



Universitat de Lleida

Impact of tillage system and crop diversification on water use efficiency, soil structure and water and gas fluxes in the soil of a Mediterranean area

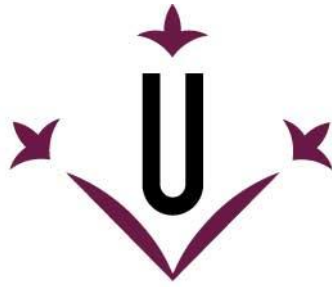
Rasendra Talukder

<http://hdl.handle.net/10803/687687>

ADVERTIMENT. L'accés als continguts d'aquesta tesi doctoral i la seva utilització ha de respectar els drets de la persona autora. Pot ser utilitzada per a consulta o estudi personal, així com en activitats o materials d'investigació i docència en els termes establerts a l'art. 32 del Text Refós de la Llei de Propietat Intel·lectual (RDL 1/1996). Per altres utilitzacions es requereix l'autorització prèvia i expressa de la persona autora. En qualsevol cas, en la utilització dels seus continguts caldrà indicar de forma clara el nom i cognoms de la persona autora i el títol de la tesi doctoral. No s'autoritza la seva reproducció o altres formes d'explotació efectuades amb finalitats de lucre ni la seva comunicació pública des d'un lloc aliè al servei TDX. Tampoc s'autoritza la presentació del seu contingut en una finestra o marc aliè a TDX (framing). Aquesta reserva de drets afecta tant als continguts de la tesi com als seus resums i índexs.

ADVERTENCIA. El acceso a los contenidos de esta tesis doctoral y su utilización debe respetar los derechos de la persona autora. Puede ser utilizada para consulta o estudio personal, así como en actividades o materiales de investigación y docencia en los términos establecidos en el art. 32 del Texto Refundido de la Ley de Propiedad Intelectual (RDL 1/1996). Para otros usos se requiere la autorización previa y expresa de la persona autora. En cualquier caso, en la utilización de sus contenidos se deberá indicar de forma clara el nombre y apellidos de la persona autora y el título de la tesis doctoral. No se autoriza su reproducción u otras formas de explotación efectuadas con fines lucrativos ni su comunicación pública desde un sitio ajeno al servicio TDR. Tampoco se autoriza la presentación de su contenido en una ventana o marco ajeno a TDR (framing). Esta reserva de derechos afecta tanto al contenido de la tesis como a sus resúmenes e índices.

WARNING. Access to the contents of this doctoral thesis and its use must respect the rights of the author. It can be used for reference or private study, as well as research and learning activities or materials in the terms established by the 32nd article of the Spanish Consolidated Copyright Act (RDL 1/1996). Express and previous authorization of the author is required for any other uses. In any case, when using its content, full name of the author and title of the thesis must be clearly indicated. Reproduction or other forms of for profit use or public communication from outside TDX service is not allowed. Presentation of its content in a window or frame external to TDX (framing) is not authorized either. These rights affect both the content of the thesis and its abstracts and indexes.



Universitat de Lleida

DOCTORAL THESIS

Impact of tillage system and crop diversification on water use efficiency, soil structure and water and gas fluxes in the soil of a Mediterranean area

Rasendra Talukder

Dissertation to obtain the degree of Doctor by the University of Lleida
Doctorate program in Agricultural and Food Science and Technology

Supervised by:
Dr. Jorge Lampurlanés Castel
Dr. Daniel Plaza-Bonilla

2022

Acknowledgments

First and foremost, my sincere gratitude and love goes to all the people who directly or indirectly helped and supported me during the hurdles in every stage of my PhD life.

This work would not have been possible without the help and encouragement of my thesis director and tutor, Dr. Jorge Lampurlanés Castel. I am grateful beyond words for the chance he has given me at this point in my life when I needed it the most. Working and studying under him was an incredible privilege. Thank you for your friendship, understanding, and unparalleled sense of humour that helped me to reach this stage.

Likewise, I offer my sincere gratitude to my thesis director Dr. Daniel Plaza Bonilla for his scholastic suggestions, guidance and critical reviews during all this time. I would want to express my deepest gratitude to Dr. Carlos Cantero Martínez (PI, DISOSMED project) and Dr. Ole Wendroth (provided the opportunity for a research stay in his lab), for his unwavering support and working by my side during this period. Thanks to the entire members of the research group especially Dr. María Concepción Ramos Martín, laboratory technician Silvia Marti, field technician Carlos Cortes, fellows and students for their assistance, generosity, and friendship. The farmer and owner of this field Ing. Xavier Penella for providing us with their field to be able to carry out this thesis.

Very deep gratitude goes to my Ma (Mother), Baba (Father), brothers and sisters, Father-in-law, Mother-in-law, for their constant support. Also, my lovely wife (Pinky) who has been great sources of hope and encouragement. She has been there for me during this difficult time of thesis writing, taking care of me and preparing traditional Bengali meals, and will be for the rest of my life. For all this and more, this thesis is dedicated to my family and wife, Pinky. I would want to thank my friends Genis, Jesus, Louise, and Gonçalo for being my companions while we enjoyed coffee and our excursion together.

A les noves zones de regadiu de la vall de l'Ebre (NE d'Espanya) se sol canviar el tradicional monocultiu de cereals d'hivern per cultius més productius com el blat de moro (*Zea mays* L.). No obstant això, en aquestes condicions, el cultiu anual únic es pot substituir per seqüències de cultiu diversificades. L'objectiu d'aquesta tesi és determinar l'efecte combinat dels sistemes de conreu i les seqüències de cultius sobre la dinàmica espai-temporal de les propietats hidrofísiques i els components del balanç hídric del sòl, el rendiment dels cultius, l'eficiència de l'ús del aigua i la seva productivitat en condicions de regadiu.

Aquest estudi es va dur a terme en un experiment de sistemes de conreu a llarg termini, establert el 1996 al NE d'Espanya, al llarg de tres anys de cultiu: 2018-19, 2019-20 i 2020-21. Es van comparar tres sistemes de conreu (conreu intensiu, IT; conreu reduït, RT i no conreu, NT) i dues seqüències de cultiu (guaret curt-panís de maduració tardana, FM; i lleguminoses-panís de maduració primerenca, LM; Pèsol, *Pisum sativum* L., o Vicia, *Vicia sativa* L.). Durant 2018-19 i 2019-20, es van realitzar 14 mostres per obtenir 288 mostres de sòl inalterades (profunditat 0.02-0.08 m) sota dos sistemes de conreu extrems (IT i NT), dues seqüències de cultius i dues posicions (dins i entre files del cultiu: W-row i B-row). En aquestes mostres es va determinar la densitat aparent, la difusivitat relativa de l'O₂, la corba de retenció d'humitat i la de conductivitat hidràulica. El 2020-21, es van dur a terme cinc campanyes d'infiltració amb el mètode Beerkan (180 infiltracions) en condicions de camp per determinar la variació espai-temporal de les propietats hidrofísiques de la superfície del sòl. A més, es va mesurar el contingut d'aigua del terra (SWC) fins a 90 cm, l'escolament superficial i la quantitat d'aigua rebuda (precipitació i reg). Es van mesurar variables del cultiu, com ara la biomassa aèria i el rendiment, i es van utilitzar per calcular l'eficiència de l'ús de l'aigua i la seva productivitat.

Els resultats van revelar que, en IT i a potencials hídrics elevats ($\Psi > -10$ cm H₂O), el sòl sota LM tenia més difusivitat, a causa d'una major quantitat de porus plens d'aire i major continuïtat de porus que FM. De la mateixa manera, es va observar una major conductivitat hidràulica específica, K_{pc} (cm dia⁻¹) corresponent a la macroporositat (> 1000 μ m) degut a un major nombre de porus efectius, N_{pc} (m⁻²), i porositat efectiva, epc (cm³ cm⁻³). Durant el cultiu d'hivern, l'absorció d'aigua per part de les lleguminoses va reduir el risc de pèrdues d'aigua per percolació profunda (DP), mentre que al cultiu d'estiu, LM va mostrar una DP similar o lleugerament més gran que FM. La introducció de lleguminoses va augmentar la biomassa aèria del panís, el rendiment en gra, l'eficiència de l'ús i la productivitat de l'aigua el 2018-19 i el 2020-21, especialment sota IT. El sòl sota NT va mostrar una difusivitat similar a l'IT a Ψ elevats (-10 cm H₂O) a causa d'una major continuïtat dels porus, particularment entre els macropors. Així mateix, el NT va mostrar més conductivitat hidràulica, K (cm dia⁻¹) a major Ψ (0, -1, -3 i -10 cm H₂O) i major K_{pc} corresponent a macropors i mesopors gruixuts (1000-60 μ m) que IT a causa de l'augment de N_{pc} , epc i de la continuïtat dels porus, C_{wpc} . La reducció en la intensitat del conreu, és a dir, RT i NT van reduir la formació de crostes superficials i la generació de escolament superficial i van augmentar la infiltració, cosa que va resultar en una biomassa aèria, rendiment en gra, eficiència en l'ús de l'aigua i productivitat de l'aigua més grans. Es van trobar variacions espaials de les propietats hidrofísiques del sòl. Així, W-row tenia més difusivitat, conductivitat hidràulica i sortivitat a causa d'una menor densitat aparent i més macroporositat i continuïtat dels porus. Les millores en les propietats hidrofísiques del sòl sota IT després del conreu no van persistir en el temps a causa de la reconsolidació del sòl amb la pluja i el reg. A més, es va trobar una major variació temporal de la conductivitat hidràulica i la sortivitat del sòl en superfície sota IT i RT en comparació amb NT a causa de la formació de la crosta del sòl.

Als agroecosistemes mediterranis, la incorporació de lleguminoses a la seqüència de cultius juntament amb el conreu de conservació seria una opció de maneig per mantenir l'estabilitat estructural del sòl i la producció dels cultius, maximitzar l'eficiència de l'ús d'aigua i la seva productivitat. Fins i tot quan l'ús del conreu de conservació no és possible, la seqüència lleguminosa-panís pot ser una opció de maneig per contrarestar l'efecte negatiu del conreu intensiu.

Resumen

En las nuevas zonas de regadío del valle del Ebro (NE de España) se suele cambiar el tradicional monocultivo de cereales de invierno por cultivos más productivos como el maíz (*Zea mays* L.). No obstante, en estas condiciones, el cultivo anual único puede sustituirse por secuencias de cultivo diversificadas. El objetivo de esta tesis es determinar el efecto combinado de los sistemas de laboreo y las secuencias de cultivos sobre la dinámica espacio-temporal de las propiedades hidrofísicas y los componentes del balance hídrico del suelo, el rendimiento de los cultivos, la eficiencia del uso del agua y su productividad en condiciones de regadío.

El presente estudio se llevó a cabo en un experimento de sistemas laboreo a largo plazo, establecido en 1996 en el NE de España, a lo largo de tres años de cultivo: 2018-19, 2019-20 y 2020-21. Se compararon tres sistemas de laboreo (laboreo intensivo, IT; laboreo reducido, RT y no laboreo, NT) y dos secuencias de cultivo (barbecho corto-maíz de maduración tardía, FM; y leguminosas-maíz de maduración temprana, LM; Guisante, *Pisum sativum* L., o Vicia, *Vicia sativa* L.). Durante 2018-19 y 2019-20, se realizaron 14 muestreos para obtener 288 muestras de suelo inalteradas (profundidad 0.02-0.08 m) bajo dos sistemas de laboreo extremos (IT y NT), dos secuencias de cultivos y dos posiciones (dentro y entre filas del cultivo: W-row y B-row). En estas muestras se determinó la densidad aparente, la difusividad relativa del O₂, la curva de retención de humedad y la de conductividad hidráulica. En 2020-21, se llevaron a cabo cinco campañas de infiltración con el método Beerkan (180 infiltraciones) en condiciones de campo para determinar la variación espacio-temporal de las propiedades hidrofísicas de la superficie del suelo. Además, se determinó el contenido de agua del suelo (SWC) hasta 90 cm, la escorrentía superficial y la cantidad de agua recibida (precipitación y riego). Se midieron variables del cultivo, como la biomasa aérea y el rendimiento, y se utilizaron para calcular la eficiencia del uso del agua y su productividad. Los resultados revelaron que, bajo IT y potenciales hídricos elevados ($\Psi > -10$ cm H₂O), el suelo bajo LM tenía una mayor difusividad, debido a una mayor cantidad de poros llenos de aire y mayor continuidad de los poros que FM. De igual forma, se observó una mayor conductividad hidráulica específica, K_{pc} (cm día⁻¹) correspondiente a la macroporosidad (> 1000 μm) debido a un mayor número de poros efectivos, N_{pc} (m⁻²), y porosidad efectiva, ε_{pc} (cm³ cm⁻³). Durante el cultivo de invierno, la absorción de agua por parte de las leguminosas redujo el riesgo de pérdidas de agua por percolación profunda (DP), mientras que en el cultivo de verano, LM mostró una DP similar o ligeramente mayor que FM. La introducción de leguminosas aumentó la biomasa aérea del maíz, su rendimiento en grano, la eficiencia del uso y la productividad del agua en 2018-19 y 2020-21, especialmente bajo IT. El suelo bajo NT mostró una difusividad similar al IT a Ψ elevados (-10 cm H₂O) debido a una mayor continuidad de los poros, particularmente entre los macroporos. Así mismo, el NT mostró mayor conductividad hidráulica, K (cm día⁻¹) a mayor Ψ (0, -1, -3 y -10 cm H₂O) y mayor K_{pc} correspondiente a macroporos y mesoporos gruesos (1000-60 μm) que IT debido al aumento de N_{pc}, ε_{pc} y de la continuidad de los poros, C_{wpc}. La reducción en la intensidad del laboreo, es decir, RT y NT previnieron la formación de costras superficiales y la generación de escorrentía superficial y aumentaron la infiltración, lo que resultó en una biomasa aérea, rendimiento en grano, eficiencia en el uso del agua y productividad del agua mayores. Se encontraron variaciones espaciales de las propiedades hidrofísicas del suelo. Así, W-row tenía mayor difusividad, conductividad hidráulica y sortividad debido a una menor densidad aparente y una mayor macroporosidad y continuidad de los poros. Las mejoras en las propiedades hidrofísicas del suelo bajo IT tras el laboreo no persistieron en el tiempo debido a la reconsolidación del suelo con la lluvia y el riego. Además, se encontró una mayor variación temporal de la conductividad hidráulica y la sortividad del suelo en superficie bajo IT y RT en comparación con NT debido a la formación de la costra del suelo. En los agroecosistemas mediterráneos, la incorporación de leguminosas en la secuencia de cultivos junto con el laboreo de conservación sería una opción de manejo para mantener la estabilidad estructural del suelo y la producción de los cultivos, maximizar la eficiencia del uso de agua y su productividad. Incluso cuando el uso del laboreo de conservación no es posible, la secuencia leguminosa-maíz puede ser una opción de manejo para contrarrestar el efecto negativo del laboreo intensivo.

Summary

Irrigated Mediterranean area of the Ebro valley (NE of Spain) has extent the possibilities of changing winter cereals to more productive crops like maize (*Zea mays* L.). Under irrigated conditions, continuous mono-cropping can be substituted by diversified crop sequences. The objective of this thesis is to determine the combined effects of tillage systems and crop sequences on spatio-temporal dynamics of soil hydro-physical properties, soil water balance components, crop productivity, crop water use efficiency and water productivity in irrigated conditions. Present study was carried out in a long-term tillage experiment, NE Spain, established in 1996 and was performed in three consecutive cropping years i.e., 2018-19, 2019-20 and 2020-21 considering only plots under medium fertilization rates (200 kg N ha⁻¹). Tillage systems (intensive tillage, IT; reduced tillage, RT and no-tillage, NT) and crop sequences (short fallow-late maturing maize, FM; and legume-early maturing maize, LM) were compared in a split plot design. During 2018-19 and 2019-20, thirteenth undisturbed soil samplings (depth: 0.02-0.08 and quantity: 288 cores) were performed under two contrasting tillage systems (IT and NT), two crop sequences, and two positions (Within and between crop rows: W-row and B-row) to determine bulk density, relative soil gas diffusivity, soil water retention and hydraulic conductivity. In 2020-21, five Beerkan infiltration campaigns (180 runs) were carried-out in field condition to measure and estimate spatio-temporal variation of surface soil hydro-physical properties. In addition, soil water content (SWC) up to 90 cm (profile), surface runoff and amount of water received e.g., precipitation and irrigation were measured and recorded from 2018-19 to 2020-21 to calculate soil water balance components. Crop variables such as above ground biomass and grain yields were measured, and used to compute crop water use efficiency, and water productivity. The results revealed that LM had greater soil gas diffusivity, due to greater air-filled porosity, macroporosity and pore continuity than FM; under IT, at higher soil water matric potentials (Ψ) (-10 cm H₂O). Similarly, greater specific hydraulic conductivity, K_{pc} (cm day⁻¹) was observed corresponding to macroporosity (> 1000 μ m) because of greater number of effective pores, N_{pc} (m⁻²) and effective porosity, ε_{pc} (cm³ cm⁻³). During winter cropping season, water uptake by legumes (Pea: *Pisum sativum* L. or Vetch: *Vicia sativa* L) reduced the risk of water losses by deep percolation (DP), whilst in summer cropping season, LM showed similar or slightly higher DP than FM. Introduction of legumes increased maize above ground biomass and grain yield, crop water use efficiency and water productivities in 2018-19 and 2020-21, especially under IT.

Soil under NT showed similar gas diffusivity than IT at higher Ψ (-10 cm H₂O) due to greater pore continuity, particularly among macropores, and less blocked pores, but no differences were observed at lower Ψ (-1000 cm H₂O). Similarly, long-term NT showed greater hydraulic conductivity, K (cm day⁻¹) at higher Ψ (0, -1, -3 and -10 cm H₂O) and greater K_{pc} corresponding to macropores and coarse mesopores (1000-60 μ m) pore size classes than IT due to increased N_{pc} , ε_{pc} , and pore continuity, C_{wpc} . Reduction in tillage intensity i.e., RT and NT prevented surface crust formation and surface runoff and increased infiltration, resulting on greater above ground biomass, grain yield water use efficiency and water productivities.

Spatial variation (i.e., B-row vs. W-row) of soil hydro-physical properties were found, and W-row had greater soil gas diffusivity, hydraulic conductivity and sorptivity due to lower bulk density, macroporosity, and pore continuity. Improvements on soil hydro-physical properties and pore characteristics under IT did not persist over time due to reconsolidation of soil after rain and irrigation. In addition, greater temporal dynamics of surface soil hydraulic conductivity and sorptivity were found under IT and RT as compared to NT because of soil crust formation.

In Mediterranean agroecosystems, incorporation of legume into crop sequence together with long-term conservation tillage i.e., RT and NT would be a management choice to maintain soil structural stability and crop production, maximize crop water use and productivity and reduce water losses. Even when the use of conservation tillage is not possible, legume-maize can be a management option to counteract the negative effect of intensive tillage.

Contents	
Acknowledgments	ii
Resum	iii
Resumen	iv
Summary.....	v
List of Tables	ix
List of Figures.....	xii
Abbreviations	xvi
General introduction	2
1. Agricultural practices towards soil and water conservation	2
2. Soil structure impact on soil hydro-physical properties	3
3. Spatio-temporal variations of soil hydro-physical properties.....	4
4. Impacts of crop sequence and tillage on soil water balance components, yields, water use efficiency and water productivity	5
General objectives	8
Chapter I.....	14
Soil gas diffusivity and pore continuity dynamics under different tillage and crop sequences in an irrigated Mediterranean area.....	14
1. Introduction	17
2. Materials and Methods	20
2.1 Experimental site and design	20
2.2 Undisturbed soil sampling	21
2.3 Laboratory measurements and calculations.....	22
2.4 Statistical analysis	25
3. Results	25
3.1 Bulk density	25
3.2 Total porosity and air-filled porosity.....	27
3.3 Relative gas diffusivity	29
3.4 Pore continuity.....	29
3.5 Relative soil gas diffusivity as a function of air-filled porosity	32
4. Discussion	35
4.1 Crop sequences effects	35
4.2 Tillage effects	37
4.3 Temporal changes and recovery	39
5. Conclusions	40
Chapter II.....	50
Soil hydraulic properties and pore dynamics under different tillage and maize-based crop sequence in an irrigated Mediterranean area	50

1. Introduction	53
2. Materials and Methods	56
2.1 Experimental site	56
2.2 Soil sampling	57
2.3 Double plate infiltrometer method	58
2.4 Evaporation method.....	59
2.5 Soil pore characteristics.....	60
2.6 Statistical analysis	62
3. Results	62
3.1 van Genuchten parameters and soil water content	62
3.2 Soil hydraulic conductivity.....	65
3.3 Soil pore characteristics.....	65
4. Discussion	75
4.1 Crop sequence effects.....	75
4.2 Tillage effects	76
4.3 Position effects	78
4.4 Temporal variations.....	78
5. Conclusions	79
Chapter III.....	87
Spatio-temporal variation of surface soil hydraulic properties under different tillage and maize-based crop sequences in a Mediterranean area	87
1. Introduction	90
2. Materials and Methods	93
2.1 Experimental site and design.....	93
2.2 Soil sampling and infiltration measurements	95
2.3 Statistical analysis	99
3. Results	99
3.1 Bulk density.....	100
3.2 Initial soil water content	100
3.3 Sorptivity	100
3.4 Saturated hydraulic conductivity	103
3.5 Mean pore size and number of pores per unit area.....	106
4. Discussion	107
4.1 Temporal variations of soil hydraulic properties.....	107
4.2 Crusting effects on soil hydraulic properties	111
5. Conclusions	112
Chapter IV	121

Soil water balance and crop water productivity under different tillage and maize-based crop sequences in a Mediterranean area	121
1. Introduction	124
2. Materials and Methods	126
2.1 Experimental site and design	126
2.2 Components of soil water balance	128
2.2.1 Precipitation	128
2.2.2 Irrigation.....	128
2.2.3 Actual evapotranspiration	129
2.2.4 Soil water content.....	129
2.2.5 Surface runoff.....	130
2.2.6 Deep percolation	130
2.3 Crop variables.....	130
2.4 Crop water use efficiency and water productivity.....	131
2.5 Statistical analysis	132
3. Results	133
3.1 Components of soil water balance.....	134
3.1.1 Crop evapotranspiration	134
3.1.2 Soil water content dynamics	134
3.1.3 Surface runoff and deep percolation	137
3.2 Crop variables.....	139
3.3 Crop water use efficiency and water productivity.....	141
4. Discussion	145
4.1 Impacts of crop sequence on soil water balance components, yield, crop water use efficiency and productivity.....	145
4.2 Impacts of tillage systems on soil water balance components, yield, crop water use and productivity	148
5. Conclusions	150
General discussion.....	160
1. Crop sequence and tillage effects on spatio-temporal variations of soil hydro-physical properties	160
2. Crop sequence and tillage effects on soil and water conservation, yields, water use efficiency and water productivity	164
General conclusions.....	168

List of Tables

Table 1: Analysis of variance (p-values) of soil bulk density (ρ_b , g cm ⁻³), relative gas diffusivity (D_s/D_o), total porosity (θ , cm ³ cm ⁻³), macroporosity (θ_{ma} , > 30 μ m), microporosity (θ_{mi} , < 30 μ m), air-filled porosity (ϵ , cm ³ cm ⁻³), pore continuity and specific pore continuity affected by tillage systems (IT, intensive tillage; NT, no-tillage and), crop sequences (FM, short fallow-maize; LM, legume-maize), sampling position (B-row, between crop rows; W-row, within crop row), soil water matric potentials (SWMP: -10, -50, -100, -333, -1000 cm H ₂ O) and their interactions (different sampling times were averaged).....	26
Table 2: Means comparisons of soil bulk density (ρ_b , g cm ⁻³), relative gas diffusivity (D_s/D_o), total porosity (θ , cm ³ cm ⁻³), macroporosity (θ_{ma} , >30 μ m), microporosity (θ_{mi} , <30 μ m), air-filled porosity (ϵ , cm ³ cm ⁻³) and pore continuity for two different tillage systems (IT, intensive tillage; NT, no-tillage), and two crop sequences (FM, short fallow-maize; LM, legume-maize), two positions (B-row, between crop rows; W-row, within crop row) and five different soil water matric potentials (SWMP: -10, -50, -100, -333, -1000 cm H ₂ O).	28
Table 3: Slope (N) and intercept (Log M) of the log (soil gas diffusivity) vs. log (air-filled porosity) relationship for two different tillage systems (IT, intensive tillage; NT, no-tillage), and two crop sequences (FM, short fallow-maize; LM, legume-maize).	33
Table 4: Analysis of variance (p-values) for van Genuchten parameters of soil water retention curve (θ_s , cm ³ cm ⁻³ : saturated water content, θ_r , cm ³ cm ⁻³ : residual soil water content, α , cm ⁻¹ and n), soil water retention ($\theta(\Psi)$, cm ³ cm ⁻³) and soil hydraulic conductivity ($K(\Psi)$, cm day ⁻¹) at different soil matric potentials (Ψ , cm H ₂ O) as affected by tillage systems (IT, intensive tillage and NT, no-tillage), crop sequences (FM, short fallow-maize and LM, legume-maize), position (W-row, within crop row and B-row, between crop rows), and their interactions (different sampling times were averaged).	64
Table 5: Mean comparisons of the van Genuchten parameters of soil water retention curve (θ_s , cm ³ cm ⁻³ : saturated water content, θ_r , cm ³ cm ⁻³ : residual soil water content, α , cm ⁻¹ and n) for two different tillage systems (IT, intensive tillage and NT, no-tillage), two crop sequences (FM, Short fallow-maize and LM, legume-maize) and two positions (W-row, within the crop row and B-row, between crop rows). Different letters within the column and factor indicate significant differences between levels (**p < 0.01 and ***p < 0.001).....	64
Table 6: Analysis of variance (p-values) for the specific hydraulic conductivity (K_{pc} , cm day ⁻¹), number of effective pores (N_{pc} , m ⁻²), effective porosity (ϵ_{pc} , cm ³ cm ⁻³), pore volume (ϕ_{pc} , cm ³ cm ⁻³) and pore continuity index (C_{wpc}) at different pore size classes (μ m) (>1000 = macroporosity, 1000-60 = coarse mesoporosity, 60-10 = fine mesoporosity, 10-3 = microporosity) affected by tillage systems (IT, intensive tillage and NT, no-tillage), crop sequences (FM, short fallow-maize and LM, legume-maize), positions (W-row, within the crop row and B-row, between crop rows) and their interactions (different sampling times were averaged). NS, non-significant (p > 0.05).	70

Table 7: Mean comparisons of specific hydraulic conductivity (K_{pc} , cm day ⁻¹) and effective porosity (ε_{pc} , cm ³ cm ⁻³) at different pore classes for two different tillage systems (IT, intensive tillage and NT, no-tillage), two crop sequences (FM, short fallow-maize, and LM, legume-maize) and two positions (W-row, within the crop row and B-row, between crop rows). Different letters within the row and factor indicate significant differences between levels (*p <0.05, **p <0.01, ***p <0.001).	70
Table 8: ANOVA (p-values) of soil bulk density (ρ_b , g cm ⁻³), initial soil water content (θ_0 , cm ³ cm ⁻³), saturated water content (θ_s , cm ³ cm ⁻³), sorptivity (S , mm s ^{-0.5}), saturated hydraulic conductivity (K_s , mm s ⁻¹), mean pore size (r, mm) and number of pores per unit area (N , m ⁻²) affected by days after autumn (18, 60, 138 days) and spring tillage (63, 205 and 177 days for FM and LM, respectively), tillage systems (IT: intensive tillage, RT: reduced tillage, and NT: no-tillage), crop sequences (FM: fallow-maize, LM: legume-maize) and their interactions.	102
Table 9: Means' comparisons of soil bulk density (ρ_b , g cm ⁻³), initial soil water content (θ_0 , cm ³ cm ⁻³), saturated water content (θ_s , cm ³ cm ⁻³), sorptivity (S , mm s ^{-0.5}), saturated hydraulic conductivity (K_s , mm s ⁻¹), mean pore size (r, mm) and number of pores per unit area (N , m ⁻²) for different days after autumn and spring tillage, three tillage systems (IT: intensive tillage, RT: reduced tillage, and NT: no-tillage) and two crop sequences (FM: fallow-maize, LM: legume-maize). Amount of rainfall and irrigation (mm) received between two consecutive samplings.	104
Table 10: Means' comparisons of soil bulk density (ρ_b , g cm ⁻³), initial soil water content (θ_0 , cm ³ cm ⁻³), saturated water content (θ_s , cm ³ cm ⁻³), sorptivity (S , mm s ^{-0.5}), saturated hydraulic conductivity (K_s , mm s ⁻¹), mean pore size (r, mm) and number of pores per unit area (N , m ⁻²) for two positions (W-row: within the crop row, B-row: between crop rows).	105
Table 11: Amount (mm) of precipitation and irrigation for three tillage systems (IT, intensive tillage; RT, reduced tillage; NT, no-tillage) and two crop sequences (FM, short fallow-maize; LM, legume-maize) during the winter and summer cropping seasons of three consecutive years.	133
Table 12: Analysis of variance (p-values) and means comparisons of crop evapotranspiration (ET_c , mm), runoff (R_{off} , mm) and deep percolation (DP , mm) affected by years (2018-19, 2019-20 and 2020-21), seasons (winter and summer cropping season), crop sequences (FM, short fallow-maize; LM, legume-maize) and tillage systems (IT, intensive tillage; RT, reduced tillage; NT, no-tillage) and their interactions. Different uppercase letters within the columns indicate significant differences between treatment means at p < 0.05; NS, Non-significant at p = 0.05.	137
Table 13: Analysis of variance (p-values) of above ground biomass (kg ha ⁻¹), grain yield (kg ha ⁻¹) and harvest index (HI) affected by tillage systems (IT, intensive tillage; RT, reduced tillage; NT, no-tillage) and crop sequence (FM, short fallow-maize; LM, legume-maize) and their interactions) during the winter and summer cropping seasons of three consecutive years.	142

Table 14: Analysis of variance (p-values) of crop water use efficiency (WUE_c), crop water productivity (WP_c), irrigation water productivity (WP_I) and input water productivity (WP_{I+P}) affected by tillage systems (IT, intensive tillage; RT, reduced tillage; NT, no-tillage), crop sequences (FM, short fallow-maize; LM, legume-maize), and their interaction) during the winter and summer cropping seasons of three consecutive years.	142
Table S1: Date of tillage, sowing or planting, chopping or harvesting, and undisturbed soil sampling for 2018-19 to 2019-20.	48
Table S2: Analysis of variance (p-values) of relative soil gas diffusivity (D_s/D_o), air-filled porosity (ϵ , $\text{cm}^3 \text{cm}^{-3}$), and pore continuity affected by sampling dates and tillage systems and their interactions in two different crop sequences (FM: short fallow-maize; LM: legume-maize).	49
Table S3: Date of tillage, sowing or planting, chopping or harvesting, and undisturbed soil sampling, amount of rainfall and irrigation for 2018-19 to 2019-20.	85
Table S4: Analysis of variance (p-values) of saturated soil water content (θ_s , $\text{cm}^3 \text{cm}^{-3}$), saturated soil hydraulic conductivity (K_s , cm day^{-1}), specific hydraulic conductivity (K_{pc} , cm day^{-1}), number of effective pores (N_{pc} , m^{-1}), pore volume (ϕ_{pc} , $\text{cm}^3 \text{cm}^{-3}$) and pore continuity index (C_{wpc}) affected by sampling dates and tillage systems and their interactions in two different crop sequences (FM: short fallow-maize; LM: legume-maize).	86
Table S5: Date of tillage operation, sowing or planting, chopping or harvesting from 2018-19 to 2020-21.	157
Table S6: Analysis of variance (p-values) of soil water content (SWC) up to 90 cm soil depth, affected by sampling dates, tillage systems (IT, intensive tillage; RT, reduced tillage; NT, no-tillage), crop sequences ((FM, short fallow-maize; LM, legume-maize) and their interactions in three consecutive years (2018-19, 2019-20 and 2020-21).	157

List of Figures

- Fig. 1: Air-filled porosity (a) (ϵ , $\text{cm}^3 \text{cm}^{-3}$) and relative soil gas diffusivity (b) (D_s/D_o) for different crop sequences (FM, short fallow-maize; LM, legume-maize) and positions (B-row, between crop rows; W-row, within crop rows). Error bars show the standard error. Different letters indicate the significant difference between treatments; ns, non-significant. 27
- Fig. 2: Pore volume ($\text{cm}^3 \text{cm}^{-3}$) and specific pore continuity for each pore size class in soils under different tillage systems (a and b), crop sequence (c and d) and position (e and f). Error bars show the standard error. Different letters indicate significant differences between treatments; ns, non-significant. Vertical dashed line separates macroporosity ($> 30 \mu\text{m}$) and microporosity ($< 30 \mu\text{m}$). 30
- Fig. 3: Relative soil gas diffusivity (D_s/D_o), air-filled porosity (ϵ , $\text{cm}^3 \text{cm}^{-3}$) and pore continuity under different tillage systems (IT, intensive tillage; NT, no-tillage) and sampling dates in short fallow-maize (a) and legume-maize (b) crop sequences. Error bars show the standard error. Different letters (lowercase letters among sampling dates and uppercase letters between tillage systems within each sampling dates) indicate the significant differences between treatments; ns, non-significant. Vertical dashed line separates the 2018-19 and 2019-20 crop seasons. 31
- Fig. 4: Pore continuity as a function of soil water matric potential (SWMP) and tillage system (IT, intensive tillage; NT, no-tillage). Error bars show the standard error. Different letters indicate significant differences between treatments for a given SWMP (-10, -50, -100, -333, -1000 $\text{cm H}_2\text{O}$); ns, non-significant. 32
- Fig. 5: Relative soil gas diffusivity as a function of air-filled porosity for two different tillage systems (IT, intensive tillage; NT, no-tillage) and two crop sequences (FM, short fallow-maize; LM, legume-maize) at five soil water matric potentials (-10, -50, -100, -333 and -1000 $\text{cm H}_2\text{O}$). Horizontal dashed lines indicate critical levels (0.005) of relative gas diffusivity. Vertical dashed lines indicate the volume of air-filled porosity ($\text{cm}^3 \text{cm}^{-3}$) required to exceed the critical limit of gas diffusivity through soils. 34
- Fig. 6: Soil water content, θ ($\text{cm}^3 \text{cm}^{-3}$) at different soil matric potentials, Ψ ($-\text{cm H}_2\text{O}$) in soils under different tillage (IT, intensive tillage and NT, no-tillage) (a), crop sequence (FM, short fallow-maize, and LM, legume-maize) (b), and position (W-row, within the crop row and B-row, between crop rows) (c). Error bars show the standard error and (*) indicates significant differences between treatments (* $p < 0.05$, ** $p < 0.01$, *** $p < 0.001$ and ns: non-significant). 66
- Fig. 7: Saturated soil water content, θ_s ($\text{cm}^3 \text{cm}^{-3}$) and saturated hydraulic conductivity, K_s (cm day^{-1}) at different sampling dates in soils under different (a and c) tillage systems (IT, Intensive tillage and NT, no-tillage), and (b and d) crop sequences (FM, short fallow-maize and LM, legume-maize). Error bars show the standard error. Different letters (lowercase letters among sampling dates and uppercase letters between tillage systems within each sampling date) indicate the significant differences between treatments at $p < 0.05$; ns, non-significant. Vertical dashed line separates the 2018-19 and 2019-20 cropping years. 67

- Fig. 8: Soil hydraulic conductivity, K (cm day^{-1}) at different soil matric potentials, Ψ ($-\text{cm H}_2\text{O}$) in soils under different tillage (IT, Intensive tillage and NT, no-tillage) (a), crop sequence (FM, short fallow-maize, and LM, legume-maize) (b), and position (W-row, within the crop row and B-row, between crop rows) (c). Error bars show the standard error and (*) indicates the significant difference between treatments (* $p < 0.05$, ** $p < 0.01$, *** $p < 0.001$ and ns: non-significant). 68
- Fig. 9: Number of effective pores, N_{pc} (m^{-2}) at different pore size classes in soils under different tillage (IT, Intensive tillage and NT, no-tillage) (a), crop sequence (FM, short fallow-maize, and LM, legume-maize) (b), and position (W-row, within the crop row and B-row, between crop rows) (c). Error bars show the standard error and (*) indicates the significant difference between treatments (* $p < 0.05$, ** $p < 0.01$, *** $p < 0.001$ and ns: non-significant). 71
- Fig. 10: Pore class volume, ϕ_{pc} ($\text{cm}^3 \text{cm}^{-3}$) and pore continuity index, C_{wpc} for different pore size classes in soils under different tillage (IT, Intensive tillage and NT, no-tillage) (a and b), crop sequence (FM, short fallow-maize, and LM, legume-maize) (c and d) and position (W-row, within the crop row and B-row, between crop rows) (e and f). Error bars show the standard error and (*) indicates the significant difference between treatments (* $p < 0.05$, ** $p < 0.01$, *** $p < 0.001$ and ns: non-significant). 72
- Fig. 11: Specific hydraulic conductivity, K_{pc} (cm day^{-1}), number of effective pores, N_{pc} (m^{-2}), pore volume, ϕ_{pc} ($\text{cm}^3 \text{cm}^{-3}$) and pore continuity index, C_{wpc} of macroporosity ($>1000 \mu\text{m}$) at different sampling dates in soils under different tillage (IT, Intensive tillage and NT, no-tillage) (a) and crop sequences (FM, short fallow-maize and LM, legume-maize) (b). Error bars show the standard error. Different letters (lowercase letters among sampling dates and uppercase letters between tillage systems within each sampling dates) indicate the significant differences between treatments; ns, non-significant. Vertical dashed line separates the 2018-19 and 2019-20 cropping years. 73
- Fig. 12: Specific hydraulic conductivity, K_{pc} (cm day^{-1}), number of effective pores, N_{pc} (m^{-2}), pore volume, ϕ_{pc} ($\text{cm}^3 \text{cm}^{-3}$) and pore continuity index, C_{wpc} of coarse mesoporosity ($1000-60 \mu\text{m}$) at different sampling dates in soils under different tillage (IT, Intensive tillage and NT, no-tillage) (a) and crop sequence (FM, short fallow-maize and LM, legume-maize) (b). Error bars show the standard error. Different letters (lowercase letters among sampling dates and uppercase letters between tillage systems within each sampling dates) indicate the significant differences between treatments; ns, non-significant. Vertical dashed line separates the 2018-19 and 2019-20 cropping years. 74
- Fig. 13: Rainfall or irrigation (mm day^{-1}), tillage practice, sowing, sampling time and harvesting for 2020-21 crop season. 101
- Fig. 14: Bulk density (a) (ρ_b , g cm^{-3}) and saturated soil water content (b) (Θ_s , $\text{cm}^3 \text{cm}^{-3}$) dynamics at different days after autumn and spring tillage under two crop sequences (FM: fallow-maize, LM: legume-maize). Error bars show the standard error. Vertical dashed line separates the days after autumn and spring tillage. ... 102

-
- Fig. 15: Sorptivity (a) (S , $\text{mm s}^{-0.5}$) and saturated hydraulic conductivity (b) (K_s , mm s^{-1}) dynamics at different days after tillage and tillage systems (IT: intensive tillage, RT: reduced tillage, and NT: no-tillage). Error bars show the standard error. Vertical dashed line separates the days after autumn and spring tillage.....105
- Fig. 16: Sorptivity (S , $\text{mm s}^{-0.5}$) under different tillage (IT: intensive tillage, RT: reduced tillage, and NT: no-tillage) and crop sequences (FM: fallow-maize, LM: legume-maize) (different sampling times were averaged). Error bars show the standard error and different uppercase letters indicates significant differences between treatments at $p < 0.05$; ns: non-significant).....106
- Fig. 17: Mean pore size (a) (r , mm) and number of pores per unit area (b) (N , m^{-2}) dynamics at different days after tillage and tillage systems (IT: intensive tillage, RT: reduced tillage, and NT: no-tillage). Error bars show the standard error. Vertical dashed line separates the days after autumn and spring tillage. 1067
- Fig. 18: Amount of precipitation and irrigation (mm) (a) received and total soil water content (mm) (b) dynamics up to 90 cm depth under different crop sequences (FM, short fallow-maize; LM, legume-maize) in three consecutive years (2018-19, 2019-20, 2020-21). Error bars show the standard error. Different lowercase and uppercase letters indicate significant differences among sampling dates and crop sequences respectively ($p < 0.05$). Vertical dashed lines separate the years..... 135
- Fig. 19: Amount of precipitation and irrigation (mm) (a) received and total soil water content (mm) (b) dynamics up to 90 cm depth under different tillage systems (IT, intensive tillage; RT, reduced tillage; NT, no-tillage) in three consecutive years (2018-19, 2019-20, 2020-21). Error bars show the standard error. Different uppercase letters indicate significant differences tillage systems for a given date ($p < 0.05$) Vertical dashed lines separate the years..... 136
- Fig. 20: Crop evapotranspiration (ET_c , mm) (a), runoff (R_{off} , mm) (b), and deep percolation (DP , mm) (c) affected by the interaction among years (2018-19, 2019-20 and 2020-21), seasons (winter and summer cropping season), and crop sequences (FM, short fallow-maize; LM, legume-maize)/tillage systems (IT, intensive tillage; RT, reduced tillage; NT, no-tillage). Error bars show the standard error. Different lowercase letters indicate significant differences between treatments within cropping season ($p < 0.05$). 138
- Fig. 21: Above ground biomass (kg ha^{-1}) production in (a) 2018-19, (b) 2019-20 and (c) 2020-21 and pea grain yield (d) (kg ha^{-1}) and harvest index, HI (c) in 2018-19 under different tillage systems (IT, intensive tillage; RT, reduced tillage; NT, no-tillage) during winter cropping season. Error bars show the standard error. Different lowercase letters indicate significant differences between treatments means for a given year and variable ($p < 0,05$). Pea grain data is shown at 0% moisture content. 139

-
- Fig. 22: Maize above ground biomass (kg ha^{-1}), grain yield (kg ha^{-1}), and harvest index (HI) in (a) 2018-19, (b) 2019-20, and (c) 2020-21 under different tillage systems (IT, intensive tillage; RT, reduced tillage; NT, no-tillage) and crop sequences (FM, short fallow-maize; LM, legume-maize) during summer cropping season. Error bars show the standard error. Different lowercase letters indicate significant differences between treatments means ($p < 0.05$). Maize grain data is shown at 0% moisture content. 140
- Fig. 23: Maize above ground biomass (kg ha^{-1}) (a) and grain yield (kg ha^{-1}) (b) in 2020-21 as affected by the interaction between tillage systems (IT, intensive tillage; RT, reduced tillage; NT, no-tillage) and crop sequences (FM, short fallow-maize; LM, legume-maize). Error bars show the standard error. Different lowercase letters indicate significant differences within each variable ($p < 0.05$). 141
- Fig. 24: Crop water use efficiency (WUE_c), crop (WP_{c1} : Yield/ET_c ; and WP_{c2} : $\text{Yield}/[\text{ET}_c + \text{N-BWU}]$), irrigation (WP_i) and input (WP_{i+p}) water productivity during the winter cropping season in (a) 2018-19 (Pea), (b) 2019-20 (Vetch) and (c) 2020-21 (Vetch) under different tillage systems (IT, intensive tillage; RT, reduced tillage; NT, no-tillage) and crop sequences (FM, short fallow-maize; LM, legume-maize). Error bars show the standard error. Different lowercase letters indicate significant differences between treatments ($p < 0.05$). 143
- Fig. 25: Crop water use efficiency (WUE_c), crop (WP_{c1} : Yield/ET_c ; and WP_{c2} : $\text{Yield}/[\text{ET}_c + \text{N-BWU}]$), irrigation (WP_i) and input (WP_{i+p}) water productivity of maize during the summer cropping season in 2018-19, 2019-20 and 2020-21 under different tillage systems (IT, intensive tillage; RT, reduced tillage; NT, no-tillage) and crop sequences (FM, short fallow-maize; LM, legume-maize). Error bars show the standard error. Different lowercase letters indicate significant differences between treatments ($p < 0.05$). 144
- Fig. 26: Maize Crop (WP_{c1}), Irrigation (WP_i) and input (WP_{i+p}) water productivity during the summer cropping season in 2020-21 as affected by the interaction between tillage systems (IT, intensive tillage; RT, reduced tillage; NT, no-tillage) and crop sequences (FM, short fallow-maize; LM, legume-maize). Error bars show the standard error. Different lowercase letters indicate significant differences within each variable ($p < 0.05$). 145
- Fig S1: Sediment yield ($\text{t ha}^{-1} \text{ year}^{-1}$) under different tillage systems (IT, intensive tillage; RT, reduced tillage; NT, no-tillage) in 2018-19 (a), 2019-20 (b) and 2020-21(c)..... 158

Abbreviations

A	Cross sectional area
B-row	Between rows of crops
C ₀	Initial oxygen concentration in the chamber
C _s	O ₂ concentration in the atmosphere
CS	Crop sequence
C _t	Oxygen concentration in the chamber at a given time
C _{wpc}	Pore continuity for water flux
DAT	Days after tillage
D ₀	Diffusion of the same gas in pure air
DP	Deep percolation
D _s	Diffusivity of gas in soil
D _s /D ₀	Relative soil gas diffusivity
D _{sT1}	Gas diffusivity at laboratory temperature
D _{sT2}	Gas diffusivity at reference temperature
E	Evaporation
ET _c	Crop evapotranspiration
ε	Air-filled porosity
f(l/l _e) ²	Pore continuity for gas flux
FM	Short fallow-maize
HI	Harvest index
I	Irrigation
IT	Intensive tillage
IWU	Irrigation water use

K _c	Crop coefficient
K(Ψ)	Hydraulic conductivity
K _{pc}	Specific hydraulic conductivity
K _s	Saturated soil hydraulic conductivity
L	Length
LM	Legume-maize
N	Number of effective pores per unit area
N-BWU	Non-beneficial water use
NT	No-tillage
O ₂	Oxygen
P	Precipitation
r	Mean pore radius
R _{off}	Runoff
RT	Reduced tillage
S	Sorptivity
SD	Sampling date
SWC	Soil water content
SWMP	Soil water matric potentials
T	Tillage
TWU	Total water use
V	Volume
WP	Water productivity
W-row	Within the row of crops
WUE _c	Crop water use efficiency
ϵ_{pc}	Effective porosity

η, m, n, ℓ	Shape parameters
θ	Soil porosity
$\theta(\Psi)$	Soil water retention
θ_0	Initial soil water content
θ_{ma}	Macroporosity
θ_{mi}	Microporosity
θ_r	Residual volumetric water content
θ_s	Saturated volumetric water content
ρ_b	Bulk density
ϕ_{pc}	Pore volume

General introduction

General introduction

1. Agricultural practices towards soil and water conservation

Conservation of Natural Resources i.e., soil and water, and profitable farming in terms of lower input and higher yield are key goals in conservation agriculture. Conservation agriculture practice includes minimum disturbance of the soil, maintenance of soil surface covered, and crop diversification (Lal, 2015). Crop diversification e.g., introduction of legumes and/or other species to cereal-based crop sequences or rotations have been recognized as a management strategy for improving the soil structure and water quality (Silva et al., 2021). In terms of soil structural quality, surface cover and crop residues obtained from additional crop helps to protect soil against soil erosion, decreases surface runoff, increases water and gas fluxes, and enhances soil fertility, compared to bare fallow systems. It also improves water quality by reducing leaching losses of agricultural inputs such as fertilizer and/or pesticides (Liu et al., 2016; Zhang et al., 2017). Moreover, crop diversification plays an important role in the soil processes by increasing the diversity of the root systems and their distribution.

Tillage is an important soil management practice which alters most soil processes and functions, but the magnitude and the direction of its effect depends on soil type, climate and cultivation history (Alvarez et al., 2014; Kargas et al., 2016; Galdos et al., 2019; Kreiselmeier et al., 2019; Silva et al., 2021). For instance, a study by Villarreal et al. (2020) reported that IT increases soil hydraulic conductivity and number of effective macropores compared to NT in Argentinian loam and sandy loam soils under maize-soybean crop rotation for 15 years. On the contrary, in silty loam soils under maize-wheat/soybean crop rotation for 34 years, no difference was found between IT and NT on these properties. Therefore, crop diversification and tillage system affect soil hydro-

physical properties in a different way according to soil conditions. Consequently, they should be properly selected to contribute to the conservation of soil and water resources. Intensification of crops in semiarid regions has often been limited because of unsuccessful crop establishment or shortage of water, while this is not the case when irrigation is available (Salmerón et al., 2011; Gabriel and Quemada, 2011). Changes in agricultural practices viz., from traditional single cropping systems (barley or wheat) to legume-maize particularly under irrigated conditions and contrasting soil tillage often changes soil hydro-physical properties and strongly influence structural stability (Lamm et al., 2009; Alfonso et al., 2020; Huynh et al., 2019). Then, it's important to investigate a variety of agricultural management practices to identify not only which has significant impact, but also whether this impact is related or interact with other practices.

2. Soil structure impact on soil hydro-physical properties

Soil structure has a great influence on soil hydro-physical properties which are related to plant growth and development, and changes on soil structure would influence these variables (Ball, 2013). The changes in soil structure are caused (i) between soils, mainly because of differences on texture, organic matter, and chemical composition, (ii) within soils, based on land use and soil management, particularly tillage, crop sequence, and irrigation. Knowing the state of soil structure in a specific agroecosystem one can infer the relationship between soil hydro-physical attributes towards agricultural management approach. Further, variations in the soil structure increase with increasing agriculture intensification as well as the risk of its degradation. Assessment of soil structure is often difficult and is performed by evaluating its components such as (i) form (organization of pores and solids, pore continuity), (ii) stability (the ability to retain structural form after certain management practices) and (iii) resilience (the ability to recover structural form) (Kay & Angers, 1999). All these components are not often measured or quantified when

assessing structural quality; instead, measurements of soil hydro-physical characteristics such as soil bulk density and porosity, water retention and hydraulic conductivity, gas diffusivity, pore characteristics, aggregate stability and penetration resistance, infiltration and percolation, resilience to soil crusting and erosion are usually used (Ball et al., 1988). In some cases, these properties can be combined to estimate indexes of soil structure i.e., pore characteristics. For instance, relative soil gas diffusivity can be divided by air-filled porosity to obtain pore continuity of existing pores in soil (Ball et al., 1988). Gas diffusivity through soils depends on the pore continuity rather than total porosity and air-filled porosity (Schjønning et al., 2002). Similarly, soil hydraulic conductivity e.g., saturated and near-saturated hydraulic conductivity changes in response to the number of active pores per unit area, effective porosity, and its continuity rather than the total volume of pores (Villarreal et al., 2020).

3. Spatio-temporal variations of soil hydro-physical properties

Soil hydraulic properties are subjected to spatio-temporal dynamics due to differences in soil management, and measurement scales (Villarreal et al., 2020). Cultivation of crops in rows, and variations of soil hydro-physical properties based on position of measurement, such as within vs. between the crops row, reflected the evidence of spatial variations (Silva et al., 2014). However, most of the studies generally measure these properties only between the crop rows. Those sometimes overestimate or underestimate the variables of concern and did not yield the best results neither comparable to real field scenarios. Beside this, using this between row values for modelling soil processes may not be representative for the whole soil.

Changes on soil hydro-physical properties before or after certain management practices such as tillage, seeding or planting can be referred as temporal changes (Hu et al., 2018). Temporal changes and recovery during each cropping season show a distinct pattern and

this pattern is affected by the agricultural practices and their intensity. For example, it is evident that soil sealing, and crusting formation are enhanced immediately after tillage operation if high intensity rainfall or irrigation event follows. Soil sealing and crusting phenomena restrict infiltration, increased surface runoff and reduce water availability for crops (Souza et al., 2014). Under these circumstances, available water for crops might be reduced, which may negatively affect the crop yield. Cropping in rows also induce spatial variations of soil structure which potential impact on soil hydro-physical properties. Studies often include annual changes on soil hydro-physical properties but did not include both temporal and spatial changes as a comprehensive assessments of management practices on these variables.

4. Impacts of crop sequence and tillage on soil water balance components, yields, water use efficiency and water productivity

Most of the Ebro valley (NE Spain), has a semiarid Mediterranean climate, where water is the most limiting factor for crop production. Most of the rain is distributed in autumn and spring and summer is very hot (Slama et al., 2019). Because of that, main production system is cereal (barley: *Hordeum vulgare* L. or wheat: *Triticum aestivum* L.) based winter mono-cropping. Seasonal rainfall and soil water storage are important factors controlling yield (ranging from 1 to 5 t ha⁻¹) of winter crop. However, some of the rain-fed agricultural fields of Ebro Valley (NE Spain) had been transformed into irrigated condition (Pareja-Sánchez et al., 2017). The establishment of irrigation system gives the possibility to cultivate more productive summer crops e.g., maize. Maize is an important grain crop which is cultivated under continuous cropping system (winter: fallow-summer: maize) a representative part of the irrigated agricultural land in Spain. Beside this, under irrigated condition, year-round cultivation of crops i.e., to change from single crop to multiple crops is possible. However, replacing winter fallow by a crop can intensify

agricultural practices such as tillage, sowing, harvesting etc. As a matter of fact, water uptake by an additional crop during the winter season would have influence on soil water content, on soil water balance i.e., inputs and outputs, and ultimately on crop yield, water use efficiency and water productivity. In an irrigated area, ensuring appropriate producer profitability and sustaining the production to meet the growing population's demand, while avoiding non-beneficial water use i.e., deep percolation, leaching and runoff, is a major challenge (Howitt, 2008; Rodrigues and Pereira, 2009; Fernández et al., 2020). The adoption of irrigation in semiarid regions not only changes soil moisture but alters many soil physical properties (e.g., soil porosity, density and infiltration) (Ramos et al., 2019) and chemical processes (i.e. dissolution of carbonate features, salt leaching) (Doner and Grossl, 2002). Moreover, the water drops action in sprinkler based irrigation systems, and wetting and drying cycles during irrigation periods modifies the soil surface structure and develops soil sealing and crusting (Assouline, 2004). To increase yields while saving water, it is necessary to assess the impact of different agricultural management strategies under irrigated conditions on soil water balance, crop yield, crop water use, and water productivity. However, depending on agricultural management practices, reliance on irrigation could change the magnitude of some of the soil water balance components at field scale (Graham et al., 2019). Water losses from surface runoff and drainage from root zone increases soil and nutrient loss, thus impacting both water quantity and quality (Gabriel and Quemada, 2011). In addition, water productivity is described as the yield produced per unit of water use, i.e., irrigation and/or precipitation (Rodrigues and Pereira, 2009; Li et al., 2016).

It is not well documented yet the consequences of legume incorporation in a maize-based crop sequence under contrasting long-term tillage systems in terms of crop yields; and whether those effects would be independent or linked with each other. To the best

knowledge, there are no reports on the impact of legume inclusion before maize crops on maize irrigation water productivity. This particular area of knowledge is highly required to quantify the benefits of crop diversification and recommending the best strategy for sustainable agroecosystem among stakeholders. This outcome can be a management option for improving soil hydraulic functions and pore system characteristics; and would stabilize maize yield compared to mono-cropping.

In Mediterranean agroecosystems, it is required to identify the best combination of soil management strategies that maintain crop productivity, and maximize crop water use efficiency and water productivity while reducing water losses through improving soil structure and enhancing water fluxes through the soils under irrigated conditions.

General objectives

The main objective of this doctoral thesis is to evaluate combined effects of tillage systems and crop diversification on soil structure, and water and gas fluxes, soil water balance components, crop productivity, water use efficiency and productivity in Agramunt, NE Spain under irrigated Mediterranean conditions.

To achieve the overall goal, four specific objectives were presented:

1. To quantify the combined impact of tillage and crop sequence (i) on soil bulk density, gas diffusivity, total porosity, macroporosity, microporosity, air-filled porosity and pore continuity within and between the crops rows, and (ii) on short-term (within a season) dynamics of soil gas transport properties (Chapter I).
2. To determine the spatio-temporal dynamics of soil hydraulic properties and pore system characteristics under various tillage systems, crop sequences and positions (Chapter II).
3. To assess the effect of crust on (i) soil physical and hydrodynamic properties and (ii) its spatio-temporal variations under various tillage, crop sequences, and position with respect to the crop row (Chapter III).
4. To determine and quantify soil water balance components, crop above ground biomass and grain yields, crop water use efficiency and productivities under various agricultural management practices (Chapter IV).

References

- Alfonso, C., Barbieri, P.A., Hernández, M.D., Lewczuk, N.A., Martínez, J.P., Echarte, M.M., Echarte, L., 2020. Water productivity in soybean following a cover crop in a humid environment. *Agric. Water Manag.* 232, 106045.
<https://doi.org/10.1016/j.agwat.2020.106045>
- Alvarez, C.R., Taboada, M.A., Perelman, S., Morrás, H.J.M., 2014. Topsoil structure in no-tilled soils in the Rolling Pampa, Argentina. *Soil Res.* 52, 533.
<https://doi.org/10.1071/SR13281>
- Assouline, S., 2004. Rainfall-Induced Soil Surface Sealing: A Critical Review of Observations, Conceptual Models, and Solutions. *Vadose Zo. J.* 3, 570–591.
<https://doi.org/10.2136/vzj2004.0570>
- Ball, B.C., 2013. Soil structure and greenhouse gas emissions: a synthesis of 20 years of experimentation. *Eur. J. Soil Sci.* 64, 357–373. <https://doi.org/10.1111/ejss.12013>
- Ball, B.C., O’Sullivan, M.F., Hunter, R., 1988. Gas diffusion, fluid flow and derived pore continuity indices in relation to vehicle traffic and tillage. *J. Soil Sci.* 39, 327–339. <https://doi.org/10.1111/j.1365-2389.1988.tb01219.x>
- Doner, H.E., Grossl, P.R., 2002. Carbonates and Evaporites, in: *Soil Mineralogy with Environmental Applications*. John Wiley & Sons, Ltd, pp. 199–228.
<https://doi.org/https://doi.org/10.2136/sssabookser7.c6>
- Lamm, F. R., Aiken, R. M., Abou Kheira, A. A., 2009. Corn Yield and Water Use Characteristics as Affected by Tillage, Plant Density, and Irrigation. *Trans. ASABE* 52, 133–143. <https://doi.org/10.13031/2013.25954>
- Fernández, J.E., Alcon, F., Diaz-Espejo, A., Hernandez-Santana, V., Cuevas, M. V., 2020. Water use indicators and economic analysis for on-farm irrigation decision: A case study of a super high density olive tree orchard. *Agric. Water Manag.* 237,

106074. <https://doi.org/10.1016/j.agwat.2020.106074>
- Gabriel, J.L., Quemada, M., 2011. Replacing bare fallow with cover crops in a maize cropping system: Yield, N uptake and fertiliser fate. *Eur. J. Agron.* 34, 133–143. <https://doi.org/10.1016/j.eja.2010.11.006>
- Galdos, M.V., Pires, L.F., Cooper, H.V., Calonego, J.C., Rosolem, C.A., Mooney, S.J., 2019. Assessing the long-term effects of zero-tillage on the macroporosity of Brazilian soils using X-ray Computed Tomography. *Geoderma* 337, 1126–1135. <https://doi.org/10.1016/j.geoderma.2018.11.031>
- Graham, S.L., Laubach, J., Hunt, J.E., Eger, A., Carrick, S., Whitehead, D., 2019. Predicting soil water balance for irrigated and non-irrigated lucerne on stony, alluvial soils. *Agric. Water Manag.* 226, 105790. <https://doi.org/10.1016/j.agwat.2019.105790>
- Howitt, R., 2008. Water Productivity in Agriculture: Limits and Opportunities for Improvement. *Vadose Zo. J.* 7, 390–391. <https://doi.org/10.2136/vzj2007.0085br>
- Hu, W., Tabley, F., Beare, M., Tregurtha, C., Gillespie, R., Qiu, W., Gosden, P., 2018. Short-Term Dynamics of Soil Physical Properties as Affected by Compaction and Tillage in a Silt Loam Soil. *Vadose Zo. J.* 17, 180115. <https://doi.org/10.2136/vzj2018.06.0115>
- Huynh, H.T., Hufnagel, J., Wurbs, A., Bellingrath-Kimura, S.D., 2019. Influences of soil tillage, irrigation and crop rotation on maize biomass yield in a 9-year field study in Müncheberg, Germany. *F. Crop. Res.* 241, 107565. <https://doi.org/10.1016/j.fcr.2019.107565>
- Kargas, G., Kerkides, P., Sotirakoglou, K., Poulouvassilis, A., 2016. Temporal variability of surface soil hydraulic properties under various tillage systems. *Soil Tillage Res.* 158, 22–31. <https://doi.org/10.1016/j.still.2015.11.011>

- Kay, B.D. & Angers, D.A. 1999. Soil structure. In: Handbook of Soil Science (ed. M.E. Sumner), pp. A229–A276. CRC Press, Boca Raton, FL.
- Kreiselmeier, J., Chandrasekhar, P., Weninger, T., Schwen, A., Julich, S., Feger, K.H., Schwärzel, K., 2019. Quantification of soil pore dynamics during a winter wheat cropping cycle under different tillage regimes. *Soil Tillage Res.* 192, 222–232. <https://doi.org/10.1016/j.still.2019.05.014>
- Lal, R., 2015. Restoring Soil Quality to Mitigate Soil Degradation. *Sustainability* 7, 5875–5895. <https://doi.org/10.3390/su7055875>
- Li, X., Zhang, X., Niu, J., Tong, L., Kang, S., Du, T., Li, S., Ding, R., 2016. Irrigation water productivity is more influenced by agronomic practice factors than by climatic factors in Hexi Corridor, Northwest China. *Sci. Rep.* 6, 37971. <https://doi.org/10.1038/srep37971>
- Liu, H., Janssen, M., Lennartz, B., 2016. Changes in flow and transport patterns in fen peat following soil degradation. *Eur. J. Soil Sci.* 67, 763–772. <https://doi.org/10.1111/ejss.12380>
- Pareja-Sánchez, E., Plaza-Bonilla, D., Ramos, M. C., Lampurlanés, J., Álvaro-Fuentes, J., & Cantero-Martínez, C. (2017). Long-term no-till as a means to maintain soil surface structure in an agroecosystem transformed into irrigation. *Soil and Tillage Research*, 174, 221–230. <https://doi.org/10.1016/j.still.2017.07.012>
- Ramos, M.C., Pareja-Sánchez, E., Plaza-Bonilla, D., Cantero-Martínez, C., Lampurlanés, J., 2019. Soil sealing and soil water content under no-tillage and conventional tillage in irrigated corn: Effects on grain yield. *Hydrol. Process.* 33, 2095–2109. <https://doi.org/10.1002/hyp.13457>
- Rodrigues, G.C., Pereira, L.S., 2009. Assessing economic impacts of deficit irrigation as related to water productivity and water costs. *Biosyst. Eng.* 103, 536–551.

<https://doi.org/10.1016/j.biosystemseng.2009.05.002>

Slama, F., Zemni, N., Bouksila, F., De Mascellis, R., & Bouhlila, R. (2019). Modelling the impact on root water uptake and solute return flow of different drip irrigation regimes with brackish water. *Water (Switzerland)*, *11*(3), 1–17.

<https://doi.org/10.3390/w11030425>

Salmerón, M., Isla, R., Cavero, J., 2011. Effect of winter cover crop species and planting methods on maize yield and N availability under irrigated Mediterranean conditions. *F. Crop. Res.* *123*, 89–99. <https://doi.org/10.1016/j.fcr.2011.05.006>

Schjønning, P., Munkholm, L.J., Moldrup, P., Jacobsen, O.H., 2002. Modelling soil pore characteristics from measurements of air exchange: the long-term effects of fertilization and crop rotation. *Eur. J. Soil Sci.* *53*, 331–339.

<https://doi.org/10.1046/J.1365-2389.2002.00438.X>

Silva, A.P. da, Ball, B.C., Tormena, C.A., Giarola, N.F.B., Guimarães, R.M.L., 2014. Soil structure and greenhouse gas production differences between row and interrow positions under no-tillage. *Sci. Agric.* *71*, 157–162. <https://doi.org/10.1590/S0103-90162014000200011>

Silva, M.F. da, Fernandes, M.M.H., Fernandes, C., Silva, A.M.R. da, Ferraudo, A.S., Coelho, A.P., 2021. Contribution of tillage systems and crop succession to soil structuring. *Soil Tillage Res.* *209*, 104924.

<https://doi.org/10.1016/j.still.2020.104924>

Souza, E.S., Antonino, A.C.D., Heck, R.J., Montenegro, S.M.G.L., Lima, J.R.S., Sampaio, E.V.S.B., Angulo-Jaramillo, R., Vauclin, M., 2014. Effect of crusting on the physical and hydraulic properties of a soil cropped with Castor beans (*Ricinus communis* L.) in the northeastern region of Brazil. *Soil Tillage Res.* *141*, 55–61.

<https://doi.org/10.1016/j.still.2014.04.004>

Villarreal, R., Lozano, L.A., Salazar, M.P., Bellora, G.L., Melani, E.M., Polich, N., Soracco, C.G., 2020. Pore system configuration and hydraulic properties. Temporal variation during the crop cycle in different soil types of Argentinean Pampas Region. *Soil Tillage Res.* 198, 104528. <https://doi.org/10.1016/j.still.2019.104528>

Zhang, Y., Niu, J., Zhang, M., Xiao, Z., Zhu, W., 2017. Interaction Between Plant Roots and Soil Water Flow in Response to Preferential Flow Paths in Northern China. *L. Degrad. Dev.* 28, 648–663. <https://doi.org/10.1002/ldr.2592>

Chapter I

Soil gas diffusivity and pore continuity dynamics under different tillage and crop sequences in an irrigated Mediterranean area

Published: Soil and Tillage Research

doi.org/10.1016/j.still.2022.105409

Soil gas diffusivity and pore continuity dynamics under different tillage and crop sequences in an irrigated Mediterranean area

Rasendra Talukder^{*a}, Daniel Plaza-Bonilla^b, Carlos Cantero-Martínez^{bc}, Ole Wendroth^d,
Jorge Lampurlanés^{ac}

^aDepartment of Agricultural and Forest Engineering - Agrotecnio-CERCA Center,
University of Lleida, Av. Rovira Roure 191, 25198 Lleida, Spain

^bDepartment of Crop and Forest Sciences - Agrotecnio-CERCA Center, University of
Lleida, Av. Rovira Roure 191, 25198 Lleida, Spain

^cAssociate Unit CSIC (Research Spanish Council), Spain

^dDepartment of Plant and Soil Science, University of Kentucky, North
Lexington, KY 40546-0091, United States

* Corresponding author: rasendra.talukder@udl.cat

Abstract

Gas diffusion can be used to quantify soil quality and structural development that is strongly affected by soil use and management practices. There is a lack of information about the quantitative effect of tillage combined with crop sequences on soil structure. This study aimed to quantify the effects of tillage and crop sequences on soil bulk density, gas diffusivity, air-filled porosity, and the resulting pore continuity and their dynamic during the cropping cycle. A total of 288 undisturbed soil samples were collected over two growing periods (2018-19 and 2019-20) on a long-term field experiment (~25 years old) in Agramunt, NE Spain. Three factors were investigated to observe their influence on the above-mentioned soil's physical characteristics: two tillage systems (intensive tillage, IT and no-tillage, NT), two crop sequences (short fallow-maize, FM; legume-maize, LM) and two positions (within the row of crops, W-row; between rows of crops,

B-row). Soil gas diffusivity was measured at five different soil water matric potentials (SWMP) (-10, -50, -100, -333 and -1000 cm H₂O). LM crop sequence showed greater air-filled porosity, macroporosity and gas diffusivity, as well as enhanced pore continuity, than FM, especially at W-row. No significant differences were observed for measured gas diffusivity between NT and IT systems though NT had lower air-filled porosity and macroporosity (> 30 µm) compared to IT. Soil under NT showed greater pore continuity, particularly among macropores and less blocked pores than IT at higher SWMP (-10 cm H₂O) but no difference was observed at lower SWMP (-1000 cm H₂O) regardless of crop sequence and position. Air-filled porosity and pore continuity changes between maize planting and harvesting were greater under IT than NT. During the legume growing seasons, IT showed comparable pore continuity values to NT. In LM crop sequence soil gas transport was favourably affected alleviating the negative effect of intensive tillage on soil structural degradation. Long-term NT also improved soil structure as indicated by higher continuity of macropores, despite a decrease in air-filled porosity and macroporosity, but did not significantly lower gas diffusivity.

Keywords: Long term no-tillage, Crop sequence, Gas diffusivity, Air-filled porosity, Pore continuity

1. Introduction

Gas transport within the soil is crucial to understand ecosystems functions, e.g., removal of greenhouse gases and volatile organic compounds from the soil and providing O₂ for root and microbial respiration in soil (Rolston and Moldrup, 2002). Understanding how agricultural management such as tillage and crop sequence affects the geometry of the soil pore space and its efficiency for gas transport, is important for maintaining essential soil ecosystem functions (Haruna et al., 2018; Malobane et al., 2021). There are two processes, i.e., gas diffusion and gas convection, by which gases move through the soil. Gas diffusion occurs because of concentration gradients within the soil and between the soil and the atmosphere, whilst convective gas transport occurs due to air pressure gradients (Rolston and Moldrup, 2002). The difference in concentration may be caused by local imbalances in gas concentration induced by plant roots and microbial respiration, as well as biological processes including nitrification, denitrification and fermentation (Masís-Meléndez et al., 2015).

The measured diffusion of gas in soil (D_s) is usually normalized by diffusion of the same gas in pure air (D_o) to minimize the influence of specific gas properties on the diffusion process. In turn, the ratio of D_s/D_o is referred to as relative soil gas diffusivity, and only soil properties influence it (Moldrup et al., 2001; Rolston, 1986; Rolston and Moldrup, 2002). Gas diffusivity through soils is regulated by soil structural properties such as bulk density, air-filled porosity and pore continuity. The air-filled porosity, however, provides little information about the oxygen content in the root zone (Troeh et al., 1982). The gas diffusivity through soils is probably more important for describing the gas movements in soils than the air-filled porosity. Moreover, gas diffusivity (D_s/D_o) as a function of air-filled porosity also represents the average pore continuity or tortuosity of the air-filled porosity in soils (Moldrup et al., 2001). Therefore, soil gas diffusivity and pore continuity

are important properties of concern for various fields of soil and environmental processes. They may vary in response to regional and temporal variability, as well as being influenced by land-use management and measurement scale (Baranian Kabir et al., 2020). Pore characteristics have been investigated extensively in relation to tillage and traffic (e.g., Abdollahi et al., 2014; Ball, 2013; Eden et al., 2012; Galdos et al., 2019). Galdos et al., (2019) reported that the average number of pores in conventional tillage (CT) was twice that in no-tillage (NT) in a long term field experiment (< 30 years) in Brazil. However, in that experiment macroporosity and pore continuity were higher in NT than in CT. In contrast, Eden et al., (2011) showed that NT decreased macroporosity; and there was no difference in pore continuity between rotovated (0.1 m depth) and NT treatments, in a long-term experiment on coarse sandy loam soil.

In Mediterranean region, water is a limited resource for agricultural crops, where most of the precipitation is distributed in autumn; summer is extremely warm and dry (Slama et al., 2019). Without irrigation, summer crops are not profitable to grow, and winter cereals are the traditional crops. Rainfed agricultural lands of the Segarra-Garrigues canal had been transformed to irrigated fields in the Ebro Valley (NE Spain) (Pareja-Sánchez et al., 2017). Establishing an irrigation system in the Ebro Valley enables the year-round cultivation of multiple crops and increases agricultural yields (Ramos et al., 2019). Cultivation of two cash crops i.e., one followed by another or cultivation of cover crops before main crops has been found to be influential on soil quality (Abdollahi et al., 2014; Chen et al., 2014; Eden et al., 2012; Malobane et al., 2021). However, the literature contains evidence of both positive and non-existent effects of crop sequences on soil structural properties. Abdollahi et al., (2014) reported that the incorporation of cover crops into crop sequences increased macropores and pore continuity, which positively influenced gas transport and water movement. Other studies did not find a significant

effect of crop sequences on soil properties such as soil air permeability, gas diffusion, pore characteristics, hydraulic conductivity etc. (Abdollahi and Munkholm, 2017; Holthusen et al., 2018). Yet, there is a knowledge gap on the effect of tillage and crop sequence on soil structure and its functioning.

Many studies have been conducted to investigate the effects of either tillage or crop sequences on gas diffusivity and soil structural properties e.g., bulk density, gas diffusivity, air-filled porosity, and pore continuity (Abdollahi et al., 2014; Chen et al., 2014; Abdollahi and Munkholm, 2017; Holthusen et al., 2018; Malobane et al., 2021). However, the impact of position (within the row or between rows of crops) on gas diffusivity and pore continuity—both of which were studied in this study—was rarely considered. For instance, Silva et al., (2014) reported that thirty days after sowing of soybean, air-filled porosity and gas diffusivity were higher within the row than between the rows, but no difference was observed with regard to pore continuity under long-term no-tillage on a clayey Oxisol in Southern Brazil. Within the row of crops, the presence of roots and the area exploited by the root systems create bypass channels or pathways, that favourably influence the soil's physical qualities. Therefore, the position where an undisturbed sample is taken affects soil structure and thus gas transport through the soil. The objectives of this study were to quantify the combined impact of tillage and crop sequence (i) on gas diffusivity, total porosity, macroporosity, microporosity, air-filled porosity and pore continuity within and between rows of crops, and (ii) on short-term (within a season) dynamics of soil gas transport properties. We hypothesized that legume-maize would enhance soil physical quality and improve air exchange in soils. In addition, it was expected that within the crop row, better soil conditions would exist for gas movement than between rows, allowing for the occurrence of localized preferential flow.

2. Materials and Methods

2.1 Experimental site and design

The experiment for this study was conducted from 2018-19 to 2019-20 at Agramunt, NE Spain (41°48' N, 1°07' E, 330 m asl). The climate of the area is the semiarid Mediterranean, with a mean annual precipitation of 401 mm and a mean air temperature of 14.1 °C. The soil was classified as Typic Xerofluvent according to USDA soil classification (Soil Survey Staff, 2014) and the upper (0–28 cm) horizon has a silt loam texture (sand, 30.8%; silt, 57.3%; clay, 11.9%). Also, at the start of the experiment (1996), the following physico-chemical properties (upper, 0–28 cm) were observed: pH (H₂O, 1:2.5): 8.5, electrical conductivity (1:5): 0.15 dS m⁻¹, soil organic carbon concentration 9 g kg⁻¹, P Olsen: 35 mg kg⁻¹; K (Amm. Ac.): 194 mg kg⁻¹; water retention (-33 kPa): 16 kg kg⁻¹; water retention (-1500 kPa): 5 kg kg⁻¹ (Cantero-Martínez et al., 2003).

The study was conducted in a long term field experiment established in 1996 to compare three tillage systems, intensive tillage (IT), reduced tillage (RT) and no-tillage (NT), and three rates of mineral nitrogen application (zero, medium and high) with a single crop (winter barley, *Hordeum vulgare* L.) under rainfed conditions (Angás et al., 2006; Cantero-Martínez et al., 2003). In 2015, a solid set sprinkler irrigation system was installed in the experimental field that was transformed from rainfed winter cereals to irrigated maize (*Zea mays* L.). In 2018, crop sequences were introduced as a new factor with two levels: the traditional short fallow-maize (FM, that is, winter short fallow and summer long-cycle maize crop: *Zea mays* L.), and legume-maize (LM, that is, winter legume crop: Pea; *Pisum sativum* L. or Vetch; *Vicia sativa* L. and summer short-cycle maize crop: *Zea mays* L.). Two tillage systems (IT and NT), two crop sequences (FM and LM), and a medium fertilization rate were considered in this study. The factors were applied to the experimental units in a split-split-plot design with three replications. Tillage

system was applied to the main plots, crop sequence to the sub-plots, and sampling position was considered as the split-split-plot. The experimental main plot size was 50 m long and 6 m width; sub-plot size was 50 m long and 3 m width.

Tillage was practised in IT plots: (i) in autumn at the same time for FM and LM, and (ii) in spring before planting maize (at different times for FM and LM) (Table S1). Autumn tillage consisted of a subsoiler pass (depth: 35 cm) followed by a chisel (depth: 15 cm) (which helped to incorporate residue into the soil nearly 100%) and a roller (to make the surface even), whereas a rototiller (15 cm), followed by a chisel pass and a roller, was used for spring tillage. Direct drilling was performed in NT plots. A pneumatic row direct drilling machine was used in both tillage systems. The machine had double disk furrow openings and two rotary residue row cleaners. Maize (both FM and LM) was planted at a density of 90,000 seeds ha⁻¹ with a row spacing of 73 cm, whilst legumes were sown at a density of 100 seeds m⁻² for pea and 267 seeds m⁻² for vetch, with 19 cm row spacing. In 2018-19, pea was harvested and in 2019-20, vetch was chopped and spread over the soil. Similarly, after commercial harvesting, the residue of maize was chopped and spread over the surface.

2.2 Undisturbed soil sampling

A total of fourteen sampling dates (LM: nine samplings and FM: five samplings) were carried out from 2018-19 to 2019-20, and a total of 288 undisturbed soil samples were collected at a depth of 0.02-0.08 m using soil corers (0.06 m height and 0.08 m diameter). To collect the samples, two positions were considered such as within the crop row (W-row) and between the crop rows (B-row). For all sampling dates, three samples were collected at each position in every sub-plot except after harvest of maize, when only two samples were taken. The samples collected were stored at low temperature (4 °C) until

they were processed. Table S1 shows the details of tillage, sowing or planting, harvesting of crops, and undisturbed soil sampling for 2018-19 to 2019-20.

2.3 Laboratory measurements and calculations

The apparent soil gas diffusivity (D_s), air-filled porosity (ϵ) and pore continuity $f(l/l_e)^2$ were quantified at five different soil water matric potentials (SWMP) such as -10, -50, -100, -333 and -1000 cm H₂O. For each matric potential, the undisturbed soil samples were placed over a ceramic plate and saturated slowly from the bottom with deaerated water for 24 hours (Kreba et al., 2017). The ceramic plate with the saturated samples was then placed in the pressure apparatus that was set to the corresponding pressure. Samples were maintained there until no more water was drained from the ceramic plate when it was assumed that the hydrostatic equilibrium of samples at this matric potential was reached. Sample weight was then measured and recorded to know soil water content from oven-dry weight at the end of the gas diffusion measurements and the air-filled porosity at each SWMP step.

For soil gas diffusivity (D_s) measurements, airtight gas diffusion chambers (height: 0.078 m, diameter: 0.19 m) were built based on the apparatus described by Rolston (1986) and equipped with a mass flow oxygen sensor (O₂-A₃ Alphasense oxygen sensor, UK) connected to a datalogger, as O₂ was used as the trace gas. It was assumed that the O₂ concentration in the atmosphere was 20.9% (C_s), and this value was used as a calibration point for the sensor readings. The soil cores were placed into chambers that were flushed with N₂ gas until the oxygen concentration in the chamber was at a relatively low value near zero percent (initial oxygen concentration, C_o). Since then, the oxygen concentration within the closed chamber was measured every 10 minutes for up to 4 hours.

The diffusion process was based on the difference in O₂ concentration between the air inside and outside the chamber that generates a gradient between the two sides of the

sample (i.e., the low concentration of O₂ in the chamber, C_o and the high concentration of O₂ in the atmosphere, C_s). The gas diffusivity was calculated from the change of the chambers oxygen concentration per unit time (Rolston and Moldrup, 2002).

The gas diffusivity (D_s) through the soil can be described as follows (Rolston and Moldrup, 2002):

$$\ln \left(\frac{C_s - C_t}{C_s - C_o} \right) = \frac{D_s \times A}{V \times L} \times t \quad (1)$$

where C_s is the ambient air O₂ concentration (g cm⁻³), C_t and C_o are the O₂ concentrations in the diffusion chamber (g cm⁻³) at a specific time t (s) and initial condition (g cm⁻³), respectively. V is the volume of the diffusion chamber (cm³), D_s is the gas diffusivity (cm² s⁻¹), L is the height of the soil core (cm) and A its cross-sectional area (cm²).

We did not expect big atmospheric pressure fluctuations as we measured the gas diffusivity only for a short period. However, in response to seasons, the temperature changed slightly, and the soil gas diffusivity was corrected at a reference temperature (20 °C). The correction was done using the formula stated by Currie (1960).

$$D_{sT_2} = D_{sT_1} \left(\frac{T_2}{T_1} \right)^{1.72} \quad (2)$$

where D_{sT_2} and D_{sT_1} represent the gas diffusivity at reference temperature (20 °C) (T_2) and laboratory temperature (T_1), respectively. The relative gas diffusivity (D_s/D_o) is then calculated by dividing the temperature corrected gas diffusivity in the soil (D_s) by the gas diffusivity in the air (O₂ diffusivity in air, $D_o = 0.206$ cm² s⁻¹).

Soil bulk density was determined as the proportion of oven-dried soil mass (g) and soil bulk volume and expressed as g cm⁻³. The oven-dried soil mass was obtained by drying the core soil at 105 °C for 24 h, and the soil volume was taken as the core inner volume.

Pore fractions corresponding to total macroporosity (θ_{ma} , diameter > 30 μm) and total microporosity (θ_{mi} , diameter < 30 μm), were calculated as the total soil porosity (θ , cm³

cm^{-3}) minus the water content at -100 cm H₂O SWMP, and the difference in soil water content between -100 and -1000 cm H₂O SWMP, respectively (Bell et al., 2011).

The pore continuity was calculated from the relative soil gas diffusivity and air-filled porosity (Ehlers et al., 1995; Troeh et al., 1982). The equation is as follows:

$$\frac{D_s}{D_0} = \varepsilon f \left(\frac{l}{l_e} \right)^2 \quad (3)$$

where l and l_e are the length of soil core (cm) and pore (cm), f is the reduction of gas diffusivity due to air-entrapped or constricted pores, and $f(l/l_e)^2$ is the pore continuity.

Specific pore continuity (Eq. 3) of total macroporosity (θ_{ma} , diameter > 30 μm) was calculated from the relative soil gas diffusivity and air-filled porosity obtained at -100 cm H₂O SWMP, and specific pore continuity of total microporosity (θ_{mi} , diameter < 30 μm) was calculated by the difference between relative soil gas diffusivity and air-filled porosity obtained at -100 and -1000 cm H₂O SWMP.

A simple exponential model was used to describe the relationship between relative soil gas diffusivity (D_s/D_0) and air-filled porosity (ε) (Marshall, 1959; Millington, 1959).

$$\frac{D_s}{D_0} = M \varepsilon^N \quad (4)$$

Which can be written as:

$$\log \left(\frac{D_s}{D_0} \right) = \log M + N \log (\varepsilon) \quad (5)$$

where M and N are empirical parameters, but N is also a measure of pore continuity being the slope of the $\log (D_s/D_0)$ vs. $\log (\varepsilon)$ relationship. Increased pore continuity is indicated by an increase in the N value. Further, the diffusion in air is 10^4 times higher than the diffusion in water (Broecker and Peng, 1974). Hence, the critical limit for effective gas diffusion under continuous air-filled pore spaces was assumed to be $D_s/D_0 = 10^{-4}$ ($D_s/D_0 = 0.005$) (Grable and Siemer, 1968).

2.4 Statistical analysis

Data analysis was performed using the statistical package JMP Pro 15 (SAS Institute Inc, 2021). The distribution (normality) and homogeneity of variance of obtained data were checked with the Shapiro-Wilk test and the Levene test, respectively. The relative gas diffusivity and pore continuity data were BoxCox-transformed before analysis when needed. Bulk density, D_s/D_o , θ , θ_{ma} , θ_{mi} , ε , pore continuity and specific pore continuity were statistically tested for treatment (main) effects and interaction with analysis of variance (ANOVA). When single effects or interactions were significant ($p < 0.05$), the comparisons among the means were performed at 0.05 probability level of significance with Student's t-test. Further, an analysis of variance (ANOVA) was performed to compare the effects of sampling dates (main plots) and tillage systems (sub-plots) on the dynamics of D_s/D_o , ε and pore continuity in FM and LM (Federer and King, 2007). An ANCOVA model was performed to examine the relationships between relative gas diffusivity and air-filled porosity, including tillage, crop sequence, and position as factors, whereas air-filled porosity as a covariate. To simplify the model, non-significant terms (high order interactions) were removed from the full model.

3. Results

3.1 Bulk density

Tillage significantly ($p < 0.002$) affected soil bulk density (Table 1), and NT had 4% higher bulk density compared to the IT systems (Table 2). Position also modified soil bulk density that was significantly higher ($p < 0.002$) between crop rows (B-row) (1.54 g cm^{-3}) compared to within the rows (W-row) (1.48 g cm^{-3}). There was no significant difference in bulk density between crop sequences, nor significant interaction among tillage, crop sequence, and position (Table 1).

Table 1: Analysis of variance (p-values) of soil bulk density (ρ_b , g cm^{-3}), relative gas diffusivity (D_s/D_o), total porosity (θ , $\text{cm}^3 \text{cm}^{-3}$), macroporosity (θ_{ma} , $> 30 \mu\text{m}$), microporosity (θ_{mi} , $< 30 \mu\text{m}$), air-filled porosity (ε , $\text{cm}^3 \text{cm}^{-3}$), pore continuity and specific pore continuity affected by tillage systems (IT, intensive tillage; NT, no-tillage and), crop sequences (FM, short fallow-maize; LM, legume-maize), sampling position (B-row, between crop rows; W-row, within crop row), soil water matric potentials (SWMP: -10, -50, -100, -333, -1000 $\text{cm H}_2\text{O}$) and their interactions (different sampling times were averaged).

Source of variation	ρ_b ,	θ	θ_{ma}	θ_{mi}	ε	D_s/D_o ‡	Pore Continuity ‡	Specific pore continuity	
	(g cm^{-3})	($\text{cm}^3 \text{cm}^{-3}$)	($\text{cm}^3 \text{cm}^{-3}$)	($\text{cm}^3 \text{cm}^{-3}$)	($\text{cm}^3 \text{cm}^{-3}$)	θ_{ma}		θ_{mi}	
Tillage (Till.)	0.002	0.012	<0.0001	NS	<0.0001	NS	<0.0001	<0.001	< 0.001
Crop sequence	NS	NS	0.044	0.040	0.009	0.0001	0.037	NS	NS
Till. *Crop sequence	NS	NS	NS	NS	NS	NS	NS	NS	NS
Position	0.002	0.003	0.023	NS	<0.0001	0.0001	NS	NS	NS
Till. *Position	NS	NS	NS	NS	NS	NS	NS	NS	NS
Crop sequence *Position	NS	NS	NS	NS	0.006	0.008	NS	NS	NS
Till. *Crop sequence*Position	NS	NS	NS	NS	NS	NS	NS	NS	NS
SWMP					<0.0001	0.0001	0.0001		
Till. *SWMP					NS	NS	0.0006		
Crop sequence *SWMP					NS	NS	NS		
Till. *Crop sequence*SWMP					NS	NS	NS		
Position *SWMP					NS	NS	NS		
Till. *Position*SWMP					NS	NS	NS		
Crop sequence *Position*SWMP					NS	NS	NS		
Till. *Crop sequence*Position*SWMP					NS	NS	NS		

‡, data were BoxCox-transformed before analysis

NS, non-significant ($p > 0.05$).

3.2 Total porosity and air-filled porosity

Total porosity was affected by tillage ($p < 0.012$) and position ($p < 0.003$) but not by crop sequence (Table 1). IT had higher total porosity ($0.44 \text{ cm}^3 \text{ cm}^{-3}$) compared to NT ($0.42 \text{ cm}^3 \text{ cm}^{-3}$), whilst W-row had higher total porosity ($0.44 \text{ cm}^3 \text{ cm}^{-3}$) than B-row ($0.42 \text{ cm}^3 \text{ cm}^{-3}$). No significant interactions were observed among tillage, crop sequence and position.

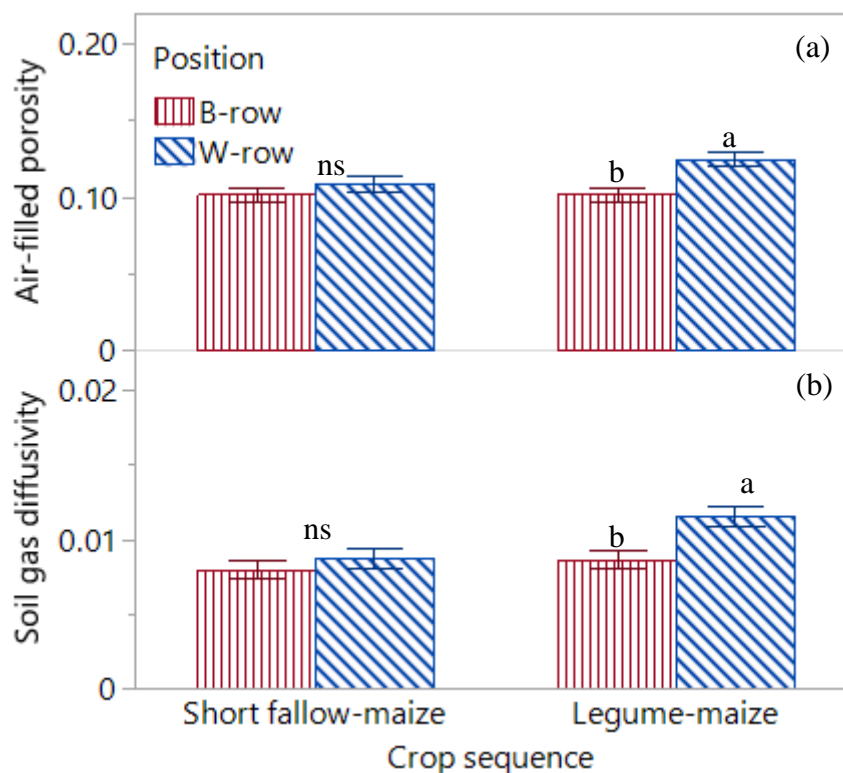


Fig. 1: Air-filled porosity (a) ($\epsilon, \text{cm}^3 \text{ cm}^{-3}$) and relative soil gas diffusivity (b) (D_s/D_0) for different crop sequences (FM, short fallow-maize; LM, legume-maize) and positions (B-row, between crop rows; W-row, within crop rows). Error bars show the standard error. Different letters indicate the significant difference between treatments; ns, non-significant.

Air-filled porosity was significantly affected by tillage ($p < 0.0001$), crop sequence ($p < 0.009$), position ($p < 0.0001$), and SWMP ($p < 0.0001$) (Table 1). IT had higher air-filled porosity ($0.129 \text{ cm}^3 \text{ cm}^{-3}$) than NT ($0.088 \text{ cm}^3 \text{ cm}^{-3}$). The interaction between crop sequence and position significantly affected air-filled porosity ($p < 0.006$). In LM, air-filled porosity was higher at W-row than at B-row (Fig. 1a).

Macroporosity ($> 30 \mu\text{m}$) was significantly affected by tillage ($p < 0.0001$), crop sequence ($p < 0.044$) and position ($p < 0.023$) whilst, microporosity ($< 30 \mu\text{m}$) was only affected by crop sequence ($p < 0.040$) (Tables 1 and 2; and Fig. 2ace). IT had greater macroporosity ($0.130 \text{ cm}^3 \text{ cm}^{-3}$) compared to NT ($0.080 \text{ cm}^3 \text{ cm}^{-3}$) and no significant difference was observed for microporosity (0.063 vs. $0.055 \text{ cm}^3 \text{ cm}^{-3}$ for IT and NT, respectively). LM had greater macroporosity ($0.120 \text{ cm}^3 \text{ cm}^{-3}$) than FM ($0.099 \text{ cm}^3 \text{ cm}^{-3}$) but lower microporosity (0.055 vs. $0.063 \text{ cm}^3 \text{ cm}^{-3}$ for LM and FM, respectively). W-row had greater macroporosity ($0.114 \text{ cm}^3 \text{ cm}^{-3}$) than B-row ($0.097 \text{ cm}^3 \text{ cm}^{-3}$) and a non-significant difference was observed for microporosity (0.060 and $0.058 \text{ cm}^3 \text{ cm}^{-3}$ for B-row and W-row, respectively). No significant interactions were observed among tillage, crop sequence and position (Table 1).

Table 2: Means comparisons of soil bulk density (ρ_b , g cm^{-3}), relative gas diffusivity (D_s/D_o), total porosity (θ , $\text{cm}^3 \text{ cm}^{-3}$), macroporosity (θ_{ma} , $>30 \mu\text{m}$), microporosity (θ_{mi} , $<30 \mu\text{m}$), air-filled porosity (ϵ , $\text{cm}^3 \text{ cm}^{-3}$) and pore continuity for two different tillage systems (IT, intensive tillage; NT, no-tillage), and two crop sequences (FM, short fallow-maize; LM, legume-maize), two positions (B-row, between crop rows; W-row, within crop row) and five different soil water matric potentials (SWMP: -10, -50, -100, -333, -1000 $\text{cm H}_2\text{O}$).

Factors	Levels	ρ_b (g cm^{-3})	D_s/D_o	θ (cm^3 cm^{-3})	θ_{ma} (cm^3 cm^{-3})	θ_{mi} (cm^3 cm^{-3})	ϵ (cm^3 cm^{-3})	Pore Continuity
Tillage	IT	1.48 b	0.001 a	0.44 a	0.13 a	0.06 a	0.13 a	0.26 b
	NT	1.53 a	0.009 a	0.42 b	0.08 b	0.06 a	0.09 b	0.33 a
Crop sequence	FM	1.52 a	0.008 b	0.43 a	0.01 b	0.06 a	0.11 b	0.29 b
	LM	1.50 a	0.010 a	0.43 a	0.12 a	0.06 b	0.11 a	0.30 a
Position	B-row	1.53 a	0.008 b	0.42 a	0.01 b	0.06 a	0.10 b	0.31 a
	W-row	1.48 b	0.010 a	0.44 b	0.11 a	0.06 a	0.12 a	0.30 a
SWMP (-cm H_2O)	1000		0.019 a				0.17 a	0.34 a
	333		0.012 b				0.14 b	0.30 b
	100		0.007 c				0.11 c	0.30 b
	50		0.005 d				0.09 d	0.27 c
	10		0.003 e				0.05 e	0.26 d

Different letters within the columns indicate significant differences between means at $p < 0.05$.

IT had higher air-filled porosity than NT, both in LM and FM, except after sowing and harvesting legumes (2018-19) (Fig. 3). The trend showed higher air-filled porosity in IT after tillage (AT, FM), after sowing legume (ASL, LM) and after planting maize (APM, FM and LM); then the difference decreased after harvesting or chopping legume (AHL or ACL, LM) and after harvesting maize (AHM, FM and LM).

3.3 Relative gas diffusivity

There was no significant difference ($p > 0.05$) between IT and NT on D_s/D_o (Table 1), but it was slightly higher in IT (0.0099) than in NT (0.0086) (Table 2). D_s/D_o was significantly affected ($p < 0.0001$) by crop sequence, position and SMWP (Table 1). A significant interaction ($p < 0.008$) between crop sequence and position was also found (Table 1). Soil gas diffusivity was higher in W-row than in B-row, and the difference was significantly greater in LM compared to FM (Fig. 1b).

A consistent trend of soil gas diffusivity was observed over time in FM, whereas a non-consistent trend was observed over time in LM (Fig. 4). In 2018-19, ASL and AHL showed higher gas diffusivity, whilst APM and AHM showed lower gas diffusivity. In contrast, in 2019-20, the opposite results were observed. There were no differences in gas diffusivity between IT and NT over time, both in FM and LM, except for AT (FM) and AHM (LM) in 2019-20.

3.4 Pore continuity

Statistically, significant effects of tillage ($p < 0.0001$), crop sequences ($p < 0.037$) and SWMP ($p < 0.0001$) on pore continuity were found but no significant difference was observed for position (Table 1). Pore continuity was greater in LM than FM (0.299 and 0.290, respectively) (Table 2). A significant ($p < 0.0006$) interaction between tillage and SWMP was observed for pore continuity (Table 1). NT showed higher pore continuity compared to IT.

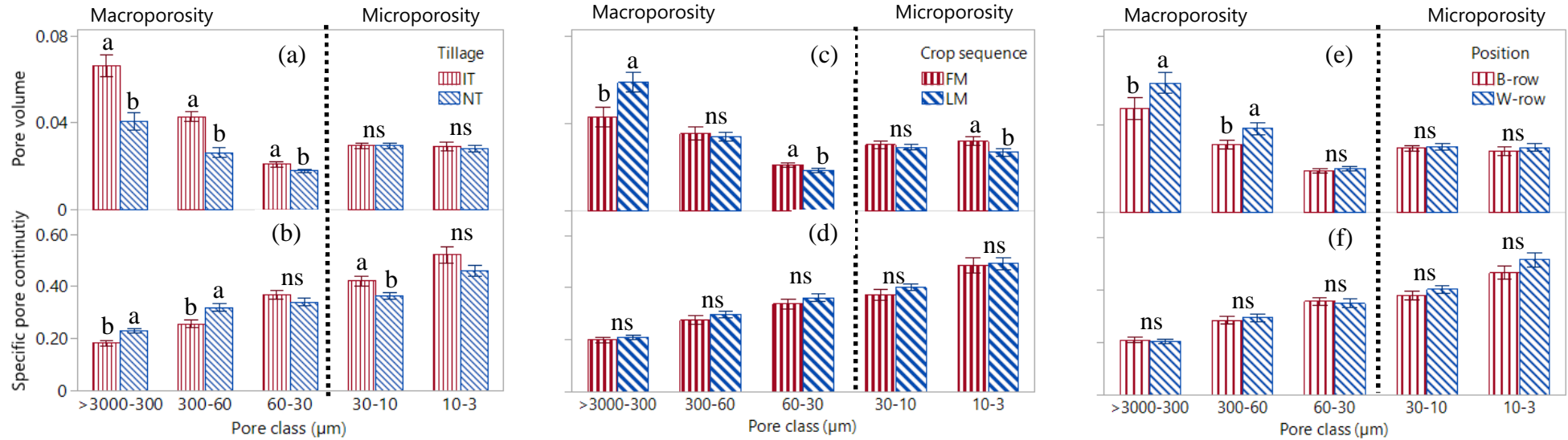


Fig. 2: Pore volume ($\text{cm}^3 \text{cm}^{-3}$) and specific pore continuity for each pore size class in soils under different tillage systems (a and b), crop sequence (c and d) and position (e and f). Error bars show the standard error. Different letters indicate significant differences between treatments; ns, non-significant. Vertical dashed line separates macroporosity ($> 30 \mu\text{m}$) and microporosity ($< 30 \mu\text{m}$).

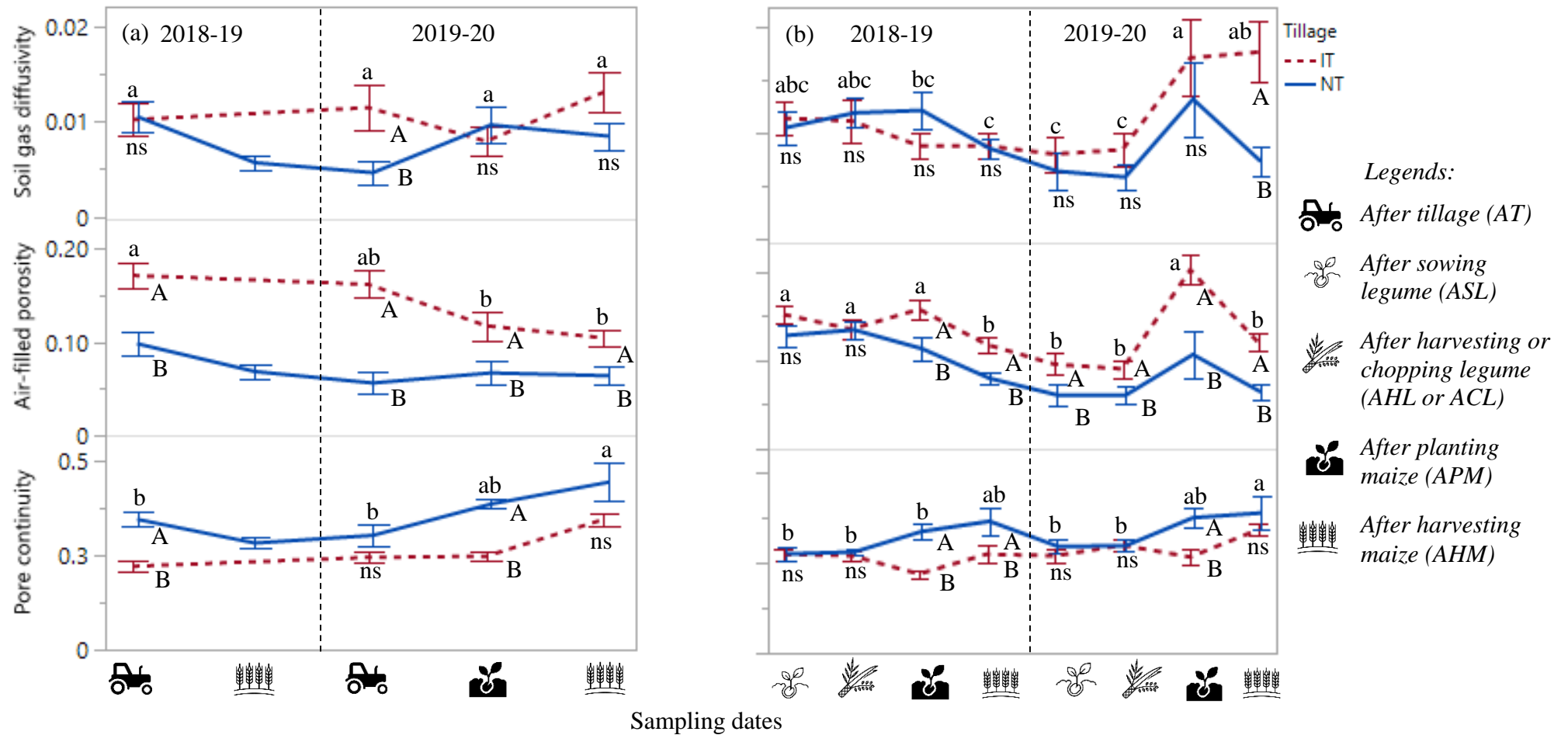


Fig. 3: Relative soil gas diffusivity (D_s/D_o), air-filled porosity (ϵ , $\text{cm}^3 \text{cm}^{-3}$) and pore continuity under different tillage systems (IT, intensive tillage; NT, no-tillage) and sampling dates in short fallow-maize (a) and legume-maize (b) crop sequences. Error bars show the standard error. Different letters (lowercase letters among sampling dates and uppercase letters between tillage systems within each sampling dates) indicate the significant differences between treatments; ns, non-significant. Vertical dashed line separates the 2018-19 and 2019-20 crop seasons.

The difference was greater at higher SWMP (-10 cm H₂O) but as SWMP declined, it became reduced. No significant difference was found at the lowest SWMP (-333 and -1000 cm H₂O) (Fig. 4).

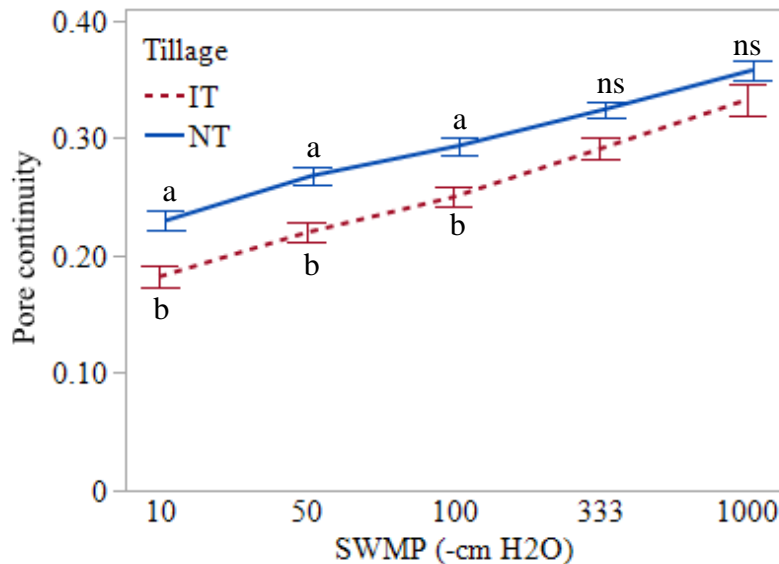


Fig. 4: Pore continuity as a function of soil water matric potential (SWMP) and tillage system (IT, intensive tillage; NT, no-tillage). Error bars show the standard error. Different letters indicate significant differences between treatments for a given SWMP (-10, -50, -100, -333, -1000 cm H₂O); ns, non-significant.

Specific pore continuity was significantly affected by tillage ($p < 0.001$) but not by crop sequence and position (Table 1). In the NT system, macropores ($> 30 \mu\text{m}$) had higher specific pore continuity than IT but the opposite result was observed for micropores ($< 30 \mu\text{m}$). Micropores had higher specific pore continuity under IT than NT (Fig. 2bdf).

An increasing trend was observed for pore continuity with time both in FM and LM (Fig. 3). NT had similar or higher pore continuity than IT regardless of crop sequence. The difference between IT and NT was greater at AT (FM) and APM (FM and LM) and then it decreased at AHM (FM and LM).

3.5 Relative soil gas diffusivity as a function of air-filled porosity

Soil gas diffusivity showed a strong linear (log-log) relationship with air-filled porosity when they were plotted for different crop sequences and tillage systems and the gas

diffusivity increased with increasing air-filled porosity. Table 3 represents the estimated parameters of the regression analysis for two different crop sequences and tillage systems. The slopes (N) and intercepts ($\log M$) of the regression lines differed statistically ($p < 0.001$) between crop sequences and were both higher under LM than under FM, independently of tillage systems. While the slopes (N) and intercepts ($\log M$) of the regression lines differed statistically ($p < 0.0001$) between tillage systems, these were both higher under NT than under IT, independently of crop sequence. Gas diffusivity was below the critical level (0.005) in both crop sequences at -10 cm H₂O SWMP (Fig. 5). FM was also remained below the critical level at -50 cm H₂O SWMP, whereas LM was not, regardless of tillage systems. Under NT system (Fig. 5b), both LM and FM exceed the critical limit of gas diffusivity when it had 0.07 cm³ cm⁻³ air-filled porosity. On the contrary, IT exceeds the critical limit of gas diffusivity at 0.11 cm³ cm⁻³ air-filled porosity (Fig. 5a).

Table 3: Slope (N) and intercept ($\log M$) of the log (soil gas diffusivity) vs. log (air-filled porosity) relationship for two different tillage systems (IT, intensive tillage; NT, no-tillage), and two crop sequences (FM, short fallow-maize; LM, legume-maize).

Tillage system	FM		LM	
	Log M	N	Log M	N
IT	-1.49 b B	0.64 b B	-1.22 a B	0.84 a B
NT	-1.26 b A	1.01 b A	-1.05 a A	1.21 a A

For a given regression parameter different letters within the row (lowercase) and column (uppercase) indicate significant differences at $p < 0.05$.

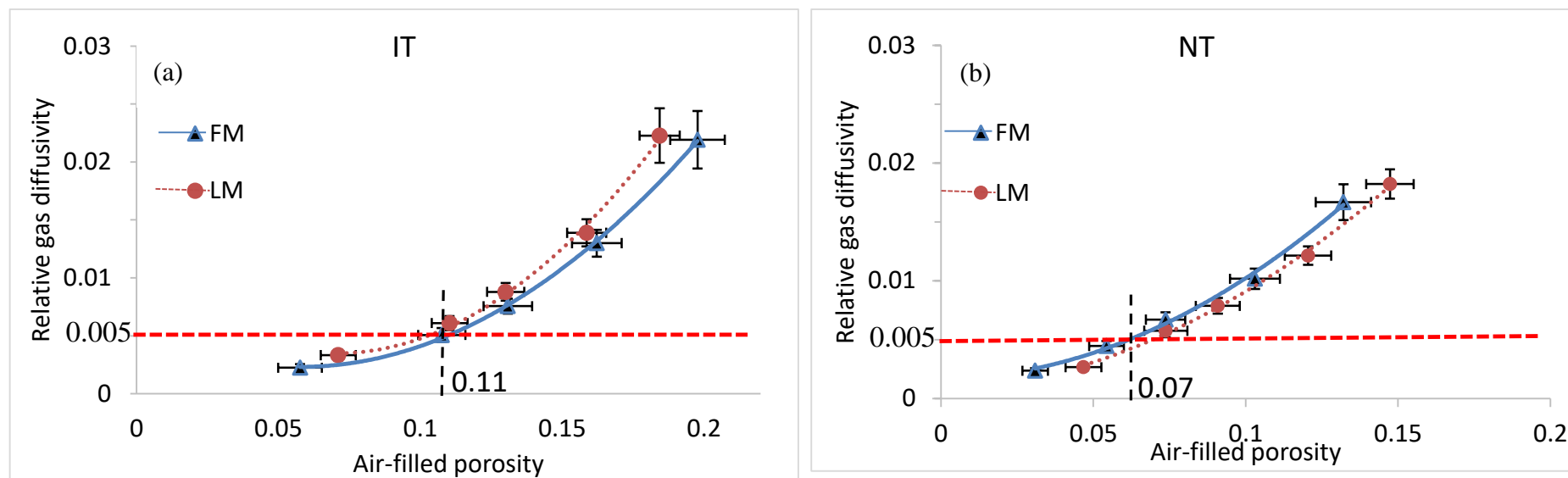


Fig. 5: Relative soil gas diffusivity as a function of air-filled porosity for two different tillage systems (IT, intensive tillage; NT, no-tillage) and two crop sequences (FM, short fallow-maize; LM, legume-maize) at five soil water matric potentials (-10, -50, -100, -333 and -1000 cm H₂O). Horizontal dashed lines indicate critical levels (0.005) of relative gas diffusivity. Vertical dashed lines indicate the volume of air-filled porosity (cm³ cm⁻³) required to exceed the critical limit of gas diffusivity through soils.

4. Discussion

4.1 Crop sequences effects

Crop sequence affected the soil gas diffusivity ($p < 0.0001$), air-filled porosity ($p < 0.009$), macroporosity ($p < 0.04$), microporosity ($p < 0.04$) and pore continuity ($p < 0.037$) (Table 1). FM had lower air-filled porosity than LM (0.105 vs. 0.113 $\text{cm}^3 \text{cm}^{-3}$), macroporosity (0.099 vs. 0.120 $\text{cm}^3 \text{cm}^{-3}$) and pore continuity (0.290 vs. 0.299) whereas FM had greater microporosity compared to LM (0.063 vs. 0.055 $\text{cm}^3 \text{cm}^{-3}$). Consequently, LM had higher relative gas diffusivity than FM (0.0101 vs. 0.0084). Our findings also matched with the results of Abdollahi et al. (2014), who compared gas transport variables between two crop sequences (cover crop vs. without cover crop) in a long-term tillage and rotation trial under Typic Hapludalf soils (USDA soil classification) at Foulum, Denmark. They found that introducing a fodder radish cover crop before barley cultivation led to increase soil gas diffusivity, air-filled porosity, pore organization, and decreased blocked pores. In contrast, no difference was observed in total soil porosity and bulk density. We also obtained similar results, but there was a trend of decreased bulk density under LM crop sequence (Table 2).

There was a significant interaction between crop sequence and position in the crop row for some variables such as air-filled porosity ($p < 0.006$) and gas diffusivity ($p < 0.008$) (Fig. 1a and b). Higher gas diffusivity and air-filled porosity were found in W-row compared to B-row, especially under the LM crop sequence. Our results are in agreement with the results of Silva et al. (2014), who compared air-filled porosity and gas diffusivity between two positions i.e., the row of crops (W-row) vs. between row of crops (B-row) under long-term no-tillage in a crop sequence trial on a clayey Oxisol in Southern Brazil. They reported that crop rows (W-row) revealed higher gas diffusivity and air-filled porosity than zones between crop rows (B-row). This result may have been caused by the

use of furrow openers (W-row position) at the seeding time, which loosened the soil surface in a specific zone, giving localized tillage. Furthermore, crop roots create channels or preferential pathways, which may contribute to maintaining pore continuity and alleviating the negative impact of compaction; instead, gas diffusivity was enhanced in the W-row positions. The results of this study indicate that legume-maize and W-row position decreased bulk density (Table 2) and increased the volume of pore space, particularly macropores, which promotes aeration.

Consequently, enhanced gas diffusivity was observed at W-row under LM in response to a larger pore space (macropores, $> 30 \mu\text{m}$). Since there was a disturbance at the W-row position by furrow openers, the pore continuity remained unaffected regardless of position. This could be a consequence of crop roots, which alleviate the negative impact of furrow openers (seeding machines) while also maintaining greater air-filled porosity. This study demonstrated that LM would positively affect soil physical quality by increasing air-filled porosity, resulting in higher gas diffusivity. Villarreal et al. (2020) observed that crop sequences such as maize cultivation followed by legume increased pore continuity compared to maize monoculture. Likewise, some other authors observed increased soil physical quality owing to the inclusion of cover crops in crop rotation vs. no cover crops (Chen et al., 2014; Haruna et al., 2018), crop rotation (continuous cropping) over maize monoculture (Malobane et al., 2021).

Moreover, the increase of gas diffusivity with increasing air-filled porosity (dependence of D_s/D_o on ϵ) was reported in many studies (Marshall, 1959; Millington, 1959), and it was the basis for D_s/D_o models (Eq. 4). We found that the relationship between relative soil gas diffusivity and air-filled porosity was influenced by crop sequence both in IT and NT (Table 3 and Fig. 5ab). The slopes of the regression lines (N) were used as an index of pore continuity (Ball et al., 1988; Dörner and Horn, 2006). Both in NT and IT, we

found that LM had significantly ($p < 0.001$) higher slope than FM, suggesting that LM increased pore continuity compared to FM (Abdollahi et al., 2014). According to Grable and Siemer, (1968), the critical value of gas diffusivity below which plant root growth is affected was 0.005. We found that LM exceeded the critical limit (0.005) of gas diffusivity at -50 cm H₂O SWMP whereas only at -10 cm H₂O SWMP for FM, regardless of the tillage system (Fig. 5ab). This finding implies that in FM soils, poor aeration may considerably restrict root growth, whereas in LM soils, this was not the case (Abdollahi and Munkholm, 2017). Besides this, higher pore continuity and well-developed pore organization are also indicators of better-structured soils under LM than under FM (Abdollahi et al., 2014; Villarreal et al., 2020).

4.2 Tillage effects

A significant effect of tillage on total porosity, air-filled porosity, macroporosity, pore continuity and specific pore continuity was found, and a tendency to higher soil gas diffusivity was observed on IT (Table 2). These results are consistent with the results of several authors (Eden et al., 2011; Jabro et al., 2012; Martínez et al., 2016; Piccoli et al., 2017).

Total porosity ($p < 0.012$), air-filled porosity ($p < 0.0001$) and macroporosity ($p < 0.0001$) were significantly greater in IT than NT (total porosity: 0.44 vs. 0.42 cm³ cm⁻³; air-filled porosity: 0.129 vs. 0.088 cm³ cm⁻³, macroporosity: 0.130 cm³ cm⁻³ vs. 0.080 cm³ cm⁻³) because tillage loosened the soil and decreased the soil bulk density compared to undisturbed soils (NT) (Jabro et al., 2012; Martínez et al., 2016). When soil porosity decreases, the volume of pores available for gas transport decreases, leading to a reduction in gas diffusion through the soil. Then, soil pore space, and more specifically, air-filled porosity controls gas diffusivity into soils (Rolston and Moldrup, 2002; Troeh et al., 1982). In this study, gas diffusivity was not significantly higher in IT compared to NT,

but it had a lower bulk density and greater total porosity, resulting in more air-filled porosity and macroporosity than NT, as found in other studies (Eden et al., 2011; Piccoli et al., 2017).

However, soil pore continuity was significantly greater (21%) under NT compared to IT (0.329 and 0.261, respectively). Besides this, a significant interaction effect between tillage systems and SWMP was observed (Fig. 4). At higher SWMP (-10 to -333 cm H₂O), NT maintained higher pore continuity, whereas no difference was found between NT and IT at lower SWMP (-1000 cm H₂O). Similarly, specific pore continuity was greater under NT among macropores than IT although macroporosity was lower (Fig. 2ab). Further, regardless of crop sequence, NT showed higher value of slopes (N) (Table 3), and exceeded the critical limit of gas diffusivity at 0.07 cm³ cm⁻³ air-filled porosity (Fig. 5ab). The results suggest that long-term NT (less disturbance) leads to increased pore continuity, particularly in macropores (> 30 μm) (Arthur et al., 2013; Galdos et al., 2019). Macropores allow greater gas movements than micropores, therefore greater gas diffusion occurs in macropores, which are also required for root growth. As a result, macropores are expected to be potentially aerated and have higher oxygen concentrations, whereas micropores are likely to be less aerated. This phenomenon is not caused by a larger air-filled pore volume but by the higher continuity of macropores compared to micropores. Moreover, the greater N value indicated that soils under NT had a higher degree of pore continuity than soils under IT, and NT exceeded the critical limit of soil gas diffusivity with a reduced number of air-filled porosity in which all pores were not isolated and actively participated in gas diffusivity. Lower N value in IT, on the other hand, imply more tortuous pores, and IT exceeded the critical limit of soil gas diffusivity with a higher number of air-filled porosity due to progressively blocked or isolated pores (Eden et al., 2011; Galdos et al., 2019; Kreba et al., 2017). Nevertheless, higher bulk density, on the

other hand, contributes to the development of well-connected pathways and decreases tortuous pores, resulting in increased gas diffusivity under NT (Eden et al., 2012).

4.3 Temporal changes and recovery

The effect of time on soil physical properties i.e., air-filled porosity and pore continuity was significant ($p < 0.0001$) in both crop sequences, but not for gas diffusivity (Table S2). Regardless of crop sequences, greater changes were observed in air-filled porosity and pore continuity from 2018-19 to 2019-20, and these were found greater between different sampling dates, particularly after tillage (AT, FM), after planting and harvesting maize (APM and AHM) (Fig. 3). This implies that, depending on the date of sampling and tillage practice, changes in air-filled porosity and pore continuity may occur both in LM and FM.

In general, IT showed greater temporal changes in air-filled porosity and pore continuity than NT, especially after tillage operations in both crop sequences (AT or APM) (Fig. 3). As expected, IT had higher air-filled porosity and lower pore continuity because soil disturbance by tillage increases air-filled porosity and decreases pore continuity. Later on, air-filled porosity under IT decreased due to settling processes induced by rainfall or irrigation events, while in NT remained unchanged because the soil was more stable and remained undisturbed. However, an increase in pore continuity, notably after harvesting maize (FM and LM) was also observed under IT, indicating that natural recovery by plant root growth may occur, which was the most likely responsible process for this improvement. Besides this, IT showed similar values of pore continuity to NT under the legume crop (after sowing and harvesting legume), both in 2018-19 and 2019-20. That could be explained by a quicker restoration of pore continuity by legume roots than by maize.

Temporal changes in soil physical properties have been widely investigated by several authors considering tillage and compaction (Hu et al., 2018), crop sequence (Villarreal et al., 2020), cropping season (Frene et al., 2020), tillage and residue retention (Alskaf et al., 2021), tillage and cover crops (Haruna et al., 2018) etc. In the Mediterranean region, where lands were transformed from rainfed to irrigated and a second crop was introduced into the crop sequence, intensified soil and crop management activities such as tillage operation, planting, and harvesting, potentially triggering temporal alterations. Our findings agreed with those of Haruna et al., (2018), who reported that IT changed the soil physical properties for a short period i.e., air-filled porosity and pore continuity, but these effects may not be persistent over a long time. On the other hand, the inclusion of legumes in the crop sequence restores pore continuity more quickly under IT than by maize, which may persist for a longer time. Our study indicates that temporal changes produced by tillage are substantially recovered during crop development. This finding also highlights the importance of including short-term changes in soil gas transport variables when modelling soil crop systems.

5. Conclusions

Introducing a legume before the maize increases soil air-filled porosity and macroporosity and produces a more continuous porous system, which increases soil gas diffusivity (better soil aeration). This can alleviate the negative effect of intensive tillage by maintaining pore continuity and reducing tillage requirements by providing increased aeration under no-tillage systems. Soil gas diffusivity, air-filled porosity and macroporosity were higher within the row of crops than between rows of crops. This should be considered when measuring soil gas emissions, as within crop row emissions can eventually be more important than between crop rows ones. Long-term no-tillage, although increases soil bulk density, reduces air-filled porosity and macroporosity,

increases pore continuity among macropores as well as reduces blocked pores avoiding deleterious effects on gas diffusivity. No-tillage creates a continuous and stable pore organization system, which is one of the driving factors in gas transport through soils. Temporal changes in air-filled porosity due to tillage operations gradually decrease over time under IT because settlement occurs due to rain and irrigation, whereas pore continuity recovers from planting to harvesting crops by crop roots. Further studies are needed to confirm the effects of long-term legume-maize on soil physical quality.

Acknowledgements

The authors thank the support given by Dr. Stefan Fenner, the visiting PhD candidate Mehrdad Soranj, Prof. Concha Ramos, the field and laboratory technicians Carlos Cortés and Silvia Martí, and the farmer Xavier Penella. The authors gratefully acknowledge support for this research from the Research Spanish Agency (DISOSMED Project-AGL2017-84529-C3-R). Rasendra Talukder also sincerely acknowledges the fund provided by University of Lleida to support PhD fellowship. Daniel Plaza-Bonilla is a Ramón y Cajal fellow (RYC-2018-024536-I) co-funded by AEI-MICIU and European Social Fund.

References

- Abdollahi, L., Munkholm, L.J., 2017. Eleven Years' Effect of Conservation Practices for Temperate Sandy Loams: II. Soil Pore Characteristics. *Soil Sci. Soc. Am. J.* 81, 392–403. <https://doi.org/10.2136/sssaj2016.07.0221>
- Abdollahi, L., Munkholm, L.J., Garbout, A., 2014. Tillage System and Cover Crop Effects on Soil Quality: II. Pore Characteristics. *Soil Sci. Soc. Am. J.* 78, 271–279. <https://doi.org/10.2136/sssaj2013.07.0302>
- Alskaf, K., Mooney, S.J., Sparkes, D.L., Wilson, P., Sjögersten, S., 2021. Short-term impacts of different tillage practices and plant residue retention on soil physical

- properties and greenhouse gas emissions. *Soil Tillage Res.* 206.
<https://doi.org/10.1016/j.still.2020.104803>
- Angás, P., Lampurlanés, J., Cantero-Martínez, C., 2006. Tillage and N fertilization: Effects on N dynamics and Barley yield under semiarid Mediterranean conditions. *Soil Tillage Res.* 87, 59–71. <https://doi.org/10.1016/j.still.2005.02.036>
- Arthur, E., Moldrup, P., Schjønning, P., de Jonge, L.W., 2013. Water Retention, Gas Transport, and Pore Network Complexity during Short-Term Regeneration of Soil Structure. *Soil Sci. Soc. Am. J.* 77, 1965–1976.
<https://doi.org/10.2136/sssaj2013.07.0270>
- Ball, B.C., 2013. Soil structure and greenhouse gas emissions: a synthesis of 20 years of experimentation. *Eur. J. Soil Sci.* 64, 357–373. <https://doi.org/10.1111/ejss.12013>
- Ball, B.C., O’Sullivan, M.F., Hunter, R., 1988. Gas diffusion, fluid flow and derived pore continuity indices in relation to vehicle traffic and tillage. *J. Soil Sci.* 39, 327–339. <https://doi.org/10.1111/j.1365-2389.1988.tb01219.x>
- Baranian Kabir, E., Bashari, H., Bassiri, M., Mosaddeghi, M.R., 2020. Effects of land-use/cover change on soil hydraulic properties and pore characteristics in a semi-arid region of central Iran. *Soil Tillage Res.* 197, 104478.
<https://doi.org/10.1016/j.still.2019.104478>
- Bell, L.W., Kirkegaard, J.A., Swan, A., Hunt, J.R., Huth, N.I., Fettell, N.A., 2011. Impacts of soil damage by grazing livestock on crop productivity. *Soil Tillage Res.* 113, 19–29. <https://doi.org/10.1016/j.still.2011.02.003>
- Broecker, W.S., Peng, T.-H., 1974. Gas exchange rates between air and sea. *Tellus* 26, 21–35. <https://doi.org/10.3402/tellusa.v26i1-2.9733>
- Cantero-Martínez, C., Angas, P., Lampurlanés, J., 2003. Growth, yield and water productivity of barley (*Hordeum vulgare* L.) affected by tillage and N fertilization

- in Mediterranean semiarid, rainfed conditions of Spain. *F. Crop. Res.* 84, 341–357.
[https://doi.org/10.1016/S0378-4290\(03\)00101-1](https://doi.org/10.1016/S0378-4290(03)00101-1)
- Chen, G., Weil, R.R., Hill, R.L., 2014. Effects of compaction and cover crops on soil least limiting water range and air permeability. *Soil Tillage Res.* 136, 61–69.
<https://doi.org/10.1016/j.still.2013.09.004>
- Currie, J.A., 1960. Gaseous diffusion in porous media Part 1. - A non-steady state method. *Br. J. Appl. Phys.* 11, 314–317. <https://doi.org/10.1088/0508-3443/11/8/302>
- Dörner, J., Horn, R., 2006. Anisotropy of pore functions in structured Stagnic Luvisols in the Weichselian moraine region in N Germany. *J. Plant Nutr. Soil Sci.* 169, 213–220. <https://doi.org/10.1002/jpln.200521844>
- Eden, M., Moldrup, P., Schjønning, P., Scow, K.M., de Jonge, L.W., 2012. Soil-Gas Phase Transport and Structure Parameters for a Soil Under Different Management Regimes and at Two Moisture Levels. *Soil Sci.* 177, 527–534.
<https://doi.org/10.1097/SS.0b013e318267ec85>
- Eden, M., Schjønning, P., Moldrup, P., De Jonge, L.W., 2011. Compaction and rotovation effects on soil pore characteristics of a loamy sand soil with contrasting organic matter content. *Soil Use Manag.* 27, 340–349.
<https://doi.org/10.1111/j.1475-2743.2011.00344.x>
- Ehlers, W., Wendroth, O., and Mol, F. de., 1995. Characterizing pore organization by soil physical parameters, in: Hartge, K.H., Stewart, B.A. (Eds.), *Soil Structure: Its Development and Function*. *Adv. Soil Sci.* CRC Press, Boca Raton, FL, pp. 257–275.
- Federer, W.T., King, F., 2007. *Variations on Split Plot and Split Block Experiment Designs*. John Wiley & Sons, Inc., Hoboken, NJ, USA.

<https://doi.org/10.1002/0470108584>

- Frene, J.P., Gabbarini, L.A., Wall, L.G., 2020. Soil physiology discriminates between no-till agricultural soils with different crop systems on winter season. *Soil Use Manag.* 36, 571–580. <https://doi.org/10.1111/sum.12568>
- Galdos, M.V., Pires, L.F., Cooper, H.V., Calonego, J.C., Rosolem, C.A., Mooney, S.J., 2019. Assessing the long-term effects of zero-tillage on the macroporosity of Brazilian soils using X-ray Computed Tomography. *Geoderma* 337, 1126–1135. <https://doi.org/10.1016/j.geoderma.2018.11.031>
- Grable, A.R., Siemer, E.G., 1968. Effects of Bulk Density, Aggregate Size, and Soil Water Suction on Oxygen Diffusion, Redox Potentials, and Elongation of Corn Roots. *Soil Sci. Soc. Am. J.* 32, 180–186. <https://doi.org/10.2136/sssaj1968.03615995003200020011x>
- Haruna, S.I., Anderson, S.H., Nkongolo, N. V., Zaibon, S., 2018. Soil Hydraulic Properties: Influence of Tillage and Cover Crops. *Pedosphere* 28, 430–442. [https://doi.org/10.1016/S1002-0160\(17\)60387-4](https://doi.org/10.1016/S1002-0160(17)60387-4)
- Holthusen, D., Brandt, A.A., Reichert, J.M., Horn, R., 2018. Soil porosity, permeability and static and dynamic strength parameters under native forest/grassland compared to no-tillage cropping. *Soil Tillage Res.* 177, 113–124. <https://doi.org/10.1016/j.still.2017.12.003>
- Hu, W., Tabley, F., Beare, M., Tregurtha, C., Gillespie, R., Qiu, W., Gosden, P., 2018. Short-Term Dynamics of Soil Physical Properties as Affected by Compaction and Tillage in a Silt Loam Soil. *Vadose Zo. J.* 17, 180115. <https://doi.org/10.2136/vzj2018.06.0115>
- Jabro, J.D., Sainju, U.M., Stevens, W.B., Evans, R.G., 2012. Estimation of CO₂ diffusion coefficient at 0–10 cm depth in undisturbed and tilled soils. *Arch. Agron.*

- Soil Sci. 58, 1–9. <https://doi.org/10.1080/03650340.2010.506482>
- Kreba, S.A., Wendroth, O., Coyne, M.S., Walton, R., 2017. Soil Gas Diffusivity, Air-Filled Porosity, and Pore Continuity: Land Use and Spatial Patterns. *Soil Sci. Soc. Am. J.* 81, 477–489. <https://doi.org/10.2136/sssaj2016.10.0344>
- Malobane, M.E., Nciizah, A.D., Bam, L.C., Mudau, F.N., Wakindiki, I.I.C., 2021. Soil microstructure as affected by tillage, rotation and residue management in a sweet sorghum-based cropping system in soils with low organic carbon content in South Africa. *Soil Tillage Res.* 209, 104972. <https://doi.org/10.1016/j.still.2021.104972>
- Marshall, T.J., 1959. The diffusion of gases through porous media. *J. Soil Sci.* 10, 79–82. <https://doi.org/10.1111/j.1365-2389.1959.tb00667.x>
- Martínez, I., Chervet, A., Weisskopf, P., Sturny, W.G., Rek, J., Keller, T., 2016. Two decades of no-till in the Oberacker long-term field experiment: Part II. Soil porosity and gas transport parameters. *Soil Tillage Res.* 163, 130–140. <https://doi.org/10.1016/j.still.2016.05.020>
- Masís-Meléndez, F., de Jonge, L.W., Chamindu Deepagoda, T.K.K., Tuller, M., Moldrup, P., 2015. Effects of Soil Bulk Density on Gas Transport Parameters and Pore-Network Properties across a Sandy Field Site. *Vadose Zo. J.* 14, vzj2014.09.0128. <https://doi.org/10.2136/vzj2014.09.0128>
- Millington, R.J., 1959. Gas Diffusion in Porous Media. *Science (80-)*. 130, 100–102. <https://doi.org/10.1126/science.130.3367.100-a>
- Moldrup, P., Olesen, T., Komatsu, T., Schjønning, P., Rolston, D.E., 2001. Tortuosity, Diffusivity, and Permeability in the Soil Liquid and Gaseous Phases Tortuosity phenomena of pore space influence the transport of. *Soil Sci. Soc. Am. J.* 65, 613–623.
- Pareja-Sánchez, E., Plaza-Bonilla, D., Ramos, M.C., Lampurlanés, J., Álvaro-Fuentes,

- J., Cantero-Martínez, C., 2017. Long-term no-till as a means to maintain soil surface structure in an agroecosystem transformed into irrigation. *Soil Tillage Res.* 174, 221–230. <https://doi.org/10.1016/j.still.2017.07.012>
- Piccoli, I., Schjønning, P., Lamandé, M., Furlan, L., Morari, F., 2017. Challenges of conservation agriculture practices on silty soils. Effects on soil pore and gas transport characteristics in North-eastern Italy. *Soil Tillage Res.* 172, 12–21. <https://doi.org/10.1016/j.still.2017.05.002>
- Ramos, M.C., Pareja-Sánchez, E., Plaza-Bonilla, D., Cantero-Martínez, C., Lampurlanés, J., 2019. Soil sealing and soil water content under no-tillage and conventional tillage in irrigated corn: Effects on grain yield. *Hydrol. Process.* 33, 2095–2109. <https://doi.org/10.1002/hyp.13457>
- Rolston, D.E., 1986. Gas Diffusivity, in: Klute, A. (Ed.), *Methods of Soil Analysis, Physical and Mineralogical Methods*. SSSA Book Ser. 5. John Wiley & Sons, Ltd, SSSA, Madison, WI., pp. 1089–1102. <https://doi.org/10.2136/sssabookser5.1.2ed.c46>
- Rolston, D.E., Moldrup, P., 2002. 4.3 Gas Diffusivity, in: Dane, J.H., Topp, G.C. (Eds.), *Methods of Soil Analysis, Physical Methods*. SSSA Book Ser. 5. John Wiley & Sons, Ltd, SSSA, Madison, WI., pp. 1113–1139. <https://doi.org/10.2136/sssabookser5.4.c45>
- Silva, A.P. da, Ball, B.C., Tormena, C.A., Giarola, N.F.B., Guimarães, R.M.L., 2014. Soil structure and greenhouse gas production differences between row and interrow positions under no-tillage. *Sci. Agric.* 71, 157–162. <https://doi.org/10.1590/S0103-90162014000200011>
- Slama, F., Zemni, N., Bouksila, F., De Mascellis, R., Bouhlila, R., 2019. Modelling the impact on root water uptake and solute return flow of different drip irrigation

regimes with brackish water. *Water (Switzerland)* 11, 425.

<https://doi.org/10.3390/w11030425>

Soil Survey Staff, 2014. *Keys to Soil Taxonomy*, 12th ed. ed. USDA-Natural Resources Conservation Service, Washington, DC.

Troeh, F.R., Jabro, J.D., Kirkham, D., 1982. Gaseous diffusion equations for porous materials. *Geoderma* 27, 239–253. [https://doi.org/10.1016/0016-7061\(82\)90033-7](https://doi.org/10.1016/0016-7061(82)90033-7)

Villarreal, R., Lozano, L.A., Salazar, M.P., Bellora, G.L., Melani, E.M., Polich, N., Soracco, C.G., 2020. Pore system configuration and hydraulic properties.

Temporal variation during the crop cycle in different soil types of Argentinean Pampas Region. *Soil Tillage Res.* 198, 104528.

<https://doi.org/10.1016/j.still.2019.104528>

Supplementary Tables

Table S1: Date of tillage, sowing or planting, chopping or harvesting, and undisturbed soil sampling for 2018-19 to 2019-20.

Date	Tillage, sowing or planting and harvesting operation	Undisturbed soil sampling	From last tillage performed		
			Days	Rainfall (mm)	Irrigation (mm)
Period: 2018-19					
19 Oct. 2018		Before tillage (Initial)			
26 Oct. 2018	Till: IT plots (FM and LM) Sowing: legume (Peas, LM)				
21 Dec. 2018		After sowing legume when soil was consolidated (LM)	56	107	0
03 Apr. 2019		After tillage when soil was consolidated (FM)	159	125	27
12 Apr. 2019	Planting: long cycle maize (FM)				
18 June 2019	Harvesting: Legume (Peas, LM) Till: IT plots (LM)	After harvesting legume	234	204	127
27 June 2019	Planting: short cycle maize (LM)				
02 Aug. 2019		After planting maize when soil was consolidated (LM)	45	39	281
14 Oct. 2019	Harvesting: long cycle maize (FM)				
15 Oct. 2019		After harvesting maize, only NT plots (FM)	354	280	758
19 Nov. 2019	Harvesting: short cycle maize (LM)	After harvesting maize	155	167	360
Period: 2019-20					
18 Dec. 2019	Till: IT plots (FM and LM)				
10 Jan. 2020	Sowing: legume (Vetch, LM)				
28 Feb. 2020		After tillage when soil was consolidated (FM) After sowing legume when soil was consolidated (LM)	72	50	0
01 May 2020	Till: IT plots (FM)		136	198	0

02 May 2020	Planting: long cycle maize (FM)				
21 May 2020	Chopping: Legume (Vetch, LM) Till: IT plots (LM)	After chopping legume (ACL)	155	239	0
28 May 2020	Planting: short cycle maize (LM)				
06 June 2020		After planting maize when soil was consolidated (FM)	36	75	2
01 July 2020		After planting maize when soil was consolidated (LM)	41	58	46
23 Sep. 2020	Harvesting: long cycle maize (FM)				
21 Oct. 2020	Harvesting: short cycle maize (LM)	After harvesting maize (FM and LM)	153	321	582

Table S2: Analysis of variance (p-values) of relative soil gas diffusivity (D_s/D_o), air-filled porosity (ϵ , $\text{cm}^3 \text{cm}^{-3}$), and pore continuity affected by sampling dates and tillage systems and their interactions in two different crop sequences (FM: short fallow-maize; LM: legume-maize).

Source of variation	D_s/D_o	ϵ ($\text{cm}^3 \text{cm}^{-3}$)	Pore Continuity [‡]
Short fallow-maize (FM)			
Sampling date	NS	<0.0001	<0.0001
Tillage	NS	<0.0001	<0.0001
Sampling date *Tillage	NS	NS	0.03
Legume-maize (LM)			
Sampling date	NS	<0.0001	<0.0001
Tillage	0.03	<0.0001	<0.0001
Sampling date *Tillage	0.004	0.03	0.002

[‡], data were BoxCox-transformed before analysis
NS, non-significant ($p > 0.05$).

Chapter II

Soil hydraulic properties and pore dynamics under different tillage and maize-based crop sequence in an irrigated Mediterranean area

Submitted: Geoderma

Soil hydraulic properties and pore dynamics under different tillage and maize-based crop sequence in an irrigated Mediterranean area

Rasendra Talukder^{*a}, Daniel Plaza-Bonilla^b, Carlos Cantero-Martínez^{bc}, Ole Wendroth^d,
Jorge Lampurlanés^{ac}

^aDepartment of Agricultural and Forest Engineering - Agrotecnio-CERCA Center,
University of Lleida, Av. Rovira Roure 191, 25198 Lleida, Spain

^bDepartment of Crop and Forest Sciences - Agrotecnio-CERCA Center, University of
Lleida, Av. Rovira Roure 191, 25198 Lleida, Spain

^cAssociate Unit CSIC (Research Spanish Council), Spain

^dDepartment of Plant and Soil Science, University of Kentucky, North
Lexington, KY 40546-0091, United States

* Corresponding author: rasendra.talukder@udl.cat

Abstract

Soil hydraulic properties and pore continuity are important parameters of soil quality and may differ among tillage systems, crop rotations, and change over time. However, there are some contrasting results, depending on soil type, climate and cultivation history on the spatial and temporal variations. The objective of this study was to determine spatio-temporal dynamics of soil hydraulic properties and pore characteristics (i.e., pore volume, effective porosity and continuity) on a silt loam long-term tillage field experiment (~25 years), in Agramunt, NE Spain, during two cropping years (2018-19 and 2019-20). Undisturbed soil samples were used to determine soil water retention, $\theta(\Psi)$, and soil hydraulic conductivity, $K(\Psi)$, curves in two different tillage systems (intensive tillage, IT vs. no-tillage, NT), two crop sequences (short fallow-maize, FM vs. legume-maize, LM) and two positions (within the row of crops, W-row vs. between the rows of crops, B-row).

The results revealed that LM had greater specific hydraulic conductivity, K_{pc} (16.6 vs. 12.9 cm day⁻¹) in its macroporosity (> 1000 μm) than FM due to greater number of effective pores, N_{pc} (m⁻²) and effective porosity, ε_{pc} (cm³ cm⁻³). Soil water content, θ (cm³ cm⁻³) was greater under IT than under NT at higher soil water matric potential, Ψ (0, - 1 and -3 cm H₂O), whilst the opposite was observed at lower Ψ (- 50, - 100, - 300 and -1000 cm H₂O). Long-term NT showed greater hydraulic conductivity, K (cm day⁻¹) at higher Ψ (0, - 1, - 3 and - 10 cm H₂O) than IT, and no difference at lower Ψ . Although IT had greater pore volume, ϕ_{pc} (cm³ cm⁻³) than NT in the macroporosity and coarse mesoporosity (1000-60 μm) pore size classes, NT had two times greater K_{pc} than IT due to increased N_{pc} , ε_{pc} , and pore continuity, C_{wpc} . $K(\Psi)$ and pore characteristics showed spatial variations (W-row vs. B-row). W-row had significantly greater $K(\Psi)$ at higher Ψ (0, - 1 and - 3 cm H₂O) than B-row. Similarly, greater K_{pc} of macroporosity and coarse mesoporosity were observed due to increased N_{pc} , ε_{pc} and C_{wpc} of that pore classes, although W-row and B-row had similar ϕ_{pc} . Temporal dynamics of soil hydraulic properties and pore characteristics were not evident under IT during crop succession. This study shows that LM increases specific hydraulic conductivity of soil macroporosity by increasing the number of effective macropores and the effective porosity. In a Mediterranean climate, this may improve the hydrological functions of agricultural soil and associated crop yield. Further, long-term NT formed a stable number of effective macropores and coarse mesopores, and showed a greater pore continuity in coarse and fine mesopores, resulting in improved soil water flux.

Keywords: Conservation agriculture, Long-term no-tillage, Crop diversification, Macroporosity, Spatio-temporal variation, Preferential flow

1. Introduction

Climate change, declining topsoil fertility, and soil degradation induced by inappropriate agricultural management pose threats to crop productivity, soil quality, and environmental sustainability. Climate-resilient and sustainable agricultural management practices can improve soil hydraulic conductivity and water retention in the soil, particularly at the soil-root zone, which are key indicators of soil quality and environmental sustainability, and hence contribute to improve crop productivity and lower water loss (Lal, 2015). Soil physical quality parameters, viz., soil structure, number of pores, and their connectivity and continuity are affected by agricultural management practices such as tillage and crop diversification (Gabriel et al., 2019; Nouri et al., 2019; Kabir et al., 2020; Silva et al., 2021). Changes in soil structure and pore configuration, may not always be evident immediately after the implementation of management practices (Nouri et al., 2019; Silva et al., 2021). This emphasizes the significance of short-term and long-term studies that reveal the full consequences of agricultural management practices for the functionality of the soil pore system.

Tillage is often considered an important factor that affects the hydraulic conductivity and water retention of soils but the magnitude and the direction of its effect depends on soil type, climate and cultivation history (Alvarez et al., 2014; Kargas et al., 2016; Galdos et al., 2019; Kreiselmeier et al., 2019; Silva et al., 2021). For instance, a study by Villarreal et al. (2020) reported that IT increases soil hydraulic conductivity and number of effective macropores compared to NT in Argentinian loam and sandy loam soils under maize-soybean crop rotation for 15 years. On the contrary, in silty loam soils under maize-wheat/soybean crop rotation for 34 years, no difference was found between IT and NT on these properties.

Besides tillage management, inclusion of legume as cover crops in the crop sequence before main crops are encouraged to sustain the agricultural production and to maintain the soil quality (Sánchez-Navarro et al., 2019). For example, barley cover cropping before main crop i.e., maize in a semiarid silty clay soil improved soil structure stability and porosity, increased soil water retention and reduced drainage loss (Gabriel et al., 2019). Alvarez et al. (2014) reported that soybean mono-culture under NT in Argentinian silt loam soil increased soil compaction. Further, maintaining the soil cropped all year around (single or multiple crops) reduces soil erosion, enhances water infiltration, retains soil moisture and ultimately improves the soil physical properties (Silva et al., 2021). In addition, crops with greater root length density such as legumes, compared with oilseeds (Liu et al., 2011), help to enhance connectivity and continuity of soil pores which increases preferential flow of water and solute transport (Liu et al., 2016; Zhang et al., 2017). Both tillage and crop sequence used directly affect number and volume of soil pores and their continuity, thus regulating various soil-plant-atmosphere relations which are responsible for plant growth and development such as soil water flux and aeration, transport of solutes and dynamics of organic matter and nutrients. Apart from that, soil hydraulic properties are subjected to spatio-temporal dynamics due to difference in soil management, and measurement scales. Seeding or row planting may improve the stability of surrounding aggregates due to plant root growth within rows (W-row) as compared to between crop rows (B-row). In this context, the position of measurements (W-row vs. B-row) would be taken into consideration while assessing the soil hydraulic characteristics. For instance, Alagna et al. (2019) reported spatial variability of saturated soil hydraulic conductivity W-row and B-row of Faba bean (*Vicia faba* L. var. minor) due to soil crust, tillage and vegetation cover on a loam soil under rain-fed Mediterranean condition. They found that soil W-row had twice ponded infiltration rate than B-row. Further, temporal

changes of soil hydraulic properties caused by management practices were documented by several authors (Kargas et al., 2016; Hu et al., 2018; Kreiselmeier et al., 2019; Vanderlinden et al., 2021) but very few studies considered dynamics of soil hydraulic properties together with pore system characteristics (Kabir et al., 2020; Villarreal et al., 2020). For example, Villarreal et al. (2020) observed that under maize-legume crop rotation, intensive tillage demonstrated higher hydraulic conductivity and water conducting macroporosity than no-tillage due to biological activity during the crop vegetative phase in a loam soil.

Changes of soil attributes particularly, soil hydraulic conductivity, $K(\Psi)$ and soil water retention, $\theta(\Psi)$ by tillage and crop sequence can be understood through the evaluation of soil pore characteristics. $K(\Psi)$ is highly dynamic and controlled by the number of effective soil macropores and their continuity. For instance, Kabir et al. (2020) reported that less than 1% of macropores ($> 1000 \mu\text{m}$) contributed more than 50% of the total water flux regardless of land-use/cover type. Continuous effective pores contribute strongly to water flow and the ratio of their volume to the total soil volume is referred to as effective porosity. Examining effective porosity and number of effective pores per unit area, which are characterized by tortuosity and pore connectivity, can provide insight into the effects of agricultural management, i.e., tillage and crop sequence on soil hydrological processes.

The aim of this work was to determine the spatio-temporal dynamics of soil hydraulic properties and pore system characteristics under various tillage systems, crop sequences and positions in an irrigated Mediterranean area. We hypothesize that temporal dynamics of soil hydraulic properties and soil pore characteristics would vary during the vegetative stage of crop depending on the tillage systems.

2. Materials and Methods

2.1 Experimental site

This study was conducted from 2018-19 to 2019-20 at Agramunt, NE Spain (41°48' N, 1°07' E, 330 m asl) in a long-term tillage experiment established in 1996. The climate of the area is semiarid Mediterranean, with a mean annual precipitation of 401 mm and 14.1 °C mean air temperature. The soil was classified as Typic Xerofluvent (Soil Survey Staff, 2014; equivalent to an Haplic Fluvisol of the WRB) and the upper (0–28 cm) horizon has a silt loam texture (sand, 30.8%; silt, 57.3%; clay, 11.9%). Also, at the start of the experiment (1996), the following physico-chemical properties (upper: 0–28 cm) were observed: pH (H₂O, 1: 2.5): 8.5, electrical conductivity (1:5): 0.15 dS m⁻¹, soil organic carbon concentration 9 g kg⁻¹, P Olsen: 35 mg kg⁻¹; K (Amm. Ac.): 194 mg kg⁻¹; water retention (-33 kPa): 16 kg kg⁻¹; water retention (-1500 kPa): 5 kg kg⁻¹ (Cantero-Martínez et al., 2003).

The experiment was established to compare three tillage systems (intensive tillage: IT, reduced tillage: RT, and no-tillage: NT), and three rates of N mineral fertilizer application (zero, medium and high) under rain-fed conditions cultivated with winter barley (*Hordeum vulgare L.*). Two changes were made to the experiment: (i) in 2015 a solid set of sprinklers was installed to transform the fields from rain-fed to irrigated, and (ii) in 2018 crop sequence was introduced as a factor. Crop sequence had two levels, i.e., the common short-term fallow-maize (FM) practice (winter fallow and summer crop: maize; *Zea mays L.*), and a legume-maize (LM) crop sequence (winter crop: Pea; *Pisum sativum L.* /Vetch; *Vicia sativa L.*, and summer crop: maize; *Zea mays L.*). There was different maturing maize in each crop sequence, namely late and early maturing maize in FM and LM, respectively. The experimental main plot size was 50 m long and 6 m width; and the sub-plot size was 50 m long and 3 m width. In this experiment, two tillage systems (IT

and NT) and two crop sequences (FM and LM) were considered in the plots under medium N fertilization rates. Treatments were replicated three times in a split-split-plot design where tillage was applied to main plots, crop sequence to sub-plots and sampling position as the split-split-plot.

Tillage was practiced twice on IT plots: (i) in autumn at the same time for FM and LM, and (ii) in spring before seeding maize (at different times for FM and LM) (Table S3). In IT plots, autumn tillage consisted of a subsoiler pass (depth: 35 cm) followed by a chisel (depth: 15 cm) (which helped to incorporate residue into the soil nearly 100%) and a roller (to make the surface even) whereas a rototiller (15 cm), followed by a chisel pass and a roller, were used for spring tillage. Direct drilling was performed in NT plots and the same pneumatic row direct drilling machine was used to plant in all tillage systems. The machine had double disk furrow openings to make the slots and rotary residue row cleaners to clear the path for the opening of the row unit. The two crops (legume and maize) were harvested using a combine harvesting machine. After harvesting, the residue was chopped and spread over the surface.

2.2 Soil sampling

We anticipated that changes in soil structure would be more pronounced at the topsoil compared to subsoil because of the direct impact of precipitation or irrigation events into surface and mechanical disturbance due to tillage practice. Therefore, soil samples were taken from the topsoil at a depth of 0.02-0.08 m. The first 0-0.02 m contained a thick crust that was fragile and easily broken during sampling and hence was discarded. A total of thirteen samplings were performed and 288 undisturbed soil samples collected (Table S3). Briefly, the 1st sampling (before the introduction of pea into the crop sequence) was done pre-sowing and data obtained were considered the baseline scenario before splitting plots into sub-plots for each crop sequence. Out of twelve sampling, eight were carried

out in legume-maize (LM) crop sequence, while the other five were carried out in short fallow-maize (FM) crop sequence (Table S3). After sowing and harvesting of each crop, undisturbed soil samples were taken in LM in 2018-19 and 2019-2020. In the case of FM, in 2018-19 two soil samplings were done: after tillage (when soil remained fallow), and after harvesting of maize, whereas in 2019-20, three samplings were done: after tillage (when soil was left fallow), after sowing, and after harvesting of maize. In each sampling, six undisturbed soil samples were collected in each sub-plot, three within the row (W-row) and three between rows (B-row) of crop, except in the last sampling, after harvesting of maize, when only four samples per sub-plot were taken. Table S3 contains details on tillage operation, undisturbed soil sampling, sowing and harvesting of crops, amount of rainfall and irrigation for 2018-19 and 2019-20.

2.3 Double plate infiltrometer method

The undisturbed soil samples were saturated over 48 hours by slowly raising the water level in a tray. Saturated undisturbed soil samples were then placed between the 20 μm pore size nylon cloth covered plates of a double plate infiltrometer (Cook, 2007). The same (zero or negative) water matric potential was applied to both ends of the sample using a Mariotte reservoir for the top plate and a hanging water column for the bottom plate. Since the soil matric potential was the same at both ends, the driving force for the water to flow through the soil sample was the vertical unit gradient of soil water potential produced by gravity. As the gradient was unitary, equilibrium infiltration rates were directly the hydraulic conductivity for the given water matric potential. The level of water in the Mariotte reservoir was recorded at regular intervals during the infiltration measurements. When the sample reached state-state-flow for a given ψ , that is constant infiltration rate, sample weight was recorded to calculate the volumetric water content.

Soil volumetric water content and hydraulic conductivity were measured at four soil water matric potentials, Ψ (0, -1, -5 and -10 cm H₂O).

Hydraulic conductivity was calculated as follows:

$$K(\Psi) = -\frac{r_r^2}{r_c^2} \frac{dh}{dt} \quad (1)$$

where dh/dt is the Mariotte reservoir water level decrease rate at a given time during hydraulic equilibrium state. r_r and r_c represent the reservoir and soil corer ring internal diameters, respectively.

2.4 Evaporation method

The same soil samples were used in a modified Wind evaporation method to determine soil water retention and hydraulic conductivity curves (Wendroth et al., 1993). In a saturated soil sample, two tensiometers: [ceramic cup (length: 0.06 m and width: 0.006 m) mounted with a pressure transducer] were inserted horizontally into pre-drilled holes. The two tensiometers were positioned 0.015 and 0.045 m below the soil surface, respectively.

Each sample and its tensiometers were mounted on a plastic sheet and placed over a balance. The balance and the pressure transducers were connected to a data logging system to monitor weight losses and soil water matric potential decreases over time. The soil sample was covered with a plastic lid before initiating the evaporation process and remained covered until hydraulic equilibrium was reached. At hydraulic equilibrium, the lid was removed, the evaporation process started, and the weight and pressure transducer values were automatically recorded (hourly). The measurement stopped when the measurement range on the dry end was reached for the upper tensiometer (Ψ : -600 cm H₂O). Finally, the sample was oven dried to determine its bulk density and compute the volumetric water content during the evaporation process from the measured weights.

To describe the soil water retention curves, the van Genuchten model (van Genuchten, 1980) was fitted iteratively to the θ - ψ data pairs with the Nonlinear Least Square function (nls) of R (R core team, 2020), until changes of estimated water content between iterations were negligible (Wendroth et al., 1993):

$$\theta(\Psi) = \theta_r + \frac{\theta_s - \theta_r}{[1 + (\alpha|\Psi|)^n]^m} \quad (2)$$

where θ_s and θ_r denote the saturated and residual soil water contents, respectively and α , n , and m ($m = 1 - 1/n$) were used as empirical fitting parameters (van Genuchten, 1980). $\theta(\Psi)$ is the volumetric water content ($\text{cm}^3 \text{ cm}^{-3}$) at soil water matric potential, Ψ ($-\text{cm H}_2\text{O}$). Soil hydraulic conductivity was calculated at each time step from the water flux density between the two tensiometers and the corresponding hydraulic head gradient (Wendroth, 2008).

θ - ψ and K - ψ data pairs obtained from double plate infiltrometer and evaporation method, and θ - ψ data pairs obtained with the pressure plate apparatus at -10 , -50 , -100 , -333 , and -1000 $\text{cm H}_2\text{O}$ soil matric potentials (Talukder et al., 2022) were merged and fitted together with RETC (van Genuchten, 1991) using van Genuchten and Mualem models (Mualem, 1976). Mualem model describes the $K(\theta)$ relationship:

$$K(S) = K_s S^\ell [1 - (1 - S^{1/m})^m]^m \quad (3)$$

where

$$S = \frac{(\theta - \theta_r)}{(\theta_s - \theta_r)} \quad (4)$$

K_s is the saturated hydraulic conductivity, m ($m = 1 - 1/n$), and ℓ are the fitting parameters (van Genuchten, 1980).

2.5 Soil pore characteristics

Soil pore characteristics were calculated using Watson and Luxmoore, (1986) methods. Four pore classes were considered, macroporosity ($> 1000 \mu\text{m}$), coarse mesoporosity

(1000- 60 μm), fine mesoporosity (60- 10 μm) and microporosity (10-3 μm) (Haruna et al., 2018). Specific hydraulic conductivity, K_{pc} , (cm day^{-1}) of each pore class was calculated from this equation:

$$K_{pc} = k(\psi_i) - k(\psi_{i-1}) \quad (5)$$

where $K(\psi_i)$ and $K(\psi_{i-1})$ is the soil hydraulic conductivity at ψ_i and ψ_{i-1} soil water matric potentials corresponding to the upper and lower pore size limits of the pore class, respectively.

The number of effective pores per unit area, N_{pc} (m^{-2}) for every pore class was obtained by this equation:

$$N_{pc} = \frac{8\mu K_{pc}}{\pi\rho g r^4} \quad (6)$$

where μ is the dynamic viscosity of water ($\text{ML}^{-1}\text{T}^{-1}$), ρ is the density of water (ML^{-3}), g is acceleration due to gravity (LT^{-2}), r is the minimum pore radius (μm) of each pore class, obtained from the capillarity equation:

$$r = -\frac{2\sigma\cos\beta}{\rho g \Psi} \cong -\frac{0.15}{\Psi} \quad (7)$$

where σ is the surface tension of water (MT^{-2}), β is the contact angle between the water and the pore wall (assumed 0).

The effective porosity, ε_{pc} ($\text{cm}^3 \text{cm}^{-3}$) of each pore class was calculated using the following equation:

$$\varepsilon_{pc} = N_{pc}\pi r^2 \quad (8)$$

The pore volume, ϕ_{pc} ($\text{cm}^3 \text{cm}^{-3}$) of each pore class was calculated as the difference in the amount of water retained at ψ_i and ψ_{i-1} soil water matric potentials.

The pore continuity index, C_{wpc} of each pore class for water flow was calculated by using this formula proposed by Ehlers et al. (1995).

$$K_{pc} = \frac{1}{96} \frac{\bar{r}^2}{4} \phi_{pc} \left(\frac{\rho g}{\mu} \right) b \left(\frac{l}{l_e} \right)^2 \quad (9)$$

where \bar{r} (μm) is the geometric mean of the maximum and minimum pore radius of the pore class, l and l_e are the lengths of soil core and pore, respectively. b is a reduction factor, and $b^{1/2}(l/l_e) = C_{wpc}$ is the pore continuity index.

2.6 Statistical analysis

All statistical analyses were performed using the statistical package JMP Pro 16 (SAS Institute Inc, 2022). Both Shapiro-Wilk and Levene test were performed to check for normality and homogeneity of variances. Soil hydraulic conductivity, K ($-3 \text{ cm H}_2\text{O}$) and some pore characteristics (K_{pc} , N_{pc} , ϕ_{pc} and C_{wpc} corresponding to coarse macroporosity) were not normally distributed and were BoxCox-transformed before analysis. θ_s , θ_r , α , n , $\theta(\Psi)$, $K(\Psi)$ and soil pore characteristics were statistically tested for treatment (main) effects and interaction with analysis of variance (ANOVA). Further, analysis of variance (ANOVA) was performed to compare effects of sampling time (main plots, Federer and King, 2007) and tillage systems (sub-plots) for temporal dynamics of θ_s , K_s and pore characteristics (K_{pc} , N_{pc} , ε_{pc} , ϕ_{pc} and C_{wpc} of macroporosity and coarse macroporosity) in FM and LM. When single effects or interactions were significant, the comparisons among the means were performed at 0.05 probability level of significance with Student's t-test.

3. Results

3.1 van Genuchten parameters and soil water content

There was a significant effect of tillage on the van Genuchten parameters ($p < 0.05$), i.e., θ_s and n ; and on soil water retention but no significant effect of crop sequence and position was found (Table 4). Both θ_s and n were significantly higher in IT compared to NT (0.46 vs. 0.43 $\text{cm}^3 \text{cm}^{-3}$ and 1.44 vs. 1.20 for IT and NT, respectively) (Table 4 and 5). At higher Ψ (-1 and $-3 \text{ cm H}_2\text{O}$), $\theta(\Psi)$ was higher under IT than NT (0.45 vs. 0.43 and 0.44 vs. 0.42 $\text{cm}^3 \text{cm}^{-3}$), whilst NT had higher $\theta(\Psi)$ than IT at lower Ψ (-50 , -100 , -300 and -1000 cm

H₂O) (Table 4 and Fig. 6a). Both IT and NT showed similar values of $\theta(\Psi)$ (0.40 vs. 0.39 cm³ cm⁻³) at -10 cm H₂O. There was no difference on θ_s between LM and FM (0.45 cm³ cm⁻³), neither on θ at all studied Ψ (Table 5 and Fig. 6b). Similarly, both B-row and W-row showed similar values of θ_s (0.44 vs 0.46 cm³ cm⁻³) and $\theta(\Psi)$ at all studied Ψ .

Both IT and NT showed relatively similar trends for θ_s over time in FM and LM (Fig. 7ab). In case of FM, IT showed non-significantly greater θ_s than NT in all sampling dates, whereas in LM, IT and NT had similar values of θ_s except after 2019-20 maize harvest.

Table 4: Analysis of variance (p-values) for van Genuchten parameters of soil water retention curve (θ_s , $\text{cm}^3 \text{cm}^{-3}$: saturated water content, θ_r , $\text{cm}^3 \text{cm}^{-3}$: residual soil water content, α , cm^{-1} and n), soil water retention ($\theta(\Psi)$, $\text{cm}^3 \text{cm}^{-3}$) and soil hydraulic conductivity ($K(\Psi)$, cm day^{-1}) at different soil matric potentials (Ψ , $\text{cm H}_2\text{O}$) as affected by tillage systems (IT, intensive tillage and NT, no-tillage), crop sequences (FM, short fallow-maize and LM, legume-maize), position (W-row, within crop row and B-row, between crop rows), and their interactions (different sampling times were averaged).

Source of variation	van Genuchten parameters			Soil water retention, $\theta(\Psi[\text{cm H}_2\text{O}])$								Soil hydraulic conductivity, $K(\Psi[\text{cm H}_2\text{O}])$							
	θ_s	θ_r	α^\ddagger	n^\ddagger	-1	-3	-	-50	-100	-300	-1000	0	-1	-3 [‡]	-10	-	-	-	-
							10								50	100	300	1000	
Tillage (T)	0.004	NS	NS	0.0009	0.005	0.011	NS	0.0001	<0.0001	0.0001	0.0001	<0.0001	0.0006	0.016	0.0008	NS	NS	NS	NS
Crop sequence (CS)	NS	NS	NS	NS	NS	NS	NS	NS	NS	NS	NS	NS	NS	NS	NS	NS	NS	NS	NS
T *CS	NS	NS	NS	NS	NS	NS	NS	NS	NS	NS	NS	NS	NS	NS	NS	NS	NS	NS	NS
Position (P)	NS	NS	NS	NS	NS	NS	NS	NS	NS	NS	NS	0.007	0.037	0.022	NS	NS	NS	NS	NS
T *P	NS	NS	NS	NS	NS	NS	NS	NS	NS	NS	NS	NS	NS	NS	NS	NS	NS	NS	NS
CS *P	NS	NS	NS	NS	NS	NS	NS	NS	NS	NS	NS	NS	NS	NS	NS	NS	NS	NS	NS
T *CS *P	NS	NS	NS	NS	NS	NS	NS	NS	NS	NS	NS	NS	NS	NS	NS	NS	NS	NS	NS

[‡] data were Box-Cox transformed before analysis. NS, non-significant ($p > 0.05$).

Table 5: Mean comparisons of the van Genuchten parameters of soil water retention curve (θ_s , $\text{cm}^3 \text{cm}^{-3}$: saturated water content, θ_r , $\text{cm}^3 \text{cm}^{-3}$: residual soil water content, α , cm^{-1} and n) for two different tillage systems (IT, intensive tillage and NT, no-tillage), two crop sequences (FM, Short fallow-maize and LM, legume-maize) and two positions (W-row, within the crop row and B-row, between crop rows). Different letters within the column and factor indicate significant differences between levels (** $p < 0.01$ and *** $p < 0.001$).

Factors	Levels	van Genuchten parameters			
		θ_s	θ_r	α	n
Tillage	IT	0.46 a ^{**}	0.21 a	0.21 a	1.44 a ^{***}
	NT	0.43 b	0.21 a	0.32 a	1.20 b
Crop sequence	FM	0.45 a	0.20 a	0.30 a	1.30 a
	LM	0.45 a	0.22 a	0.23 a	1.34 a
Position	B-row	0.44 a	0.20 a	0.33 a	1.30 a
	W-row	0.46 a	0.23 a	0.21 a	1.34 a

3.2 Soil hydraulic conductivity

Soil hydraulic conductivity was significantly affected by tillage and position ($p < 0.05$), but not by crop sequence (Table 4). NT had greater K than IT at higher Ψ (31 vs. 14, 19 vs. 8, 11 vs. 5, 3 vs. 1 cm day^{-1} at 0, -1, -3 and -10 $\text{cm H}_2\text{O}$, respectively) but no significant differences were observed at lower Ψ (-50, -100, -300 and -1000 $\text{cm H}_2\text{O}$) (Fig. 8a). Similarly, W-row had greater K than B-row at higher Ψ (26 vs. 19, 16 vs. 11, 10 vs. 7 cm day^{-1} at 0, -1, and -3 $\text{cm H}_2\text{O}$, respectively) but no significant difference was observed at lower Ψ (-10, -50, -100, -300 and -1000 $\text{cm H}_2\text{O}$) (Fig. 8c). LM showed non-significantly higher K than FM ($p = 0.08$) only at 0 and -1 $\text{cm H}_2\text{O}$ (25 vs. 19 and 14 vs. 13 cm day^{-1} , respectively) (Fig. 8b).

Both IT and NT showed relatively similar trends for K_s over time in FM and LM (Fig. 7cd) except in LM where NT showed greater K_s than IT after sowing and after harvest of legume in 2018-19. In addition, an increasing trend in K_s was observed under IT from legume to maize crop succession in 2018-2019.

3.3 Soil pore characteristics

There was a significant effect of tillage, crop sequence and position ($p < 0.05$) on specific hydraulic conductivity, number of effective pores, and effective porosity at different pore classes (Table 6). NT showed greater K_{pc} (20 vs. 9 and 11 vs. 5 cm day^{-1}), N_{pc} (9 vs. 4 and 367812 vs. 176883 m^{-2}), and ε_{pc} (0.0006 vs. 0.0004 and 0.10 vs 0.05 $\text{cm}^3 \text{cm}^{-3}$) than IT for macroporosity ($> 1000 \mu\text{m}$) and coarse mesoporosity (1000-60 μm), whilst no differences were observed for fine mesoporosity (60-10 μm) and microporosity (10-3 μm) (Table 7 and Fig. 9a). LM showed significantly greater K_{pc} (17 vs. 13 cm day^{-1}), N_{pc} (7 vs. 5 m^{-2}), and ε_{pc} (0.0006 vs. 0.0004 $\text{cm}^3 \text{cm}^{-3}$) than FM for macroporosity, whereas no differences were observed for coarse mesoporosity, fine mesoporosity and microporosity (Table 7 and Fig. 9b).

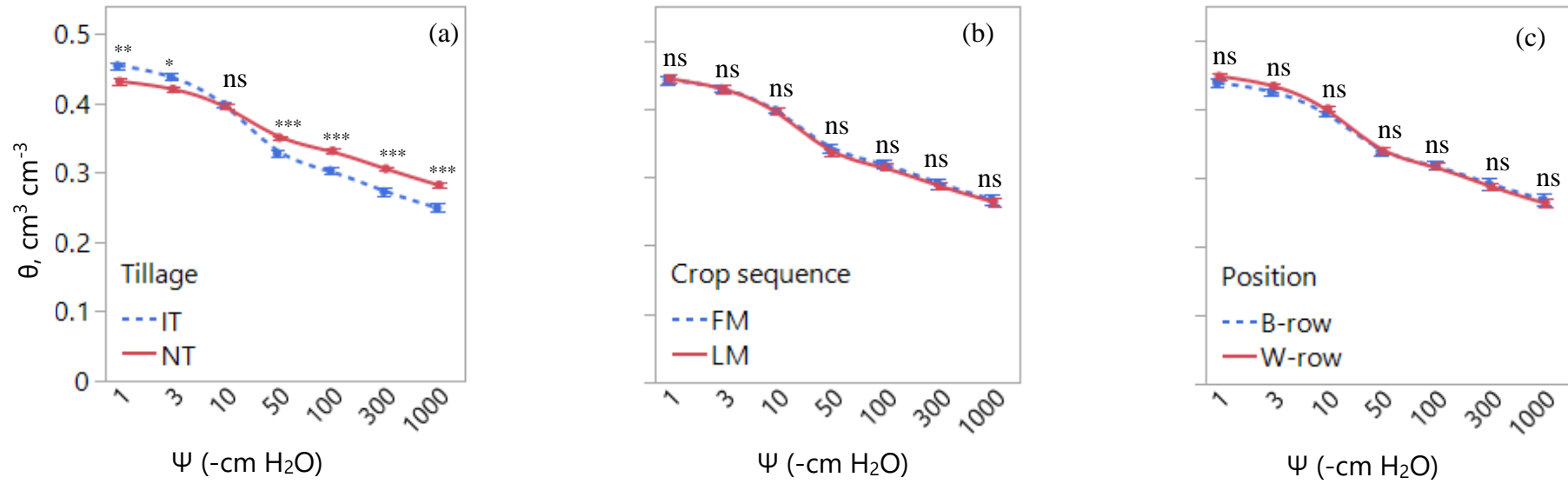


Fig. 6: Soil water content, θ ($\text{cm}^3 \text{cm}^{-3}$) at different soil matric potentials, Ψ ($-\text{cm H}_2\text{O}$) in soils under different tillage (IT, intensive tillage and NT, no-tillage) (a), crop sequence (FM, short fallow-maize, and LM, legume-maize) (b), and position (W-row, within the crop row and B-row, between crop rows) (c). Error bars show the standard error and (*) indicates significant differences between treatments (* $p < 0.05$, ** $p < 0.01$, *** $p < 0.001$ and ns: non-significant).

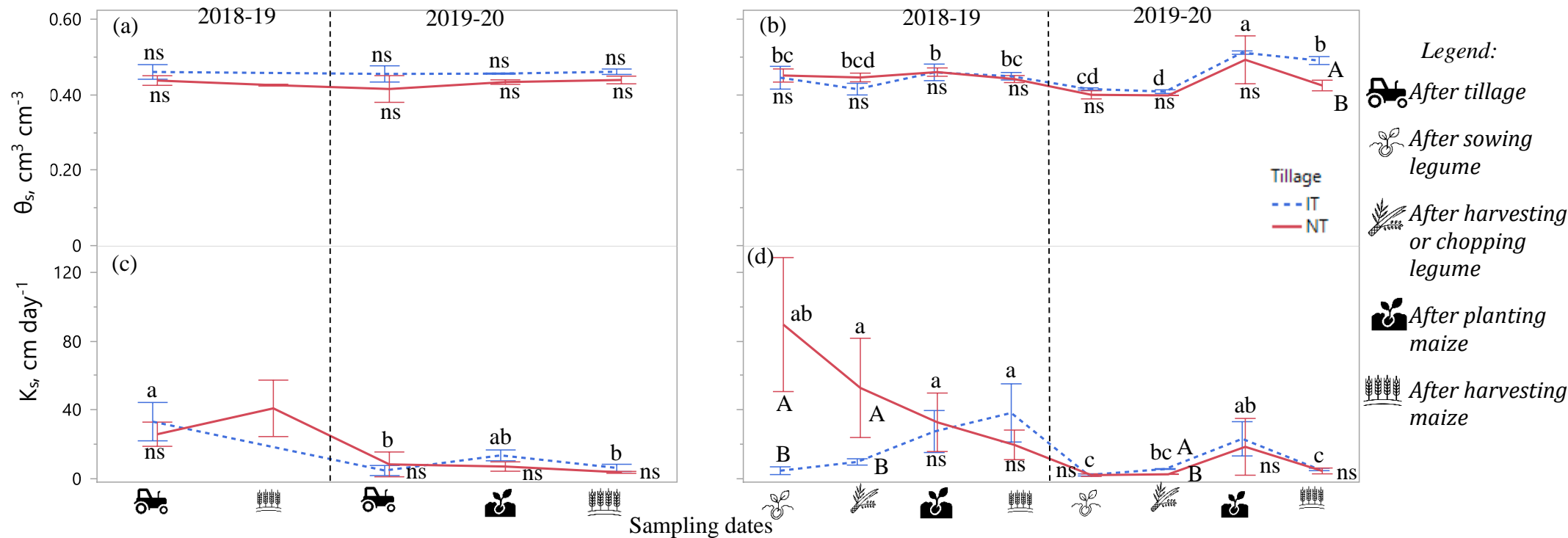


Fig. 7: Saturated soil water content, θ_s ($\text{cm}^3 \text{cm}^{-3}$) and saturated hydraulic conductivity, K_s (cm day^{-1}) at different sampling dates in soils under different (a and c) tillage systems (IT, Intensive tillage and NT, no-tillage), and (b and d) crop sequences (FM, short fallow-maize and LM, legume-maize). Error bars show the standard error. Different letters (lowercase letters among sampling dates and uppercase letters between tillage systems within each sampling date) indicate the significant differences between treatments at $p < 0.05$; ns, non-significant. Vertical dashed line separates the 2018-19 and 2019-20 cropping years.

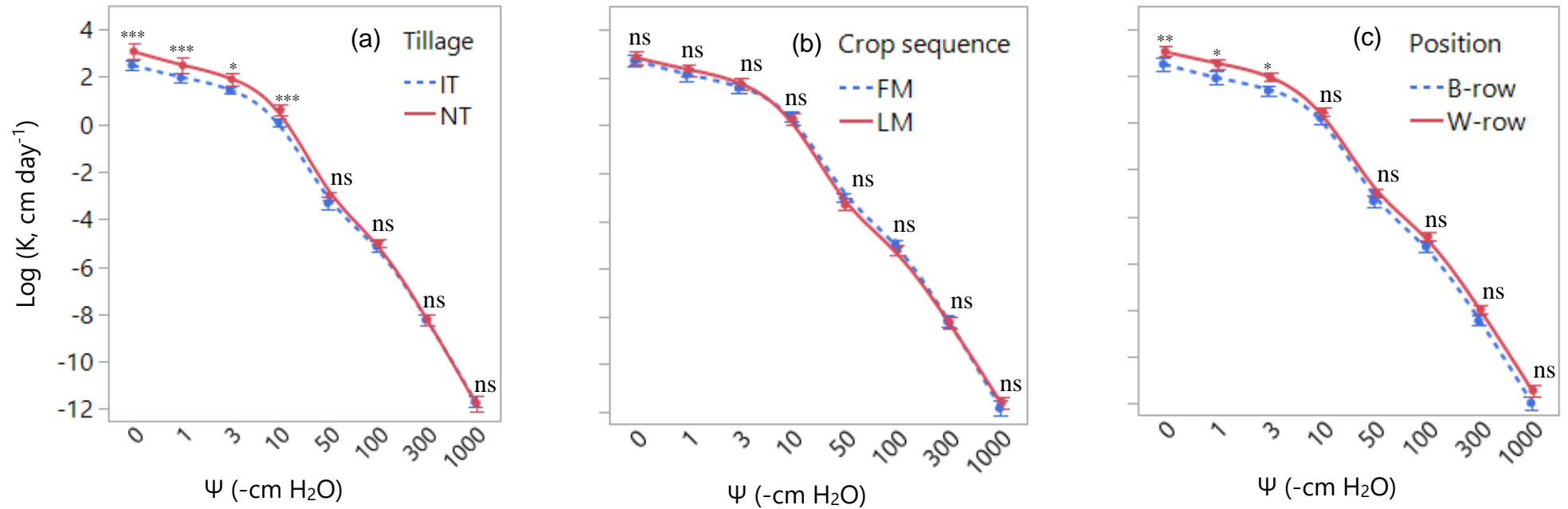


Fig. 8: Soil hydraulic conductivity, K (cm day^{-1}) at different soil matric potentials, Ψ (-cm H_2O) in soils under different tillage (IT, Intensive tillage and NT, no-tillage) (a), crop sequence (FM, short fallow-maize, and LM, legume-maize) (b), and position (W-row, within the crop row and B-row, between crop rows) (c). Error bars show the standard error and (*) indicates the significant difference between treatments ($*p < 0.05$, $**p < 0.01$, $***p < 0.001$ and ns: non-significant).

W-row had greater K_{pc} (17 vs. 12 and 9 vs. 7 cm day⁻¹), N_{pc} (7 vs. 5 and 312618 vs. 232077 m⁻²), and ε_{pc} (0.0006 vs. 0.0004 and 0.09 vs 0.07 cm³ cm⁻³) than B-row for macroporosity and coarse mesoporosity, whilst no differences were observed for fine mesoporosity and microporosity (Table 7 and Fig. 9c).

Pore volume was significantly affected by tillage ($p < 0.05$) but not by crop sequence and position (Table 6 and Fig. 10ace). IT had significantly greater ϕ_{pc} of coarse mesoporosity (0.018 vs. 0.017 cm³ cm⁻³) and fine mesoporosity (0.11 vs. 0.07 cm³cm⁻³) than NT, whilst no significant difference was observed for macroporosity and microporosity (Fig. 10a). Pore continuity index was significantly affected by tillage and position, ($p < 0.05$) but not by crop sequence (Table 6 and Fig. 10bdf). NT had greater C_{wpc} of coarse mesoporosity (0.09 vs. 0.06) and fine mesoporosity (0.08 vs. 0.06) than IT, whilst no significant differences were observed for macroporosity and microporosity (Fig. 10b). W-row, C_{wpc} for macroporosity (0.04 vs. 0.03) was greater than B-row whilst no differences were observed for coarse mesoporosity, fine mesoporosity and microporosity (Fig. 10f).

Regardless of crop sequences, K_{pc} , N_{pc} , ϕ_{pc} and C_{wpc} of macroporosity showed similar trends over time for NT and IT (Fig. 11ab) except after sowing and harvesting of legume in LM. In 2018-19, macroporosity showed greater K_{pc} , N_{pc} , and C_{wpc} under NT, whereas tended to increase under IT from legume to maize crop succession. In case of FM, coarse mesoporosity showed similar K_{pc} and N_{pc} under both NT and IT (Fig. 12a). Further, IT showed greater ϕ_{pc} and similar or lower C_{wpc} than NT. In case of LM, coarse mesoporosity showed non-significantly higher K_{pc} and N_{pc} under NT than under IT after sowing and harvesting of legume in 2018-19 (Fig. 12b). NT showed lower ϕ_{pc} and similar or higher C_{wpc} at different sampling dates.

Table 6: Analysis of variance (p-values) for the specific hydraulic conductivity (K_{pc} , cm day⁻¹), number of effective pores (N_{pc} , m⁻²), effective porosity (ε_{pc} , cm³ cm⁻³), pore volume (ϕ_{pc} , cm³ cm⁻³) and pore continuity index (C_{wpc}) at different pore size classes (μ m) (>1000 = macroporosity, 1000-60 = coarse mesoporosity, 60-10 = fine mesoporosity, 10-3 = microporosity) affected by tillage systems (IT, intensive tillage and NT, no-tillage), crop sequences (FM, short fallow-maize and LM, legume-maize), positions (W-row, within the crop row and B-row, between crop rows) and their interactions (different sampling times were averaged). NS, non-significant ($p > 0.05$).

Source of variation	K_{pc} cm day ⁻¹				N_{pc} m ⁻²				ε_{pc} cm ³ cm ⁻³				ϕ_{pc} cm ³ cm ⁻³				C_{wpc}			
	>1000	1000-60	60-10	10-3	>1000	1000-60	60-10	10-3	>1000	1000-60	60-10	10-3	>1000	1000-60	60-10	10-3	>1000	1000-60	60-10	10-3
Tillage (T)	<.0001	0.016	NS	NS	<.0001	0.016	NS	NS	<.0001	0.016	NS	NS	NS	<0.001	0.002	NS	NS	0.0003	0.036	NS
Crop sequence (CS)	0.048	NS	NS	NS	0.048	NS	NS	NS	0.048	NS	NS	NS	NS	NS	NS	NS	NS	NS	NS	NS
T *CS	NS	NS	NS	NS	NS	NS	NS	NS	NS	NS	NS	NS	NS	NS	NS	NS	NS	NS	NS	NS
Position (P)	0.014	0.022	NS	NS	0.014	0.022	NS	NS	0.014	0.022	NS	NS	NS	NS	NS	NS	0.041	NS	NS	NS
T *P	NS	NS	NS	NS	NS	NS	NS	NS	NS	NS	NS	NS	NS	NS	NS	NS	NS	NS	NS	NS
CS *P	NS	NS	NS	NS	NS	NS	NS	NS	NS	NS	NS	NS	NS	NS	NS	NS	NS	NS	NS	NS
T *CS *P	NS	NS	NS	NS	NS	NS	NS	NS	NS	NS	NS	NS	NS	NS	NS	NS	NS	NS	NS	NS

Table 7: Mean comparisons of specific hydraulic conductivity (K_{pc} , cm day⁻¹) and effective porosity (ε_{pc} , cm³ cm⁻³) at different pore classes for two different tillage systems (IT, intensive tillage and NT, no-tillage), two crop sequences (FM, short fallow-maize, and LM, legume-maize) and two positions (W-row, within the crop row and B-row, between crop rows). Different letters within the row and factor indicate significant differences between levels (* $p < 0.05$, ** $p < 0.01$, *** $p < 0.001$).

Soil water matric potential, Ψ (cm H ₂ O)	Pore size class (μ m)	Pore size category	Tillage		Crop sequence		Position	
			IT	NT	BM	LM	B-row	W-row
Specific hydraulic conductivity, K_{pc} (cm day ⁻¹)								
0 to -3	>1000	Macroporosity	9.05 b	20.44 a ^{***}	12.89 b	16.61 a [*]	12.30 b	17.20 a [*]
-3 to -50	1000-60	Coarse Mesoporosity	5.35 b	11.13 a [*]	8.06 a	8.42 a	7.02 b	9.46 a [*]
-50 to -300	60-10	Fine Mesoporosity	0.05 a	0.06 a	0.06 a	0.05 a	0.04 a	0.06 a
-300 to -1000	10-3	Microporosity	0.0003 a	0.0003 a	0.0003 a	0.0003 a	0.0003 a	0.0004 a
Effective porosity, ε_{pc} (cm ³ cm ⁻³)								
0 to -3	>1000	Macroporosity	0.0003 b	0.0007 a ^{***}	0.0004 b	0.0006 a [*]	0.0004 b	0.0006 a [*]
-3 to -50	1000-60	Coarse Mesoporosity	0.05 b	0.10 a [*]	0.08 a	0.08 a	0.07 b	0.09 a [*]
-50 to -300	60-10	Fine Mesoporosity	0.02 a	0.02 a	0.02 a	0.02 a	0.01 a	0.02 a
-300 to -1000	10-3	Microporosity	0.001 a	0.001 a	0.001 a	0.001 a	0.001 a	0.001 a

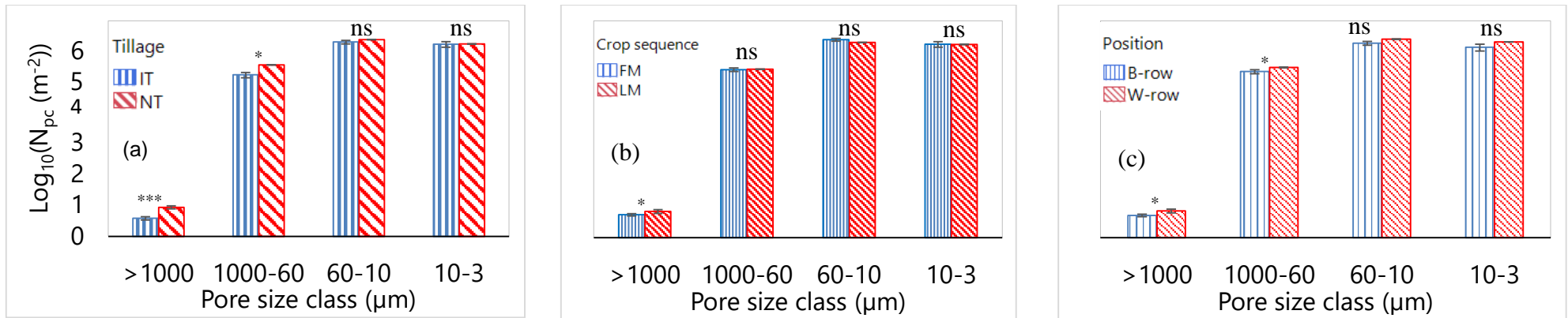


Fig. 9: Number of effective pores, N_{pc} (m^{-2}) at different pore size classes in soils under different tillage (IT, Intensive tillage and NT, no-tillage) (a), crop sequence (FM, short fallow-maize, and LM, legume-maize) (b), and position (W-row, within the crop row and B-row, between crop rows) (c). Error bars show the standard error and (*) indicates the significant difference between treatments (* $p < 0.05$, ** $p < 0.01$, *** $p < 0.001$ and ns: non-significant).

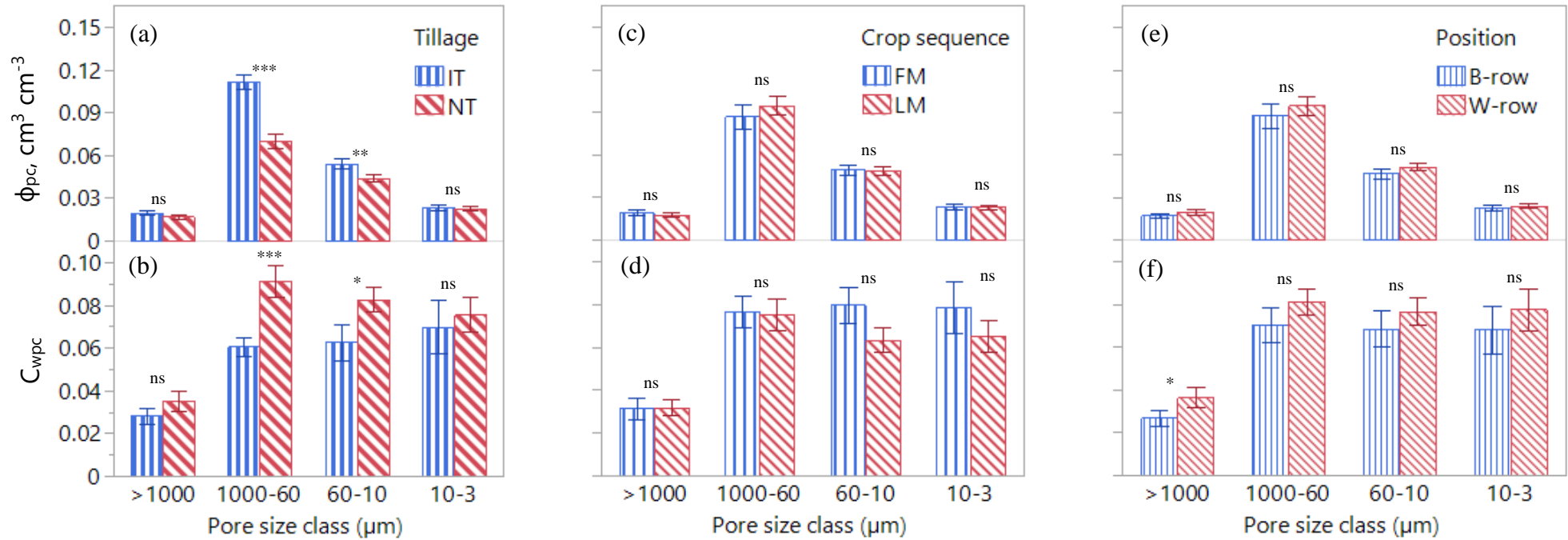


Fig. 10: Pore class volume, ϕ_{pc} ($\text{cm}^3 \text{cm}^{-3}$) and pore continuity index, C_{wpc} for different pore size classes in soils under different tillage (IT, Intensive tillage and NT, no-tillage) (a and b), crop sequence (FM, short fallow-maize, and LM, legume-maize) (c and d) and position (W-row, within the crop row and B-row, between crop rows) (e and f). Error bars show the standard error and (*) indicates the significant different between treatments ($*p < 0.05$, $**p < 0.01$, $***p < 0.001$ and ns: non-significant).

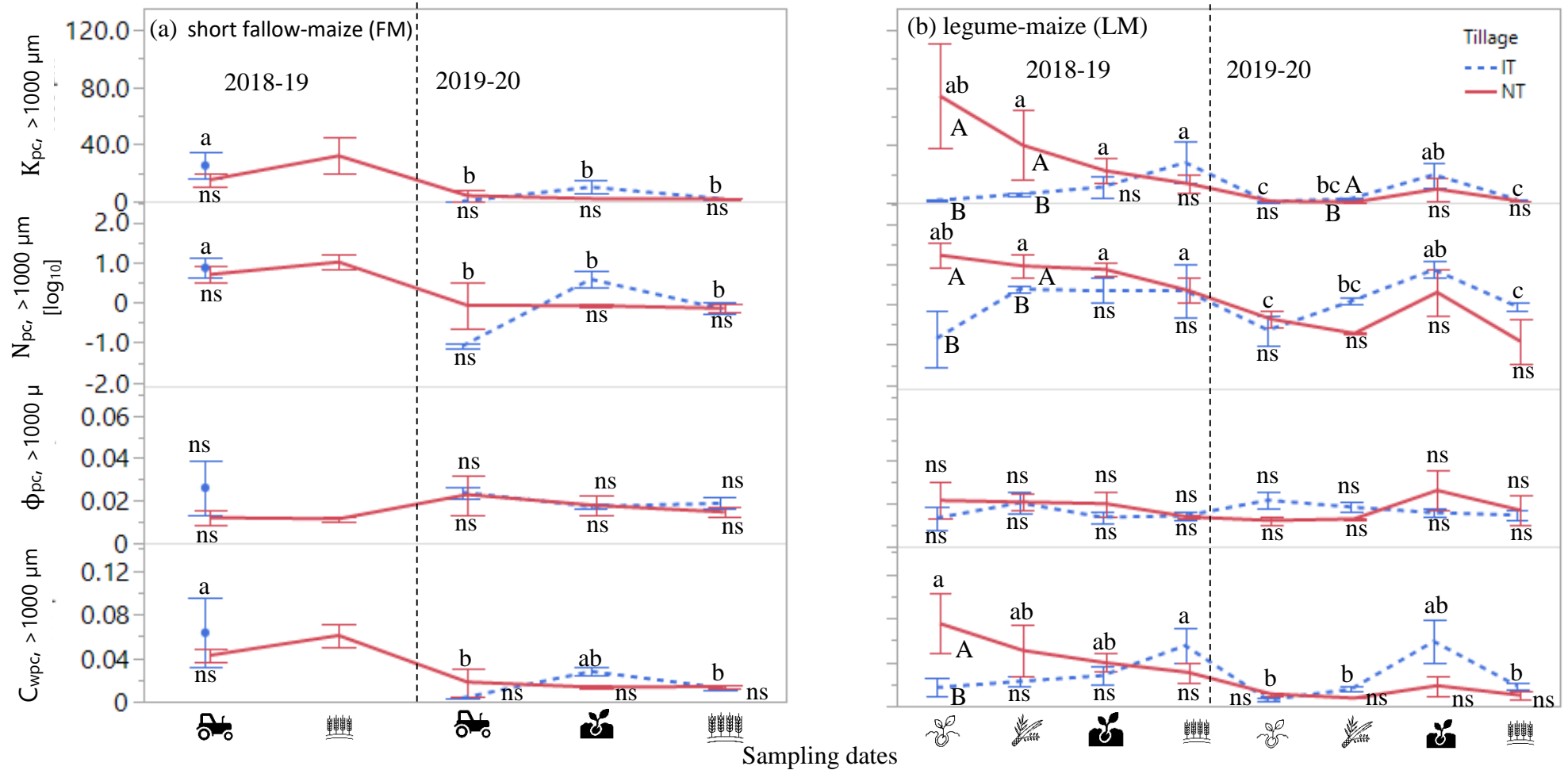


Fig. 11: Specific hydraulic conductivity, K_{pc} (cm day^{-1}), number of effective pores, N_{pc} (m^{-2}), pore volume, ϕ_{pc} ($\text{cm}^3 \text{cm}^{-3}$) and pore continuity index, C_{wpc} of macroporosity ($>1000 \mu\text{m}$) at different sampling dates in soils under different tillage (IT, Intensive tillage and NT, no-tillage) (a) and crop sequences (FM, short fallow-maize and LM, legume-maize) (b). Error bars show the standard error. Different letters (lowercase letters among sampling dates and uppercase letters between tillage systems within each sampling dates) indicate the significant differences between treatments; ns, non-significant. Vertical dashed line separates the 2018-19 and 2019-20 cropping years.

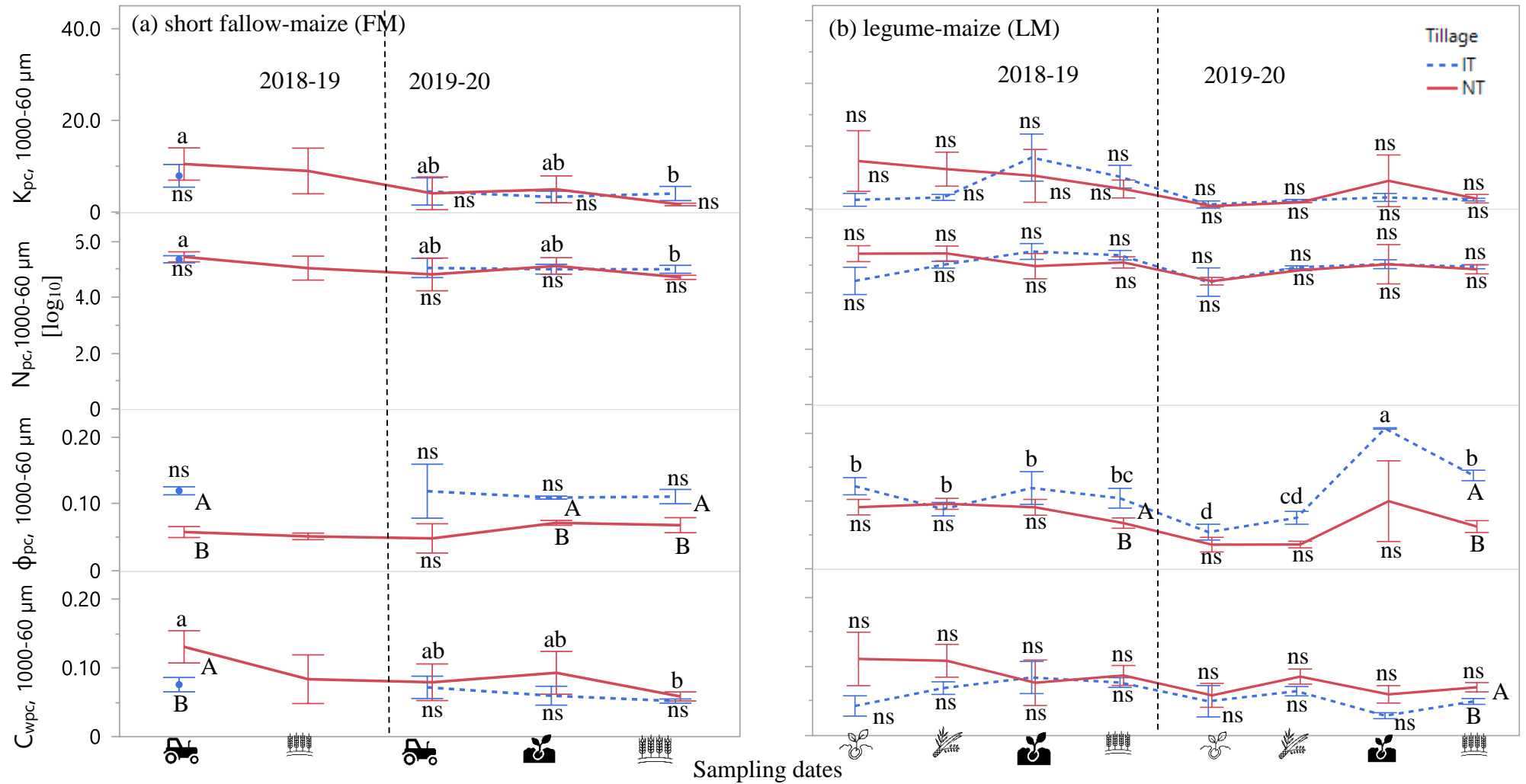


Fig. 12: Specific hydraulic conductivity, K_{pc} (cm day^{-1}), number of effective pores, N_{pc} (m^{-2}), pore volume, ϕ_{pc} ($\text{cm}^3 \text{cm}^{-3}$) and pore continuity index, C_{wpc} of coarse mesoporosity (1000-60 μm) at different sampling dates in soils under different tillage (IT, Intensive tillage and NT, no-tillage) (a) and crop sequence (FM, short fallow-maize and LM, legume-maize) (b). Error bars show the standard error. Different letters (lowercase letters among sampling dates and uppercase letters between tillage systems within each sampling dates) indicate the significant differences between treatments; ns, non-significant. Vertical dashed line separates the 2018-19 and 2019-20 cropping years.

4. Discussion

4.1 Crop sequence effects

Both LM and FM had similar values of van Genuchten soil water retention parameters (θ_s , θ_r , α and n), $\theta(\Psi)$, and ϕ_{pc} and C_{wpc} of different pore classes (Tables 5 and 7; Figs. 6, 8 and 10). However, hydraulic conductivity $K(\Psi)$ tended to be higher under LM at higher Ψ (0 and -1 cm H₂O) (Fig. 8b) and greater K_{pc} of macroporosity was observed in LM compared to FM (Table 7). Saturated and near saturated (0 to -3 cm H₂O) soil hydraulic conductivity is likely controlled by macro-pores that contributed to 53% of total water flux both in FM and LM (data not shown). Therefore, water flow by macro-pores could significantly determine processes such as infiltration and water or solute transport (Kabir et al., 2020). Our results are consistent with the results of Gabriel et al. (2019) and Nouri et al. (2019). In a long-term study (10 years), Gabriel et al. (2019) found that inclusion of winter barley in crop rotations before main crops (maize) increased soil macroporosity and microporosity on a silty clay loam soil in a semiarid Mediterranean climate under irrigated conditions. They pointed out that barley cover cropping increased soil water retention and improved soil structure. Nouri et al. (2019) observed that long-term vetch cover cropping (34 years) compared with no cover cropping before cotton increased initial infiltration and field-saturated hydraulic conductivity on a silt loam soil in a humid subtropical climate. This increased infiltration and hydraulic conductivity was caused by improvements in soil microaggregation. In case of LM, greater K_{pc} of macro-pores may be explained by the following reasons. Firstly, inclusion of a legume before maize provides further crop residues of a low C: N ratio that are returned to the soil, resulting a greater residue turn over in LM than FM. Under NT, residue retention on soil surface and lack of soil mechanical disturbance might have created favourable conditions for soil fauna and soil flora (Castellanos-Navarrete et al., 2012), thus might have increased number of bio-pores in soils. Secondly, tap root systems of legume comprising numerous secondary branches might have helped to create preferential paths within macro-pores, i.e., bio-pores, and burrows (Zhang et al., 2017; Patra et al., 2019). Furthermore,

preferential flow paths left by those roots after decaying, are regarded as main root channels that remain activated up to the next crop and the following succession (Zhang et al., 2017). Finally, LM had more effective macropores (Table 7) that increased water infiltration and redistribution, which is usually coupled with better aeration (Imhoff et al., 2010). Overall, compared to a winter fallow, introducing a legume before maize increased soil hydraulic conductivity of macropores by generating preferential paths and improved soil pore system characteristics i.e., greater effective porosity and numbers of pores per unit area.

4.2 Tillage effects

Total porosity was equal to saturated soil water content or water content at 0 cm H₂O soil matric potential, and IT showed 7% higher θ_s than NT (Table 5) which was directly related to greater total soil porosity observed under IT caused by tillage operation (Talukder et al., 2022). Tillage often increases soil porosity by loosening the soil surface (Kargas et al., 2016; Patra et al., 2019; Vanderlinden et al., 2021). Again, IT had greater soil water content at Ψ from -1 to -3 cm H₂O, whilst at Ψ from -50 to -1000 cm H₂O, NT showed constantly greater soil water content than IT (Fig. 6). These results indicate that macropores (pore size > 1000 μm), under IT would drain water away readily, favouring improved aeration, but a greater number of relatively small pores ($\leq 60 \mu\text{m}$) under NT would allow water retention and storage (Nouri et al., 2019). As a consequence, IT showed greater n compared to NT (1.44 vs. 1.20) (Table 5) (Gabriel et al., 2019). Long-term NT had a significantly greater soil hydraulic conductivity than IT at Ψ from 0 to -10 cm H₂O, but no differences were observed from -10 to -1000 cm H₂O (Fig. 8). Ψ from 0 to -10 cm H₂O, corresponding to pores of diameter $\geq 300 \mu\text{m}$, includes macroporosity (> 1000 μm) and part of the coarse mesoporosity (1000-60 μm). This suggests that macropores and coarse mesopores were likely controlling $K(\Psi)$ in soils under NT. Similar findings were also reported by Patra et al. (2019) on semiarid irrigated conditions. In a long-term tilled cereal-based cropping system experiment they observed higher soil hydraulic conductivity under NT compared to IT due to formation of greater, and more continuous macropores.

Although we found an equal volume of macropores, and the volume of coarse mesopores was higher in IT, specific hydraulic conductivities for those classes were higher under NT due to higher number of effective pores, effective porosity and pore continuity (Fig. 10ab). The number of macropores, that increases after tillage, decreases over time due to low aggregate stability and wetting and drying cycles, indicating soil physical quality deterioration (Kargas et al., 2016; Villarreal et al., 2020). A study by Imhoff et al. (2010) reported that larger pores, such as macropores, created by tillage, changed into coarse and fine mesopores over time in a silty-loam soil in Argentina, lowering soil hydraulic conductivity by blocking pores and reducing pore continuity. Our results show a similar trend, as we collected soil samples one month after tillage operations and obtained a similar volume of macropores in IT and NT, but a greater volume of coarse mesopores and fine mesopores under IT. On the other hand, similar values of macropores and higher continuity under NT could be linked to long-term NT (~ 26 years). We hypothesized that prolonged periods of undisturbed faunal and floral activity as well as plant roots growth could be responsible for the development of macropores on NT. For instance, Galdos et al. (2019) reported that long-term NT (~ 30 years) increased the volume of macropores and its continuity compared to IT in a Brazilian Typic Rhodudalf soil under semiarid conditions.

Despite having greater pore volume under IT, such as coarse and fine mesopores, these pore size classes had lower specific hydraulic conductivity (Fig. 10ab). These findings highlighted that the porous system of long-term NT was highly connected, although the pore volume was lower. Tillage operations, on the other hand, helped to increase the volume of coarse and fine mesopores but those pores were poorly interconnected under IT. As a result, IT showed lower number of effective pores and effective porosity and consequently, decreased K_{pc} of that pore classes. Our results suggest that tillage does not succeed in creating long-lasting macropores. Beside this, greater volume of coarse and fine mesopores created by IT does not increase the soil hydraulic conductivity because of lower pore continuity and number of effective pores per unit area.

4.3 Position effects

Within the row of crops, soil hydraulic conductivity, $K(\Psi)$ was significantly greater than B-row at Ψ 's from 0 to -3 cm H₂O, but no difference was observed from -3 to -1000 cm H₂O (Fig 8c). Spatial variations of $K(\Psi)$ might be due to presence of plant roots and its growth and development W-row that creates preferential flow channels. Therefore, soil water flow is significantly greater along the root-soil interface (W-row) than distant from the plants (B-row) (Zhang et al., 2017). K_{pc} of macropores and coarse mesopores were approximately 1.4 times higher W-row than B-row (Table 7). This could be due to significantly greater effective porosity (Table 7) and number of effective pores per unit area (Fig. 9c). Although the pore volume of the different pore classes was similar W-row and B-row, pore continuity tended to be higher W-row, but only significantly higher for macropores (Fig. 10ef). Our results are in agreement with the results of Liu et al. (2016), who stated that K_s was controlled by the number of effective macropores and pore continuity. We hypothesized that greater K_{pc} W-row could be due to the presence of plant roots that improved pore continuity. Working in a long-term NT experiment on a Brazilian clayey Oxisol soil, Silva et al. (2014) reported that W-row had more favourable soil physical and structural properties such as bulk density, air-filled porosity and air permeability compared to B-row.

4.4 Temporal variations

Both tillage systems showed relatively similar trends on θ_s , K_s and pore characteristics (K_{pc} , N_{pc} , ϕ_{pc} and C_{wpc} of macroporosity and coarse mesoporosity) over time (Figs. 7, 11 and 12) except between sowing and harvesting of legume in 2018-19. Few temporal variations on soil hydro-physical properties were observed under IT because the effects of mechanical disturbance by tillage were lost within a short period of time. Undisturbed soil sampling was performed one month after sowing, when the soil was reconsolidated either by rain or irrigation (Table S3). Freshly tilled soil was difficult to sample due to very fragile structure and was not suitable to be analyzed under laboratory conditions. Therefore, wetting and drying cycles as well as reconsolidation due to rain and irrigation

events decrease the effects of tillage under IT. Effects of tillage on the short-term dynamics of soil hydro-physical properties were reported by several authors (Kargas et al., 2016; Hu et al., 2018; Villarreal et al., 2020) but those effects were lost during the period of crop succession or soil reconsolidation. For instance, Hu et al. (2018) reported that effects of tillage were immediate and temporary, and changes on soil hydro-dynamic or physical properties did not persist for long. Moreover, regardless of crop sequence, greater volume of coarse mesopores at different sampling dates under IT did not change K_{pc} of that pore class. On the other hand, long-term NT showed a consistent trend of soil hydro-physical properties over time which implies that soil under NT has a more stable structure and improved soil hydraulic conductivity due to a more effective porous system i.e., higher number of effective pores and pore continuity. Nevertheless, crop diversification i.e., incorporation of legume in comparison to fallow, increased soil K_s , K_{pc} , N_{pc} and C_{wpc} of macropores and coarse mesopores after sowing of legume under NT than IT in 2018-19 (Fig. 7cd and Fig. 11ab). However, such differences between IT and NT did not remain over time, thanks to legumes that mitigated the deleterious effect of tillage in IT. This indicates importance of leguminous crops on soil hydro-dynamic properties on the short term but the long-term effects need to be study further.

5. Conclusions

Long-term no-tillage helps to form stable macropores and a system of continuous and vertically oriented effective porosity that improves soil water transport. Temporal changes on soil hydraulic properties and pore characteristics under IT do not last over time due to reconsolidation of soil after rain and irrigation. Regardless of tillage system, the inclusion of winter legumes replacing fallow in crop sequences, positively influences soil hydraulic functions and pore characteristics. Growing a legume before maize, where irrigation or weather conditions allows it, can be a management choice to improve soil hydraulic properties by the development of a more effective macroporosity. Within the row of crops, effective porosity, number of effective pores and pore continuity are greater, leading to higher saturated and unsaturated hydraulic conductivity. Therefore, spatial variations of soil

hydraulic properties and pore characteristics should be taken into account when measuring soil water flux as those variables may vary depending on the position of measurements. Estimates of soil water content and pore volume based on soil water retention data are not good predictors of soil water flux since they do not account for pore continuity, which is one of the most influential parameters in soil water flux.

Acknowledgments

The authors thank the support given by Dr. Stefan Fenner, the visiting Ph.D. candidate Mehrdad Soranj, Prof. Concha Ramos, the field and laboratory technicians Carlos Cortés and Silvia Martí, and the farmer Xavier Penella. The authors gratefully acknowledge support for this research from the Research Spanish Agency (DISOSMED Project - AGL2017-84529-C3-R). Rasendra Talukder also sincerely acknowledges the fund provided by University of Lleida to support its PhD fellowship. Daniel Plaza-Bonilla is Ramón y Cajal fellow (RYC-2018-024536-I) co-funded by MICIN/AEI/10.13039/501100011033 and European Social Fund.

References

- Alagna, V., Bagarello, V., Di Prima, S., Guaitoli, F., Iovino, M., Keesstra, S., Cerdà, A., 2019. Using Beerkan experiments to estimate hydraulic conductivity of a crusted loamy soil in a Mediterranean vineyard. *J. Hydrol. Hydromechanics* 67, 191–200. <https://doi.org/10.2478/johh-2018-0023>
- Alvarez, C.R., Taboada, M.A., Perelman, S., Morrás, H.J.M., 2014. Topsoil structure in no-tilled soils in the Rolling Pampa, Argentina. *Soil Res.* 52, 533. <https://doi.org/10.1071/SR13281>
- Baranian Kabir, E., Bashari, H., Bassiri, M., Mosaddeghi, M.R., 2020. Effects of land-use/cover change on soil hydraulic properties and pore characteristics in a semi-arid region of central Iran. *Soil Tillage Res.* 197, 104478. <https://doi.org/10.1016/j.still.2019.104478>
- Cantero-Martínez, C., Angas, P., Lampurlanés, J., 2003. Growth, yield and water productivity of

barley (*Hordeum vulgare* L.) affected by tillage and N fertilization in Mediterranean semiarid, rainfed conditions of Spain. *F. Crop. Res.* 84, 341–357. [https://doi.org/10.1016/S0378-4290\(03\)00101-1](https://doi.org/10.1016/S0378-4290(03)00101-1)

Castellanos-Navarrete, A., Rodríguez-Aragónés, C., De Goede, R.G.M., Kooistra, M.J., Sayre, K.D., Brussaard, L., Pulleman, M.M., 2012. Earthworm activity and soil structural changes under conservation agriculture in central Mexico. *Soil Tillage Res.* 123, 61–70. <https://doi.org/10.1016/j.still.2012.03.011>

Cook, F. J., 2007. Near-saturated hydraulic conductivity and sorptivity: Laboratory measurement, in: Carter, M.R., Gregorich, E.G. (Eds.), *Soil Sampling and Methods of Analysis*. CRC Press, pp. 1075–1087.

Ehlers, W., Wendroth, O., and Mol, F. de., 1995. Characterizing pore organization by soil physical parameters, in: Hartge, K.H., Stewart, B.A. (Eds.), *Soil Structure: Its Development and Function*. *Adv. Soil Sci.* CRC Press, Boca Raton, FL, pp. 257–275.

Federer, W.T., King, F., 2007. *Variations on Split Plot and Split Block Experiment Designs*. John Wiley & Sons, Inc., Hoboken, NJ, USA. <https://doi.org/10.1002/0470108584>

Gabriel, J.L., Quemada, M., Martín-Lammerding, D., Vanclooster, M., 2019. Assessing the cover crop effect on soil hydraulic properties by inverse modelling in a 10-year field trial. *Agric. Water Manag.* 222, 62–71. <https://doi.org/10.1016/j.agwat.2019.05.034>

Galdos, M.V., Pires, L.F., Cooper, H.V., Calonego, J.C., Rosolem, C.A., Mooney, S.J., 2019. Assessing the long-term effects of zero-tillage on the macroporosity of Brazilian soils using X-ray Computed Tomography. *Geoderma* 337, 1126–1135. <https://doi.org/10.1016/j.geoderma.2018.11.031>

Haruna, S.I., Anderson, S.H., Nkongolo, N. V., Zaibon, S., 2018. Soil Hydraulic Properties: Influence of Tillage and Cover Crops. *Pedosphere* 28, 430–442.

[https://doi.org/10.1016/S1002-0160\(17\)60387-4](https://doi.org/10.1016/S1002-0160(17)60387-4)

- Hu, W., Tabley, F., Beare, M., Tregurtha, C., Gillespie, R., Qiu, W., Gosden, P., 2018. Short-Term Dynamics of Soil Physical Properties as Affected by Compaction and Tillage in a Silt Loam Soil. *Vadose Zo. J.* 17, 180115. <https://doi.org/10.2136/vzj2018.06.0115>
- Imhoff, S., Ghiberto, P.J., Grioni, A., Gay, J.P., 2010. Porosity characterization of Argiudolls under different management systems in the Argentine Flat Pampa. *Geoderma* 158, 268–274. <https://doi.org/10.1016/j.geoderma.2010.05.005>
- Kargas, G., Kerkides, P., Sotirakoglou, K., Poulouvasilis, A., 2016. Temporal variability of surface soil hydraulic properties under various tillage systems. *Soil Tillage Res.* 158, 22–31. <https://doi.org/10.1016/j.still.2015.11.011>
- Kreiselmeier, J., Chandrasekhar, P., Weninger, T., Schwen, A., Julich, S., Feger, K.H., Schwärzel, K., 2019. Quantification of soil pore dynamics during a winter wheat cropping cycle under different tillage regimes. *Soil Tillage Res.* 192, 222–232. <https://doi.org/10.1016/j.still.2019.05.014>
- Lal, R., 2015. Restoring Soil Quality to Mitigate Soil Degradation. *Sustainability* 7, 5875–5895. <https://doi.org/10.3390/su7055875>
- Liu, H., Janssen, M., Lennartz, B., 2016. Changes in flow and transport patterns in fen peat following soil degradation. *Eur. J. Soil Sci.* 67, 763–772. <https://doi.org/10.1111/ejss.12380>
- Liu, L., Gan, Y., Bueckert, R., Van Rees, K., 2011. Rooting systems of oilseed and pulse crops. II: Vertical distribution patterns across the soil profile. *F. Crop. Res.* 122, 248–255. <https://doi.org/10.1016/j.fcr.2011.04.003>
- Mualem, Y., 1976. A new model for predicting the hydraulic conduc. *Water Resour. Res.* 12, 513–522.
- Nouri, A., Lee, J., Yin, X., Tyler, D.D., Saxton, A.M., 2019. Thirty-four years of no-tillage and

cover crops improve soil quality and increase cotton yield in Alfisols, Southeastern USA.

Geoderma 337, 998–1008. <https://doi.org/10.1016/j.geoderma.2018.10.016>

Patra, S., Julich, S., Feger, K.H., Jat, M.L., Jat, H., Sharma, P.C., Schwärzel, K., 2019. Soil

hydraulic response to conservation agriculture under irrigated intensive cereal-based cropping systems in a semiarid climate. *Soil Tillage Res.* 192, 151–163.

<https://doi.org/10.1016/j.still.2019.05.003>

Sánchez-Navarro, V., Zornoza, R., Faz, Á., Fernández, J.A., 2019. Comparing legumes for use in

multiple cropping to enhance soil organic carbon, soil fertility, aggregates stability and vegetables yields under semi-arid conditions. *Sci. Hortic. (Amsterdam)*. 246, 835–841.

<https://doi.org/10.1016/j.scienta.2018.11.065>

Silva, A.P. da, Ball, B.C., Tormena, C.A., Giarola, N.F.B., Guimarães, R.M.L., 2014. Soil structure

and greenhouse gas production differences between row and interrow positions under no-tillage. *Sci. Agric.* 71, 157–162. <https://doi.org/10.1590/S0103-90162014000200011>

Silva, M.F. da, Fernandes, M.M.H., Fernandes, C., Silva, A.M.R. da, Ferraudo, A.S., Coelho, A.P.,

2021. Contribution of tillage systems and crop succession to soil structuring. *Soil Tillage Res.*

209, 104924. <https://doi.org/10.1016/j.still.2020.104924>

Soil Survey Staff, 2014. *Keys to Soil Taxonomy*, 12th ed. ed. USDA-Natural Resources

Conservation Service, Washington, DC.

Talukder, R., Plaza-Bonilla, D., Cantero-Martínez, C., Wendroth, O., Castel, J.L., 2022. Soil gas

diffusivity and pore continuity dynamics under different tillage and crop sequences in an irrigated Mediterranean area. *Soil Tillage Res.* 221, 105409.

<https://doi.org/10.1016/j.still.2022.105409>

van Genuchten, 1980. A closed-form equation for predicting the hydraulic conductivity of

unsaturated soils. *Soil Sci. Soc. Am. J.* 44, 892–898.

- Vanderlinden, K., Pachepsky, Y., Pedrera-Parrilla, A., Martinez, G., Espejo-Pérez, A., Perea, F., Giráldez, J., 2021. Water retention and field soil water states in a vertisol under Long-Term direct drill and conventional tillage. *Eur. J. Soil Sci.* 72, 667–678.
<https://doi.org/10.1111/ejss.12967>
- Villarreal, R., Lozano, L.A., Salazar, M.P., Bellora, G.L., Melani, E.M., Polich, N., Soracco, C.G., 2020. Pore system configuration and hydraulic properties. Temporal variation during the crop cycle in different soil types of Argentinean Pampas Region. *Soil Tillage Res.* 198, 104528.
<https://doi.org/10.1016/j.still.2019.104528>
- Watson, K.W., Luxmoore, R.J., 1986. Estimating Macroporosity in a Forest Watershed by use of a Tension Infiltrometer. *Soil Sci. Soc. Am. J.* 50, 578–582.
<https://doi.org/10.2136/sssaj1986.03615995005000030007x>
- Wendroth, O., Ehlers, W., Hopmans, J.W., Kage, H., Halbertsma, J., Wösten, J.H.M., 1993. Reevaluation of the Evaporation Method for Determining Hydraulic Functions in Unsaturated Soils. *Soil Sci. Soc. Am. J.* 57, 1436–1443.
<https://doi.org/10.2136/sssaj1993.03615995005700060007x>
- Zhang, Y., Niu, J., Zhang, M., Xiao, Z., Zhu, W., 2017. Interaction Between Plant Roots and Soil Water Flow in Response to Preferential Flow Paths in Northern China. *L. Degrad. Dev.* 28, 648–663. <https://doi.org/10.1002/ldr.2592>

Supplementary Tables

Table S3: Date of tillage, sowing or planting, chopping or harvesting, and undisturbed soil sampling, amount of rainfall and irrigation for 2018-19 to 2019-20.

Date	Tillage, sowing or planting and harvesting operation	Undisturbed soil sampling	From last tillage performed		
			Days	Rainfall (mm)	Irrigation (mm)
Period: 2018-19					
19 Oct. 2018		Before tillage (Initial)			
26 Oct. 2018	Till: IT plots (FM and LM) Sowing: legume (Peas, LM)				
21 Dec. 2018		After sowing legume when soil was consolidated (LM)	56	107	0
03 Apr. 2019		After tillage when soil was consolidated (FM)	159	125	27
12 Apr. 2019	Planting: long cycle maize (FM)				
18 June 2019	Harvesting: Legume (Peas, LM) Till: IT plots (LM)	After harvesting legume	234	204	127
27 June 2019	Planting: short cycle maize (LM)				
02 Aug. 2019		After planting maize when soil was consolidated (LM)	45	39	281
14 Oct. 2019	Harvesting: long cycle maize (FM)				
15 Oct. 2019		After harvesting maize, only NT plots (FM)	354	280	758
19 Nov. 2019	Harvesting: short cycle maize (LM)	After harvesting maize	155	167	360
Period: 2019-20					
18 Dec. 2019	Till: IT plots (FM and LM)				
10 Jan. 2020	Sowing: legume (Vetch, LM)				
28 Feb. 2020		After tillage when soil was consolidated (FM) After sowing legume when soil was consolidated (LM)	72	50	0

01 May 2020	Till: IT plots (FM)		136	198	0
02 May 2020	Planting: long cycle maize (FM)				
21 May 2020	Chopping: Legume (Vetch, LM)	After chopping legume (ACL)	155	239	0
	Till: IT plots (LM)				
28 May 2020	Planting: short cycle maize (LM)				
06 June 2020		After planting maize when soil was consolidated (FM)	36	75	2
01 July 2020		After planting maize when soil was consolidated (LM)	41	58	46
23 Sep. 2020	Harvesting: long cycle maize (FM)				
21 Oct. 2020	Harvesting: short cycle maize (LM)	After harvesting maize (FM and LM)	153	321	582

Table S4: Analysis of variance (p-values) of saturated soil water content (θ_s , $\text{cm}^3 \text{cm}^{-3}$), saturated soil hydraulic conductivity (K_s , cm day^{-1}), specific hydraulic conductivity (K_{pc} , cm day^{-1}), number of effective pores (N_{pc} , m^{-1}), pore volume (ϕ_{pc} , $\text{cm}^3 \text{cm}^{-3}$) and pore continuity index (C_{wpc}) affected by sampling dates and tillage systems and their interactions in two different crop sequences (FM: short fallow-maize; LM: legume-maize).

Source of variation	θ_s $\text{cm}^3 \text{cm}^{-3}$	K_s^\ddagger cm day^{-1}	K_{pc} cm day^{-1}	N_{pc} m^{-1}	θ_{pc} $\text{cm}^3 \text{cm}^{-3}$	C_{wpc}
Pore class (μm)			>1000 1000-60	>1000 1000-60	>1000 1000-60	>1000 1000-60
Short fallow-maize (FM)						
Sampling date (SD)	NS	0.0007	0.0007	0.03	0.0007	0.03
Tillage (T)	0.03	NS	NS	NS	NS	NS
SD *T	NS	NS	NS	NS	NS	NS
Legume-maize (LM)						
Sampling date (SD)	0.002	<0.0001	0.005	NS	0.005	NS
Tillage (T)	NS	NS	NS	NS	NS	NS
SD *T	NS	0.007	0.01	NS	0.009	NS

\ddagger , data were BoxCox-transformed before analysis. NS, non-significant ($p > 0.05$).

Chapter III

Spatio-temporal variation of surface soil hydraulic properties under different tillage and maize-based crop sequences in a Mediterranean area

Accepted: Plant and Soil

Spatio-temporal variation of surface soil hydraulic properties under different tillage and maize-based crop sequences in a Mediterranean area

Rasendra Talukder^{*a}, Daniel Plaza-Bonilla^b, Carlos Cantero-Martínez^{bc}, Simone Di Prima^d, Jorge Lampurlanés^{ac},

^aDepartment of Agricultural and Forest Engineering, University of Lleida-AGROTECNIO-CERCA Center, Av. Rovira Roure 191, 25198 Lleida, Spain

^b Department of Crop and Forest Sciences - Agrotecnio-CERCA Center, Universitat de Lleida, Av. Rovira Roure 191, 25198 Lleida, Spain.

^cAssociate Unit CSIC (Research Spanish Council)

^dDepartment of Agriculture, Università degli Studi di Sassari, Piazza Università 21, Sassari, Italy

* corresponding author: rasendra.talukder@udl.cat

Abstract

Aims

The surface crust formed by the drop impact of rainfall and/or irrigation is a prevalent characteristic in many Mediterranean soils. However, the temporal variation of soil hydraulic properties induced by surface crust during the high-frequency irrigation has rarely been investigated.

Methods

Beerkan infiltration tests in conjunction with the BEST method were used to investigate the effects of surface crusting on the spatio-temporal variation of saturated soil hydraulic conductivity (K_s , mm s⁻¹), sorptivity (S , mm s^{-0.5}), mean pore size (r , mm), number of effective pores per unit area (N , m⁻²) in Agramunt, NE Spain.

Results

In response to autumn tillage, intensive tillage (IT) increased K_s and S due to higher r and N , but both declined after 60 days. Reduced tillage (RT), maintained comparable K_s and S values, despite having a lower N value. After the spring tillage, both IT and RT developed crusted layers, resulting in decreased K_s , S and N . Long-term no-tillage (NT) showed an increasing trend of K_s and S over time, except for the last sampling. Spatial variation (i.e., between the rows, B-row vs. within the row of crops, W-row) of K_s and S was found, and non-crustrated soils (W-row) had consistently higher K_s (LM: 0.021 vs. 0.009 mm s⁻¹, and FM: 0.015 vs. 0.005 mm s⁻¹) and S than crusted soils (B-row).

Conclusions

Conservation tillage i.e., RT and NT improve the surface soil structure and reduce the risk of crust development. Surface cover by crops may help to prevent crust formation within the row of crops, improving soil hydraulic conductivity.

Keywords: Soil crust, Crop diversification, Conservation agriculture, Saturated hydraulic conductivity, Sorptivity, BEST method

1. Introduction

Many soils, particularly in arable arid and semi-arid areas, form thin, compacted, dense surface layers with lower porosities and higher bulk densities than the soils underneath (Neave and Rayburg, 2007). These layers, also known as "structural crusts," are formed by two complex mechanisms i.e., (i) physical dispersion and (ii) chemical dispersion (Agassi et al., 1981). A physical dispersion of aggregates may happen, when soils are subjected to high-intensity water drops, whether by rain and/or irrigation. Since rainfall or irrigation began, the surface soil starts to wet rapidly, non-stable soil aggregates are broken and soil particles isolated, reorganized, and consolidated, clogging the pores, which in turn, form an unstructured layer. Further, splashing of fine particles transported in suspension by runoff in soil depressions and the subsequent drying form a thick soil layer (Badorreck et al., 2013). A chemical dispersion (or leaching of fine particles), on the other hand, is determined by the soil mineralogy, soil exchangeable sodium percentage (ESP), sodium absorption ration (SAR), and the electrolyte concentration (EC) of rain or irrigation water. The wet phase of this layer is referred as a "seal" and when dries is called "crust" (Moore and Singer, 1990; Assouline, 2004). Surface crusting is an indicator of land degradation for a variety of reasons. For instance, it impaired infiltration and percolation (Souza et al., 2014; Alagna et al., 2019), which generates runoff and erodes the soil surface (Wu et al., 2016), limiting solute and gas transport, seedling emergence, and root penetration (Baumhardt et al., 2004; Gabriel et al., 2021), and ultimately reducing crop yields (Souza et al., 2014; Ramos et al., 2019). Soil inherent properties like silt and clay content, and exchangeable sodium percentage increases the likelihood of soil sealing and crusting, while aggregate stability, organic matter content and electrolyte concentration reduces it (Agassi et al., 1981; Vandervaere et al., 1997; Šimůnek et al., 1998; Chen et al., 2013). Soils rich in silt and clay were found more prone to soil sealing with a low-intensity rainfall than sandy soils. When rain drops (distilled water) lowers the electrolyte concentration below the flocculation

threshold at the soil surface, particle dispersion (and leaching) takes place and stimulate the soil sealing (Chen et al., 2013). Similarly, soils rich in quartz content significantly increases crust strength due to its inertness, which makes the soil highly dispersive (Nciizah and Wakindiki, 2014). Beside this, soil with a high ESP (≥ 6.4) can promote particle dispersion, crust formation, and a significant decrease in infiltration (Agassi et al., 1981), while an increase in EC decreases the chemical dispersion.

In addition, soil management practices have a substantial impact on surface soil crusting that is dependent on pedo-climatic conditions, soil textural type. For instance, Usón and Poch (2000) reported that crusting on a silty loam soils under rain-fed semiarid conditions was unaffected by tillage practices, whilst Palese et al. (2014) observed the opposite results on a sandy soils under rain-fed semiarid conditions (slope gradient was 0 to 16%). They noted that continuous IT made the soil much more vulnerable to crusting due to lower aggregate stability and reduced surface cover by crop residues (residue incorporation by tillage). In contrast, absence of disturbance (tillage) and surface cover by crop residues in NT reduced the risk of crusting.

Furthermore, crop residues improvesoil structural properties directly by preventing waterdrop impact and indirectly by promoting biological activity i.e., earthworms which help to create bio-channels and facilitating water flow. Crop sequences can also modify some soil properties related to soil crusting. For instance, cultivation of winter crop before summer crop can cover bare soil with living crops or residues, lowering water drop impact and protecting soils. In this regard, replacing the fallow season with a crop is a good practise for lowering soil crust development (Wu et al., 2016; Gabriel et al., 2021). Gabriel et al. (2021) reported that under irrigated condition replacemnet of bare fallow by cover crops (barley, *Hordeum vulgare L.*, or vetch, *Vicia sp. L.*) together with summer crops (maize, *Zea mays L.*, or sunflower, *Helianthus annuus L.*) enhanced the soil surface conditions and prevent the crust formation under reduced tillage in a long-term field experiment in Spain. However, studies on soil crusting were

conducted separately to determine the differences between vegetation cover and bare or fallow conditions (Neave and Rayburg, 2007; Ries and Hirt, 2008; Gabriel et al., 2021), as well as various tillage treatments (Usón and Poch, 2000; Wu et al., 2016; Ramos et al., 2019). Yet, there is a knowledge gap on soil crusting effects on soil hydro-physical properties under different tillage and crop sequences.

Rainfall and irrigation events after tillage and sowing can induce changes on soil hydraulic properties during the growing season due to modification of soil surface, and crust formation. Pareja-Sánchez et al. (2017), working on the same experimental field, found that the potential route of irrigation water and soil losses (by splashing and soil sealing) occurred between rows (B-row), and it was more evident in IT than in NT. They explained this was due to lack of vegetation cover B-row, and lack of crop residues on the soil surface during most part of the crop growing season when IT is used. Moreover, infiltration shows a highly dynamic behaviour during rainfall and irrigation events, intensity and time (Mubarak et al., 2009; Badorreck et al., 2013). For instance, Mubarak et al. (2009) reported that, soil hydraulic conductivity reached a very low value at the end of irrigation period compared to initial under high frequency drip irrigation during a maize growing season. However, given the importance of soil surface crusting on soil water balance, most studies were conducted in rain-fed conditions (Moore and Singer, 1990; Vandervaere et al., 1997; Baumhardt et al., 2004; Neave and Rayburg, 2007; Ries and Hirt, 2008; Alagna et al., 2013, 2019; Nciizah and Wakindiki, 2014), with only a few undertaken under irrigated conditions (Gabriel et al., 2021).

In Mediterranean area, evapotranspiration in summer periods, with rising temperatures and lower precipitation, is mostly balanced by high-frequency water applications in newly irrigated areas. During the irrigation period, water supply would have to cover a growing water demand; hence, knowledge about crust development and associated impact on soil hydraulic properties over time is required to establish an appropriate irrigation plan preventing soil and water losses

by overflow. This is especially important in non-flat areas with sprinkler irrigation systems. As a matter of fact, penetration resistance (PR) was measured in the same experimental field to characterize crust strength and it was reported that PR increased over time after tillage under IT and RT between row of crops (B-row). Beside this, PR was lower within the row of crops (W-row) and similar regardless of tillage treatment (Pareja-Sánchez et al., 2017). However, this previous study did not investigate the consequence of crusting on surface soil hydro-physical properties dynamics. Therefore, research concerning the effect of crusting on soil hydro-physical properties over time under different management practices in irrigation conditions is still scarce.

This study used the Beerkan Estimation of Soil Transfer (BEST) method (Lassabatère et al., 2006) to obtain the soil water characteristics from small shallow circular ponds transient infiltration measurements in a field with high-frequency sprinkler irrigation and 2% slope. The objectives of this investigation were to assess the effect of crust on (i) soil physical and hydrodynamic properties and (ii) its spatio-temporal variations under various tillage, crop sequences, and position with respect to the crop row.

2. Materials and Methods

2.1 Experimental site and design

This research was carried out on a long-term field experiment (26 years) in Agramunt, NE Spain (41°48' N, 1°07' E, 330 m asl). The climate of the area is semiarid Mediterranean, with 401 mm mean annual precipitation and 14.1 °C mean temperature. The soil has a 2% slope and was classified as Typic Xerofluvent according to USDA (Soil Survey Staff, 2014). The upper (0–5 cm) horizon has a silt loam texture (Ramos et al., 2019). Other soil properties were pH (H₂O, 1:2.5): 8.5 and electrical conductivity (1:5): 0.15 dS m⁻¹ (Cantero-Martínez et al., 2003).

The field was established in 1996 to compare three tillage systems, intensive tillage (IT), reduced tillage (RT), and no-tillage (NT), as well as three levels of mineral nitrogen (zero,

medium, and high), with a single crop (barley) grown under rain-fed conditions (Angás et al., 2006). In 2015, a solid set sprinkler irrigation system was installed in the experimental field and transformed to irrigated conditions (Pareja-Sánchez et al., 2017).

Crop sequence was added as a factor in 2018 and it has two levels: short-term fallow-maize (*Zea mays* L.) (FM) and legume (pea; *Pisum sativum* L. or vetch; *Vicia sativa* L.)-maize (LM). Summer and winter crops, respectively, were maize and legume. A split-plot with three replications was used for the experimental design (three blocks). The tillage plots were 50 m long and 6 m in width, and the crop sequence plots were 50 m long and 3 m in width. The present work was done in 2020-21, during the third year after introducing the crop sequences, using vetch as winter crop for LM. Only the plots under medium fertilization rate were included in the experiment. Soil organic carbon concentration (0-5 cm depth) was 21.1, 14.8 and 10.3 g C kg⁻¹ soil for NT, RT and CT, respectively (Pareja-Sánchez et al., 2017).

On the IT and RT plots, tillage was performed twice: autumn and spring. Autumn tillage was done on the same day for both FM and LM, however spring tillage took place before planting maize at different times, one month earlier for FM (late maturing maize) than for LM (early maturing maize) (Fig. 1). In IT plots, autumn tillage consisted of a subsoiler pass (depth: 35 cm) followed by a chisel (depth: 15 cm) (which helped to incorporate crop residues into the soil nearly 100%) and a roller (to make the surface even). The spring tillage consisted of a rototiller (15 cm depth) followed by a chisel pass and a roller. In contrast, RT plots had similar tillage practices in both autumn and spring, a chisel pass (15 cm depth) and a roller. In NT plots, glyphosate spraying was done prior to planting. In the three tillage systems, vetch and maize were both planted using the pneumatic row direct drilling machine. Double disc furrow openers were used to make the slots, and rotary residue row cleaners were used to clear the path for the opening of the row unit.

Irrigation was scheduled weekly using the crop evapotranspiration (ET_c) estimations of the Department of Agriculture of the Generalitat de Catalunya for the specific site, crops and growing stage. Due to the irrigation system design constraints, every irrigation sector included plots with different crops or growing stages, and the irrigation doses were selected according to the most demanding crop. During 2018-19, the irrigation dose was applied in one event per day, and water losses by runoff were observed, especially in IT. Then, from 2019-20, the irrigation dose was split in two events per day to reduce runoff. Maximum daily irrigation dose was $90 \text{ m}^3 \text{ ha}^{-1}$, and the precipitation rate of the sprinklers 6 mm h^{-1} (Christiansen Uniformity Coefficient: 78.10). Irrigation water comes from a snow-fed river's dam, which explain its low EC (0.237 dS/m) and SAR is also low (0.30). According to Ayers and Westcot (1985), with these values, there is no risk of reduced water availability nor toxicity for the plants, but irrigation water can have a slight to moderate effect on infiltration rate.

Vetch was mowed as fodder, and maize was harvested using a commercial combine harvesting machine. After harvesting, the residue was chopped and spread over the soil surface.

2.2 Soil sampling and infiltration measurements

A total of 180 infiltration runs covering approximately a total of 318 m^2 were carried out at five sampling times, with two runs per plot. The first three samplings were done 18, 60, and 137 days after the autumn tillage (30 November 2020), while vetch was grown in LM and FM was left fallow (Fig. 13). The last two samplings were conducted 63, and 205 (FM)/177 (LM) days after the spring tillage (21 April 2021 for FM, and 19 May 2021 for LM). LM plots had two distinct positions for the infiltration runs: W-row, and B-row. Similarly, FM plots had two samplings, during the fallow period, when there was no distinguishable position.

Infiltration runs were carried out with the Beerkan method following Lassabatère et al. (2006). Briefly, at every infiltration run, a stainless-steel ring of known inner diameter (135 or 150 mm) and height (100 mm) was installed on a relatively flat place. The ring was inserted into the soil

surface a shallow depth (approximately 10 mm) to avoid lateral losses of water. In case of RT and NT, the crop residue and litter were removed prior to ring installation. Initial soil water content ranged between 0.17-0.29 $\text{cm}^3 \text{cm}^{-3}$, which helped to prevent crust alteration during ring installation. When soil surface was too dry, before ring installation, a syringe was used to introduce some water to the ring wall to avoid crust breakdown. Then, known volumes of water, usually 100 mL, were repeatedly poured into the ring, and the elapsed time to complete infiltration recorded. To reduce the possibility of crust alteration, water was added from a close distance at low rate. The time to infiltrate was increasing with each pouring. In some cases, when filtration was low owing to the crust and time to infiltrate was too long, the volume of water poured was reduced from 100 to 50 mL. This adjustment helped to obtain enough points of the cumulative infiltration curve for fitting the BEST algorithms. The infiltration test was continued until the difference in infiltration time between successive pouring's was negligible, indicating essentially steady-state infiltration, or until a pre-determined amount of water pouring's, never less than eight, were applied (Lassabatère et al., 2006). Additionally, soil samples (0-0.05 m depth) were collected close to the point of infiltration runs to determine the dry soil bulk density, ρ_b and initial soil water content, θ_0 . The bulk density (g cm^{-3}) was calculated as the ratio of oven-dried soil mass (g) to soil bulk volume (cm^3). To obtain oven-dried soil mass, the core soil (diameter: 0.06 m, and height: 0.05 m) was dried at 105 °C for 24 h. Soil water content was determined gravimetrically and multiplied by ρ_b to obtain volumetric soil water content.

To determine soil hydraulic properties, the BEST algorithms were used (Lassabatère et al., 2006). BEST algorithms determine the soil water retention curve $\theta(h)$ using the van Genuchten (1980) equation (Eq. (1a)), and the hydraulic conductivity function $K(\theta)$ using the Brooks and Corey (1964) equation (Eq. 2a), following Burdine (1953) conditions (Eq. 1b) and (Eq. 2b), respectively.

$$\frac{\theta - \theta_r}{\theta_s - \theta_r} = \left(1 + \left(\frac{h}{h_g}\right)^n\right)^{-m} \quad (1a)$$

$$m = 1 - \frac{2}{n} \quad (1b)$$

$$\frac{K(\theta)}{K_s} = \left(\frac{\theta - \theta_r}{\theta_s - \theta_r}\right)^\eta \quad (2a)$$

$$\eta = \frac{2}{mn} + 2 + p \quad (2b)$$

where θ_r and θ_s are the residual and saturated volumetric water content ($\text{cm}^3 \text{cm}^{-3}$), respectively; n and m are shape parameters, and h_g is the pressure head scale parameter (mm) representing the inflexion point of the water retention curve $\theta(h)$, K_s is the saturated hydraulic conductivity (mm s^{-1}) and η is the shape parameter of the soil hydraulic conductivity function $K(\theta)$; p is the tortuosity factor set equal to 1 when the m and n relationship is described by Eq. 1b. According to Haverkamp et al. (2006), shape parameters n , m , and η are dependent on soil texture (soil management practices would not change those parameters), whilst θ_s , K_s , and h_g are scaling parameters dependent on soil structure (soil management practices would change those parameters).

In BEST, the θ_r is assumed to be zero. The θ_s was assumed to equal total porosity that was estimated from soil bulk density and soil mineral particles density (2.65 g cm^{-3}). The n parameter was computed from soil sand ($>0.05 \text{ mm}$) and clay ($<0.002 \text{ mm}$) percent (Minasny and McBarney, 2007) which were 22.5 % and 13.7% in block 1, 29.9 % and 11.7% in block 2, and 41.6% and 9.5% in block 3, and m and η from Eq. (1b) and (2b) respectively.

The h_g shape parameter was estimated by the following relationship:

$$h_g = - \frac{S^2}{C_p(\theta_s - \theta_0) \left[1 - \left(\frac{\theta_0}{\theta_s}\right)^\eta\right] K_s} \quad (3)$$

where S ($\text{mm s}^{-0.5}$) and θ_r ($\text{cm}^3 \text{cm}^{-3}$) are the soil sorptivity and initial soil water content, respectively. C_p is a coefficient dependent on n , m , and η (Lassabatère et al., 2006), and hence on soil texture. In BEST, S and K_s are estimated by fitting the Haverkamp's three-dimensional infiltration model (Haverkamp et al., 1994) to the experimental infiltration data.

Three alternative BEST algorithms are used i.e., BEST-slope (Lassabatère et al., 2006), that uses the slope of the regression of the last points (steady-state) to link S and K_s before fitting the transient model to the cumulative infiltration data while optimizing S , BEST-intercept (Yilmaz et al., 2010), that uses the intercept instead of the slope of the regression of the last points (steady-state) to link S and K_s before optimizing S with the transient data, and BEST-steady (Bagarello et al., 2014), that uses both the intercept and the slope of the regression of the last points (steady-state) to estimate S and K_s without fitting the transient state. All three fittings were done using the workbook from Di Prima (2013), available at <https://bestsoilhydro.net/downloads/>. Lassabatère et al. (2019) recommended to combine the estimates of all three algorithms. However, the BEST-slope algorithm results were not considered to estimate soil hydraulic parameters in this experiment because it failed to converge most of the times, particularly for crusted soil (Angulo-Jaramillo et al., 2019). Then, the results from the BEST-intercept and the BEST-steady algorithms were averaged to obtain the scale parameters θ_s , S , and K_s before statistical analysis.

Using capillary theory (Philip, 1987), the “mean” characteristic pore size (radius) can be obtained from the following equation (Mubarak et al., 2009b):

$$r = -\frac{2\sigma\cos\beta}{\rho g\alpha_h} \quad (4)$$

where σ is the soil-water surface tension (MT^{-2}), ρ is the density of water (ML^{-3}), g is the acceleration due to gravity (LT^{-2}), β is the contact angle between the water and the pore wall (assumed to be 0) and α_h is the capillary length (mm). The r (Eq. 5) represents the mean diameter of pores that are hydraulically functional at the time of infiltration. As r increases, capillary forces decrease, and gravity forces progressively dominate the infiltration process.

α_h was calculated from the following simplified equation proposed by Di Prima et al. (2020).

$$\alpha_h = 0.861 \frac{b_s}{\Delta\theta} \quad (5)$$

where b_s is the intercept of the linear regression obtained from the steady-state portion of the cumulative infiltration curve. $\Delta\theta$ is the difference between saturated (θ_s) and initial (θ_i) soil water content. The α_h indicates the relative magnitude of capillary and gravity forces ($\alpha_h > 1000$ mm capillarity forces dominant, $\alpha_h < 10$ gravity forces dominant) that were present at the time of infiltration process from initial (θ_i) to saturated (θ_s) soil water content (Angulo-Jaramillo et al., 2000).

The number of effective pores N per unit area (m^{-2}), was calculated according to Watson and Luxmoore (1986), using r values and the Poiseuille equation:

$$N = \frac{8\mu K_s}{\pi\rho g r^4} \quad (6)$$

where μ is the dynamic viscosity of water ($\text{ML}^{-1}\text{T}^{-1}$). The N illustrates the number of hydraulically active pores present per unit area.

2.3 Statistical analysis

All the statistical analyses were done with the statistical package JMP Pro 16 (SAS Institute Inc, 2022). Data were checked for distribution (normality) and homogeneity of variance by the Shapiro-Wilk test and the Levene test, respectively. Variables such as S , K_s , r and N were BoxCox-transformed before analysis. An analysis of variance (ANOVA) was performed for measured (ρ_b and θ_i) and estimated (θ_s , S , K_s , r , and N) data to test the treatment (main) and their interactions effects. According to Federer and King (2006), sampling times were taken into account for main plot, following subplots included tillage systems and crop sequences. When the effects of treatments or interactions were significant, Student's t-tests were used to compare means at the 0.05 level of significance.

3. Results

The amount of rainfall + irrigation that was received on 18, 60, and 138 days after autumn tillage, was the same for LM and FM: $11 + 0 = 11$ mm, $29 + 0 = 29$ mm, and $45 + 27 = 72$ mm,

respectively (Fig. 13). After the spring tillage, a varying amount of rainfall + irrigation was received by FM and LM, notably on 63 days, FM: $63 + 102 = 165$ mm, and LM: $23 + 242 = 265$ mm; 205/177 days, FM: $60 + 565 = 625$ mm, and LM: $55 + 398 = 453$ mm.

3.1 Bulk density

A significant interaction was observed between DAT and crop sequence ($p = 0.005$) on bulk density (ρ_b) (Table 8). ρ_b changed over time and significant differences between crop sequences were observed after autumn and spring tillage. LM had higher ρ_b at 18 days after autumn tillage, whilst lower ρ_b at 63 days after spring tillage, compared to FM (Table 9, and Fig. 14).

ρ_b differences between the two positions considered, W-row and B-row, were always significant in LM ($p = 0.0003$) and FM ($p = 0.0001$) (Table 10). W-row had lower ρ_b compared to B-row (1.25 vs. 1.35 g cm⁻³ in LM, and 1.25 vs. 1.37 g cm⁻³ in FM).

3.2 Initial soil water content

Initial soil water content (θ_0) was significantly affected by DAT ($p < 0.001$) and tillage ($p < 0.001$) but not by crop sequences (Table 8). After autumn tillage at 60 days and spring tillage at 63 days, the highest (0.29 cm³ cm⁻³) and the lowest (0.17 cm³ cm⁻³) θ_0 were observed, respectively (Table 9). From highest to lowest, θ_0 followed the order NT > RT > IT (0.30, 0.22, and 0.19 cm³ cm⁻³, respectively) (Table 9). No significant interaction was observed among days after tillage (DAT), tillage, and crop sequences.

The difference between the two positions was always significant ($p = 0.04$ in LM, $p = 0.02$ in FM) (Table 10). W-row θ_0 was lower than the B-row (0.22 vs. 0.24 cm³ cm⁻³ in LM, and 0.20 vs. 0.22 cm³ cm⁻³ in FM).

3.3 Sorptivity

A significant interaction between DAT and tillage ($p < 0.0001$), and between tillage and crop sequence ($p = 0.03$) were observed on sorptivity (S) (Table 8)

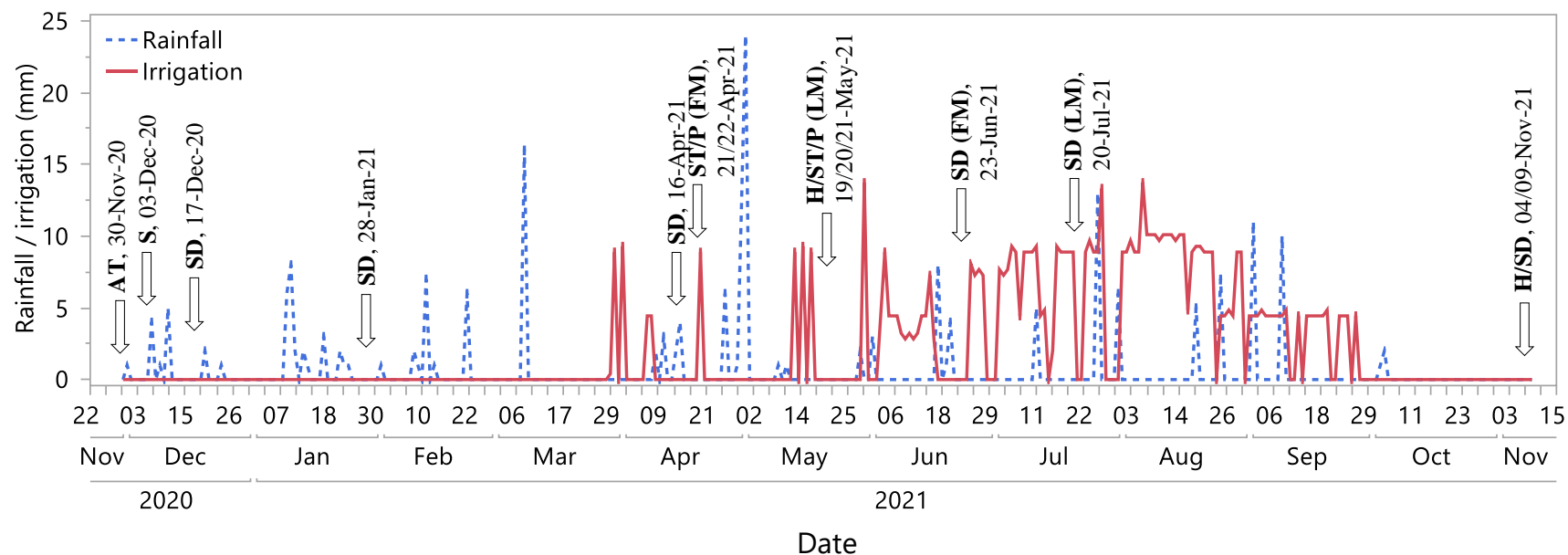


Fig. 13: Rainfall or irrigation (mm day^{-1}) during the experimental year (2020-21). Arrows represent key dates of management practice and sampling (AT, autumn tillage; S, sowing vetch, SD; sampling date, ST, spring tillage; P, planting maize; H, harvesting).

Table 8: ANOVA (p-values) of soil bulk density (ρ_b , g cm^{-3}), initial soil water content (Θ_0 , $\text{cm}^3 \text{cm}^{-3}$), sorptivity (S , $\text{mm s}^{-0.5}$), saturated hydraulic conductivity (K_s , mm s^{-1}), mean pore size (r , mm) and number of pores per unit area (N , m^{-2}) affected by days after autumn (18, 60, 138 days) and spring tillage (63, 205 and 177 days for FM and LM, respectively), tillage systems (IT: intensive tillage, RT: reduced tillage, and NT: no-tillage), crop sequences (FM: fallow-maize, LM: legume-maize) and their interactions.

Source of variation	ρ_b (g cm^{-3})	Θ_0 ($\text{cm}^3 \text{cm}^{-3}$)	S * ($\text{mm s}^{-0.5}$)	K_s * (mm s^{-1})	r * (mm)	N * (m^{-2})
Days after tillage (DAT)	0.004	<.0001	0.0002	0.0003	<.0001	<.0001
Tillage (Till.)	<.0001	<.0001	<.0001	<.0001	0.005	0.0003
DAT *Till.	NS	NS	<.0001	<.0001	0.002	0.0006
Crop sequence (CS)	NS	NS	NS	NS	NS	NS
DAT *CS	0.005	NS	NS	NS	NS	NS
Till. * CS	NS	NS	0.03	NS	NS	NS
DAT *Till. *CS	NS	NS	NS	NS	NS	NS

*, data were BoxCox transformed before analysis; NS, non-significant at $p > 0.05$.

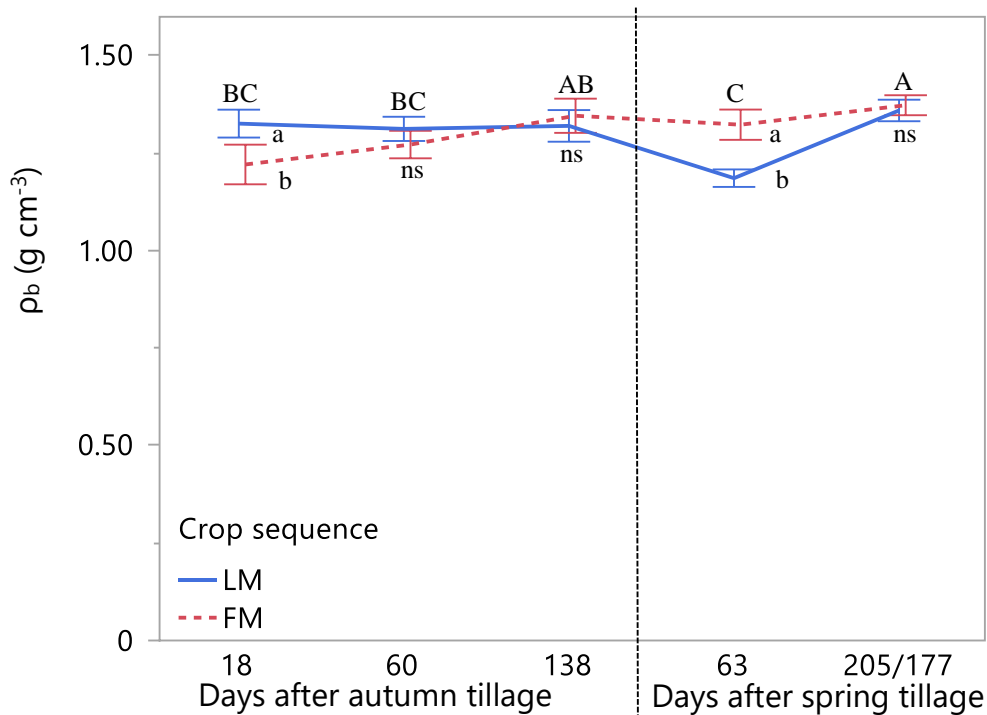


Fig. 14: Bulk density (ρ_b , g cm^{-3}) dynamics at different days after autumn and spring tillage under two crop sequences (FM: fallow-maize, LM: legume-maize). Error bars show the standard error. Vertical dashed line separates the days after autumn and spring tillage. Different letters (uppercase letters among days after tillage and lowercase letters between crop sequences within each sampling date) indicate significant differences between treatments at $p < 0.05$; ns, non-significant.

Apart from 205/177 days after spring tillage (Fig. 15), the differences between IT and NT on S were substantially greater, as they were changes over time. On the other hand, RT showed little variation on S over time. Differences between LM and FM on S were only significant under NT (Table 8 and Fig. 16), with greater values for FM compared to LM.

Position always had a significant effect on S ($p = 0.0003$ in LM, $p = 0.0004$ in FM) (Table 10). W-row S was remarkably greater than B-row (0.65 vs. 0.38 $\text{mm s}^{-0.5}$ in LM, and 0.66 vs. 0.37 $\text{mm s}^{-0.5}$ in FM).

3.4 Saturated hydraulic conductivity

A significant interaction between DAT and tillage was observed on saturated hydraulic conductivity (K_s) (Table 8). Regardless of the tillage systems, K_s experienced significant changes over time (Fig. 15). IT increased K_s from 18 days after the autumn tillage up to 60 days, then decreased to 138 days and maintained similar or slightly higher K_s after the spring tillage. RT maintained a high K_s after the autumn tillage, which decreased remarkably after the spring tillage. NT had lower K_s at 18 and 60 days after the autumn sowing, then increased K_s until 138 days. K_s was maintained up to 63 days after the spring sowing and then decreased to 205/177 days.

The effect of position on K_s was always significant in LM ($p = 0.0001$), and FM ($p = 0.001$) (Table 10). W-row K_s was greater compared to B-row (0.021 vs. 0.009 mm s^{-1} in LM, and 0.015 vs. 0.005 mm s^{-1} in FM).

Table 9: Means' comparisons of soil bulk density (ρ_b , g cm^{-3}), initial soil water content (Θ_0 , $\text{cm}^3 \text{cm}^{-3}$), sorptivity (S , $\text{mm s}^{-0.5}$), saturated hydraulic conductivity (K_s , mm s^{-1}), mean pore size (r , mm) and number of pores per unit area (N , m^{-2}) for different days after autumn and spring tillage, three tillage systems (IT: intensive tillage, RT: reduced tillage, and NT: no-tillage) and two crop sequences (FM: fallow-maize, LM: legume-maize). Amount of rainfall and irrigation (mm) received between two consecutive samplings.

Factors	Levels	ρ_b (g cm^{-3})	Θ_0 ($\text{cm}^3 \text{cm}^{-3}$)	S * ($\text{mm s}^{-0.5}$)	K_s * (mm s^{-1})	r * (mm)	N * (m^{-2})	Rainfall (mm)	Irrigation (mm)
Days after tillage									
Autumn tillage									
	18	1.27 bc	0.25 b	0.62 ab	0.018 ab	0.18 bc	8.43×10^7 a	11	0
	60	1.29 bc	0.29 a	0.66 a	0.020 a	0.14 c	8.95×10^7 a	29	0
	138	1.33 ab	0.20 c	0.39 c	0.016 b	0.37 a	6.17×10^7 b	45	27
Spring tillage									
	63 (FM)	1.25 c	0.17 d	0.55 ab	0.013 b	0.28 ab	7.05×10^7 b	63	102
	(LM)							23	242
	205 (FM)	1.37 a	0.25 b	0.43 b	0.007 c	0.11 d	9.21×10^7 a	60	565
	177 (LM)							55	398
Tillage									
	IT	1.30 b	0.19 c	0.44 c	0.010 b	0.29 a	6.83×10^7 b		
	RT	1.23 c	0.22 b	0.67 a	0.018 a	0.19 b	8.38×10^7 a		
	NT	1.38 a	0.30 a	0.47 b	0.015 a	0.16 b	8.68×10^7 a		
Crop sequence									
	FM	1.31 a	0.24 a	0.57 a	0.015 a	0.21 a	8.10×10^7 a		
	LM	1.30 a	0.23 a	0.48 a	0.014 a	0.22 a	7.83×10^7 a		

*, data were BoxCox transformed before analysis; different letters within the column indicate significant differences at $p < 0.05$.

Table 10: Means' comparisons of soil bulk density (ρ_b , g cm^{-3}), initial soil water content (Θ_0 , $\text{cm}^3 \text{cm}^{-3}$), sorptivity (S , $\text{mm s}^{-0.5}$), saturated hydraulic conductivity (K_s , mm s^{-1}), mean pore size (r , mm) and number of pores per unit area (N , m^{-2}) for two positions (W-row: within the crop row, B-row: between crop rows).

Factors	Levels	ρ_b (g cm^{-3})	Θ_0 ($\text{cm}^3 \text{cm}^{-3}$)	S^* ($\text{mm s}^{-0.5}$)	K_s^* (mm s^{-1})	r^* (mm)	N^* (m^{-2})
LM (all sampling time had distinguished position)							
Position	B-row	1.35 a	0.24 a	0.38 b	0.009 b	0.20 a	6.90×10^7 b
	W-row	1.25 b	0.22 b	0.65 a	0.021 a	0.20 a	7.88×10^7 a
p value		0.0003	0.04	0.0003	0.0001	NS	0.0003
FM (after spring tillage, FM had distinguished position at 63 and 205/177 days)							
Position	B-row	1.37 a	0.22 a	0.37 b	0.005 b	0.17 a	7.68×10^7 b
	W-row	1.25 b	0.20 b	0.66 a	0.015 a	0.17 a	8.02×10^7 a
p value		0.0001	0.02	0.0004	0.001	NS	0.005

*, data were BoxCox transformed before analysis; different letters within the column indicate significant differences at $p < 0.05$.

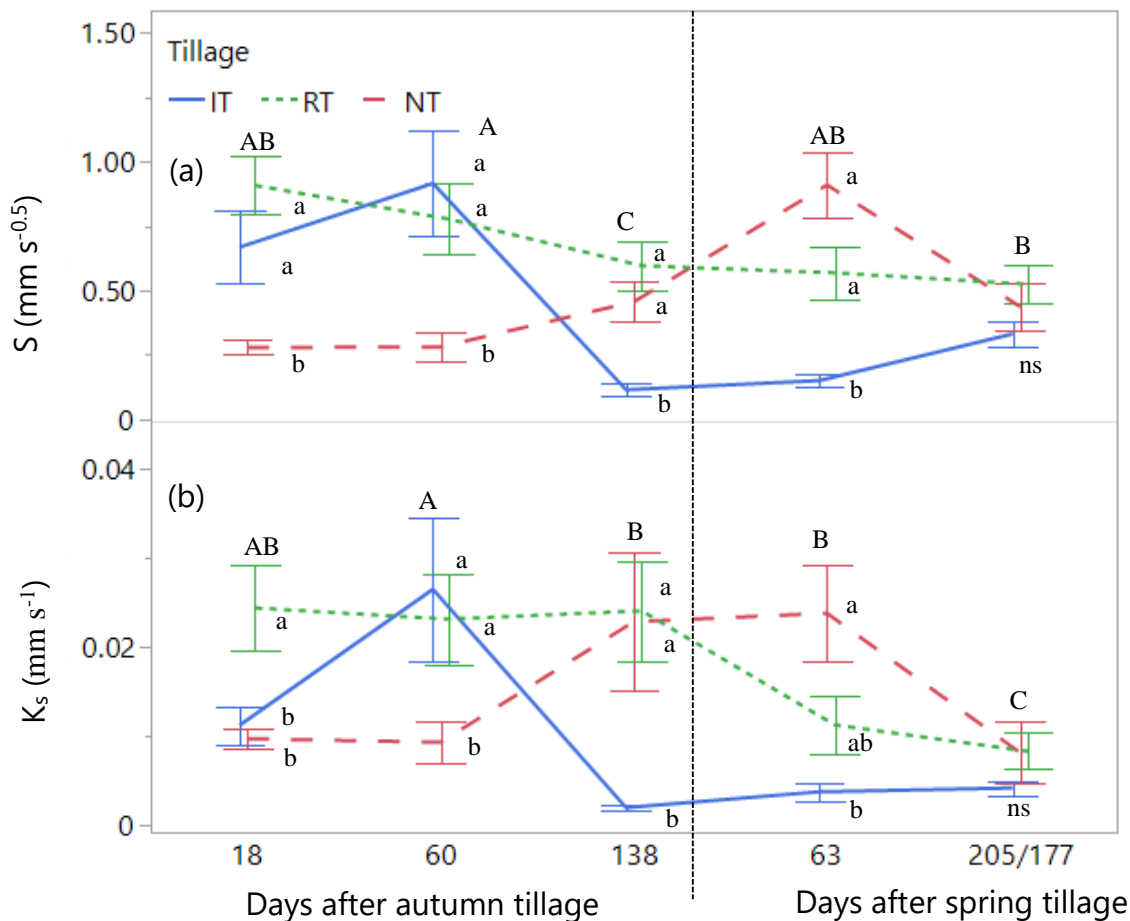


Fig. 15: Sorptivity (a) (S , $\text{mm s}^{-0.5}$) and saturated hydraulic conductivity (b) (K_s , mm s^{-1}) dynamics at different days after tillage and tillage systems (IT: intensive tillage, RT: reduced tillage, and NT: no-tillage). Error bars show the standard error. Vertical dashed line separates the days after autumn and spring tillage. Different letters (uppercase letters among days after tillage and lowercase letters among tillage systems within each sampling date) indicate significant differences between treatments at $p < 0.05$; ns, non-significant.

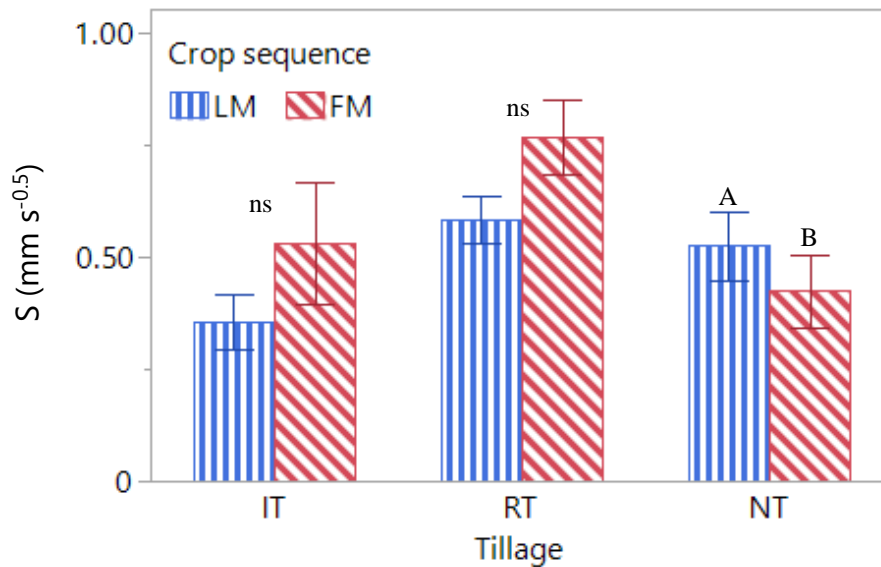


Fig. 16: Sorptivity (S , $\text{mm s}^{-0.5}$) under different tillage (IT: intensive tillage, RT: reduced tillage, and NT: no-tillage) and crop sequences (FM: fallow-maize, LM: legume-maize) (different sampling times were averaged). Error bars show the standard error and different uppercase letters indicates significant differences between treatments at $p < 0.05$; ns: non-significant).

3.5 Mean pore size and number of pores per unit area

A significant interaction was observed between DAT and tillage on mean pore size (r , mm) ($p = 0.002$) and number of pores per unit area (N , m^{-2}) ($p = 0.0006$) (Table 8). Regardless of tillage, r and N varied greatly with time, especially in IT (Fig. 17). Both IT and RT showed lower and relatively similar r at 18 and 60 days after the autumn tillage, then increased at 138 days, maintaining this high value up to 63 days after the spring tillage, decreasing later on up to 205/177 days. On the contrary, N was found higher at 18 and 60 days after the autumn tillage, then decreased at 138 days, was maintained, or even slightly increased at 63 days after spring tillage and increased again at 205/177 days. NT showed greater r at 18, 60, and 138 days after the autumn sowing, then decreased slowly up to 205/177 days after the spring sowing. On the other hand, N increased slowly over time and reached its maximum at 205/177 days after spring sowing.

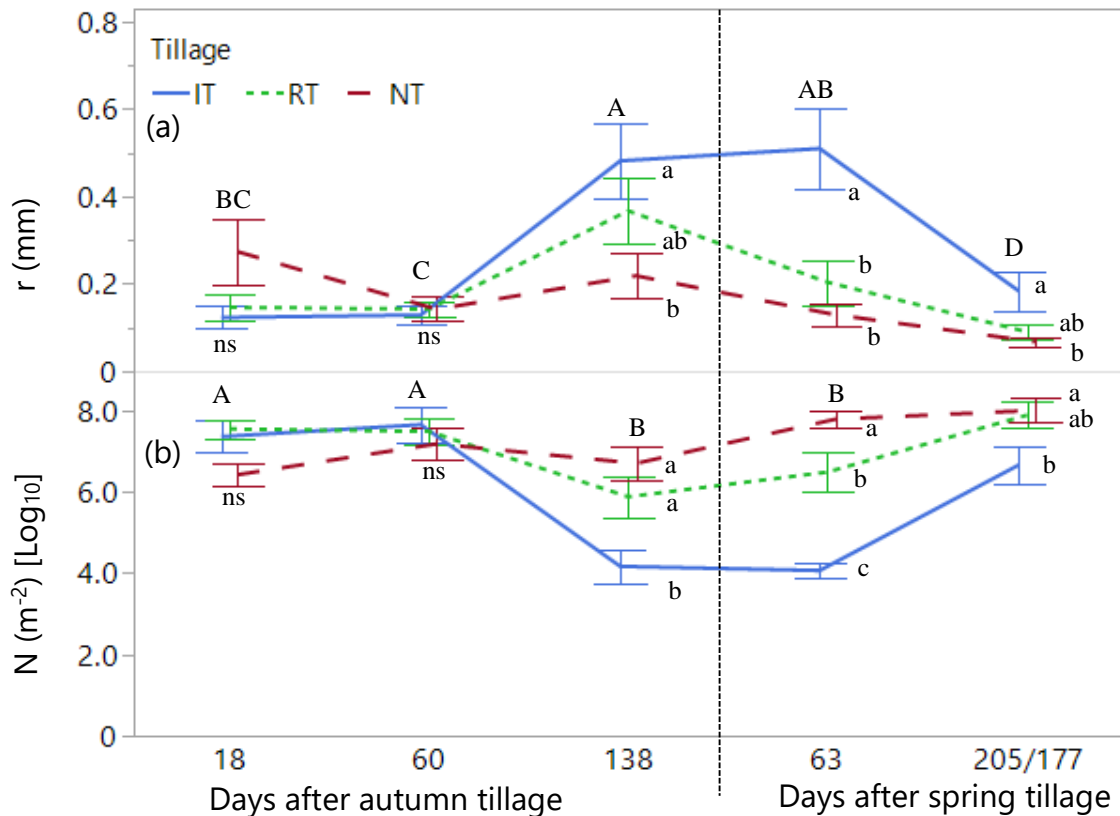


Fig. 17: Mean pore size (a) (r , mm) and number of pores per unit area (b) (N , m^{-2}) dynamics at different days after tillage and tillage systems (IT: intensive tillage, RT: reduced tillage, and NT: no-tillage). Error bars show the standard error. Vertical dashed line separates the days after autumn and spring tillage. Different letters (uppercase letters among days after tillage and lowercase letters among tillage systems within each sampling date) indicate significant differences between treatments at $p < 0.05$; ns, non-significant.

The effect of position was not significant on r but a significant effect was found on N ($p = 0.0003$ in LM, $p = 0.005$ in FM) (Table 10). Both B-row and W-row showed similar r (0.20 mm in LM, and 0.17 mm in FM) (Table 10). In addition, W-row had greater N compared to B-row (7.88×10^7 vs. 6.90×10^7 m^{-2} in LM, and 8.03×10^7 vs. 7.68×10^7 m^{-2} in FM) (Table 10).

4. Discussion

4.1 Temporal variations of soil hydraulic properties

Temporal variations of soil hydraulic properties (S , K_s , r and N) caused by soil crust were great under IT and RT, less evident under long-term NT (Figs. 15 and 17), whilst no significant difference was observed between LM and FM (Table 8 and 9). Figures 15 and 17, can be divided

into two separate stages, viz., (i) 18, 60 and 138 days after autumn tillage, and (ii) 63 and 205/177 days after spring tillage. After the autumn tillage, IT showed an increasing trend on both S and K_s from 18 to 60 days, and then they declined and reached extremely low values at 138 days (Fig. 15). However, 63 and 205/177 days after spring tillage, IT showed mostly similar K_s values and slightly higher than 138 days after autumn tillage. Tillage, in general, alters the soil structure and pore systems, leading to the formation of macro-pores (Jirků et al., 2013). However, soil surface structure is expected to be fragile and unstable with regards to macro-pores (Feng et al., 2011). In this line clogging or blocking of the macro-pores could occur as a result of aggregate breakdown during rainfall or irrigation events (Nciizah and Wakindiki, 2014). Tillage effects on S and K_s were easily mitigated, and variations on hydraulic properties occurred based on the rate and intensity of rainfall events and irrigation applications (Feng et al., 2011). The higher K_s that was observed at 18 and 60 days after autumn tillage could be attributed to macro-pores created by tillage, resulting in temporary increases in K_s . Besides this, in those two periods were received 11 and 29 mm of rainfall, respectively, with an intensity lower than 10 mm day^{-1} (Table 9, and Fig. 13). This amount of rainfall was not enough to form a strong crust to reduce K_s . On the contrary, an extremely low K_s value was recorded at 138 days after autumn tillage in IT because of crust formed by raindrops and irrigation application. This period received a total of 72 mm of rain and irrigation water, intensity of rain exceeded 10 mm day^{-1} , which was sufficient to form a seal and crust on the surface soil (Fig. 13). After the spring tillage, multiple rainfall and irrigation events with greater intensity (Fig. 13) developed a strong surface crust. As a consequence, tillage induced K_s and S enhancement were not found at 63 days after spring tillage, earlier than autumn tillage. In contrast, both K_s and S were reduced due to crust formation. Our results suggest that the crust development process was time-dependent, and was primarily governed by the overall rain or irrigation and their intensity (Figs. 13 and 15). Further, mean pore size (r) showed an increasing trend at 138 days after

autumn tillage, whilst after spring tillage, found greater value at 63 days and then decreased at 205/177 days. In contrast, the opposite result was observed for number of pores per unit area (N). An increasing trend in pore size can be attributed by tillage operations, as well as biological activity and plant root development. At the same time mean pore size increased, the number of pores per unit area decreased greatly. This finding indicates that, although IT had greater r particularly at 138 and 63 days, it showed a lower value of K_s because of lower N . We hypothesized that lower N under those sampling date could be linked to poor connection between pores. In a study in the same experimental field, it was documented that due to lower pore continuity IT had similar gas diffusivity to NT, although IT had greater air-filled porosity than NT (Talukder et al., 2022).

After the autumn tillage, S and K_s did not change significantly under RT, whereas an increasing trend of r and a decreasing trend of N were observed over time. After the spring tillage, both S and K_s showed a decreasing trend over time. r showed a maximum value at 63 days and then declined. Again, N showed a lower value at 63 days and then increased slightly (Fig. 17). Rainfall and irrigation after autumn tillage were not enough to create a strong crust, and consequently, S and K_s were high up to 138 days in RT. After spring tillage, multiple rainfall and especially irrigation events following tillage quickly formed a strong crust, and as a consequence, K_s was low under RT from the beginning. Similarly, NT showed an increasing trend on S and K_s over time and then declined at the end (205/177). A slightly decreasing trend over time was observed for r , whereas N showed the opposite, an increasing trend. These findings illustrate that, with reduction of tillage intensity from IT to NT crust formation was lowered. It was well documented that long-term RT and NT formed a more stable soil structure than IT. As a result, RT and NT were more resilient to crust formation than IT. Due to less disturbance, Palese et al. (2014) found that the effect of crusting was lower under reduced (RT) and no-tillage (NT) compared to conventional tillage (IT) on semi-arid sandy loam soils.

Because of the occurrence of crusting and compacted layers in IT, they observed lower infiltration of rainfall water. In addition, findings of this study are supported by the previous studies conducted in the same experimental field indicating that the soil structure was improved under NT compared to RT and IT (Pareja-Sánchez et al., 2017; Talukder et al., 2022). In these studies, soil physical properties such as gas diffusivity, and macropore continuity were greater under NT than IT (Talukder et al., 2022), the macroaggregates water stability was lower under IT and RT due to decreased soil organic content than NT (Pareja-Sánchez et al., 2017). Notwithstanding, the results of the surface runoff and sediment yield measurements made over the course of 2018-19 to 2020-21 in the same study area revealed that crusting impacts based on tillage practice. It was demonstrated that regardless of the year, surface runoff and sediment yield were greater under IT and RT than NT (unpublished work). Beside this, some other possible reasons can be (i) IT (100%) incorporates greater quantity of crop residues into the soil than RT (70%), whereas crop residues remain in NT (85%), (ii) crop establishment was delayed under IT and RT compared to NT (Pareja-Sánchez et al., 2017) and both biomass and grain yield were greater under RT and NT. Therefore, strong surface crust under IT could be attributed to lower surface cover by crop residues or living crops than RT and NT, making the soil aggregates exposed to water drop impact. Additionally, in the same study area (Cantero-Martínez et al., 2004) reported that greater activity of earthworms in the top soil (0-30 cm depth) of NT system than IT. We hypothesized that under conservation tillage, especially in NT channelling and burrowing by earthworms loosens the surface soil and creates preferential paths for infiltration and percolation of water. As a consequence, NT had greater hydraulic conductivity during the high frequency irrigation period. Moreover, both S and K_s were decreased 205/177 days after the spring tillage under NT. The reason can be that maximum amount of rainfall + irrigation (566 and 398 mm for FM and LM, respectively) was received during this period. In this line, Angulo-Jaramillo et al. (2000) reported soil hydraulic properties

variation over time under two kinds of soils (sand and sandy loam). Under furrow irrigation, K_s values declined from the beginning of irrigation period towards the end. At the end of the irrigation period, both S and K_s showed lower values compared to the beginning of irrigation. Our results are consistent with Angulo-Jaramillo et al. (2000) and observed a similar trend.

In summary, raindrops and irrigation water following tillage contributed to settle down the fragile structure created by the tillage and developed surface crusting; consequently, temporal variation on S , K_s , r , and N due to tillage did not persist over a long time. Beside this, multiple rainfall events and irrigation applications and their intensities were capable to create a strong crust. The negative effects of soil crust on S and K_s were greater under IT than RT, and little under long-term NT. Nevertheless, the effect of crust on temporal variation of soil hydraulic properties was potentially greater at the end of irrigation period and less at the beginning of irrigation particularly under RT and NT.

4.2 Crusting effects on soil hydraulic properties

The saturated hydraulic conductivity (K_s) was around three times higher W-row than B-row in FM and LM (Table 10). The difference in K_s values was due to crust formation and was more prominent B-row. Seeding or row planting (W-row) is insufficient to cover the whole soil surface, especially during the vegetative stage of crops, which exposes more soil surface to water drop impact. The presence of the crops W-row, led to the weakening or lowering of crust development by intercepting raindrops and irrigation water, and reducing the falling energy when reaching the surface (Neave and Rayburg, 2007). In contrast, B-row was directly exposed to rain or irrigation water and formed a well-developed crust. Furthermore, plant roots strengthened the stability of surrounding aggregates by decaying roots biomass at the W-row, leading to a reduction in aggregate physical dispersion and transportation caused by water action (Fageria and Stone, 2006). This last process is aggravated by the presence of soil sediment prevailed in between rows of crops, particularly under IT as observed by Pareja-

Sánchez et al. (2017) in the same field. Several authors working under different environmental conditions found similar results (Alagna et al., 2019; Neave and Rayburg, 2007; Ries and Hirt, 2008; Souza et al., 2014). For instance, Alagna et al. (2019) reported that B-row areas had lower K_s (by a factor of 1.6) than W-row due to crust formation under rain-fed Mediterranean vineyard loamy soils. In addition, it was observed that W-row had lower bulk density (ρ_b), and a higher number of hydraulically active pores per unit area (N), with the same pore size, (r) than B-row (Table 10). This indicates that the W-row was more conductive due to an increased number of pores per unit area. Our results match with the results of Souza et al. (2014) who used BEST method in a Brazilian Oxisol cultivated with castor bean (*Ricinus communis L.*). They found that non-crust (W-row) soils were 3 times more conductive (K_s) than crusted soils (B-row) due to higher number of hydraulically active pores per unit area, and also recorded lower bulk density for non-crust soils. Moreover, Jirků et al. (2013) reported that K_s increased proportionally with θ_s , whereas decreased inversely in relation to ρ_b . Our results showed a similar pattern; a negative relation between ρ_b and K_s was observed B-row (greater ρ_b and lower K_s).

Likewise, K_s , sorptivity (S) was always significantly higher W-row, around 1.70 times higher than B-row. S represents how fast/readily a soil absorbs water at the initial stage of a rainfall event or irrigation application due to capillary force (Castellini et al., 2016). Our results suggested that presence of crust B-row impaired the soil's ability to infiltrate water compared to W-row, as Alagna et al. (2019) found. Castellini et al. (2016) reported that S increased proportionally to soil organic content and was inversely related to ρ_b . Our results correspond the findings, exhibiting a negative relationship between ρ_b and S .

5. Conclusions

Two-fold higher hydraulic conductivity and sorptivity were found under the crop row compared to between rows because of greater number of pores per unit area. Between rows soil remain

unprotected in the first stages of the crop development, highlight the protective effect of the crop canopy on the soil that prevents crusting. Furthermore, this preferential water flow path should not be neglected when conducting infiltration experiments in row crops, or at least the sampling position must be indicated when comparing results.

The initial enhancements of porosity by intensive tillage, are lost very easily in the short-term because of weak structural stability of surface soil which becomes prone to crust formation. This surface crusting leads to decrease sorptivity, hydraulic conductivity and number of actively conducting pores. On the contrary, no-tillage and reduced tillage can be a management choice in Mediterranean areas, also under irrigated conditions, due to better structural stability. Structurally stable soils are resilient to crust formation, and enhanced soil hydraulic properties, which can improve the efficiency of rain and irrigation water use by reducing runoff. Incorporation of pea or vetch before maize lowered bulk density during the maize growing period, but it did not improve soil hydraulic properties after three years. Long-term impacts of legume-maize sequence on soil crusting needs to be assessed in future research. Finally, effects of crust should be considered while modelling or simulating soil water movement and/or scheduling irrigation.

Acknowledgments

The authors thank the support given by MD. Elena Nadal who helped in the field measurements, the field and laboratory technicians Carlos Cortés and Silvia Martí, and the farmer Xavier Penella. The authors gratefully acknowledge support for this research from the Research Spanish Agency (DISOSMED Project - AGL2017-84529-C3-R). Rasendra Talukder also sincerely acknowledges the fund provided by University of Lleida to support PhD fellowship. Daniel Plaza-Bonilla is Ramón y Cajal fellow (RYC-2018-024536-I) co-funded by MICIN/AEI/10.13039/501100011033 and European Social Fund.

References

- Agassi, M., Shainberg, I., Morin, J., 1981. Effect of Electrolyte Concentration and Soil Sodicity on Infiltration Rate and Crust Formation. *Soil Sci. Soc. Am. J.* 45, 848–851. <https://doi.org/10.2136/sssaj1981.03615995004500050004x>
- Alagna, V., Bagarello, V., Di Prima, S., Giordano, G., Iovino, M., 2013. A simple field method to measure the hydrodynamic properties of soil surface crust. *J. Agric. Eng.* 44, 74–79. [https://doi.org/10.4081/jae.2013.\(s1\):e14](https://doi.org/10.4081/jae.2013.(s1):e14)
- Alagna, V., Bagarello, V., Di Prima, S., Guaitoli, F., Iovino, M., Keesstra, S., Cerdà, A., 2019. Using Beerkan experiments to estimate hydraulic conductivity of a crusted loamy soil in a Mediterranean vineyard. *J. Hydrol. Hydromechanics* 67, 191–200. <https://doi.org/10.2478/johh-2018-0023>
- Angás, P., Lampurlanés, J., Cantero-Martínez, C., 2006. Tillage and N fertilization: Effects on N dynamics and Barley yield under semiarid Mediterranean conditions. *Soil Tillage Res.* 87, 59–71. <https://doi.org/10.1016/j.still.2005.02.036>
- Angulo-Jaramillo, R., Bagarello, V., Di Prima, S., Gosset, A., Iovino, M., Lassabatere, L., 2019. Beerkan Estimation of Soil Transfer parameters (BEST) across soils and scales. *J. Hydrol.* 576, 239–261. <https://doi.org/10.1016/j.jhydrol.2019.06.007>
- Angulo-Jaramillo, R., Vandervaere, J.-P., Roulier, S., Thony, J.-L., Gaudet, J.-P., Vauclin, M., 2000. Field measurement of soil surface hydraulic properties by disc and ring infiltrometers. *Soil Tillage Res.* 55, 1–29. [https://doi.org/10.1016/S0167-1987\(00\)00098-2](https://doi.org/10.1016/S0167-1987(00)00098-2)
- Assouline, S., 2004. Rainfall-Induced Soil Surface Sealing: A Critical Review of Observations, Conceptual Models, and Solutions. *Vadose Zo. J.* 3, 570–591. <https://doi.org/10.2136/vzj2004.0570>
- Badorreck, A., Gerke, H.H., Hüttl, R.F., 2013. Morphology of physical soil crusts and

- infiltration patterns in an artificial catchment. *Soil Tillage Res.* 129, 1–8.
<https://doi.org/10.1016/j.still.2013.01.001>
- Bagarello, V., Di Prima, S., Iovino, M., 2014. Comparing Alternative Algorithms to Analyze the Beerkan Infiltration Experiment. *Soil Sci. Soc. Am. J.* 78, 724–736.
<https://doi.org/10.2136/sssaj2013.06.0231>
- Baumhardt, R.L., Unger, P.W., Dao, T.H., 2004. Seedbed Surface Geometry Effects on Soil Crusting and Seedling Emergence. *Agron. J.* 96, 1112–1117.
<https://doi.org/10.2134/agronj2004.1112>
- Brooks, R.H., Corey, A.T., 1964. Hydraulic Properties of Porous Media, Colorado State University Hydrology Paper. Colorado State University.
- Burdine, N.T., 1953. Relative Permeability Calculations From Pore Size Distribution Data. *J. Pet. Technol.* 5, 71–78. <https://doi.org/10.2118/225-G>
- Cantero-Martínez, C., Ojeda, L., Ángas, P., Santiveri, P., 2004. Técnicas de laboreo del suelo en zonas de secano semi-árido; Efecto sobre la población de lombrices. Departamento de Production Vegetal Y Ciencia Forestal, Universitat Lleida, ETSEA. 724–729.
- Cantero-Martínez, C., Angas, P., Lampurlanés, J., 2003. Growth, yield and water productivity of barley (*Hordeum vulgare* L.) affected by tillage and N fertilization in Mediterranean semiarid, rainfed conditions of Spain. *F. Crop. Res.* 84, 341–357.
[https://doi.org/10.1016/S0378-4290\(03\)00101-1](https://doi.org/10.1016/S0378-4290(03)00101-1)
- Castellini, M., Iovino, M., Pirastru, M., Niedda, M., Bagarello, V., 2016. Use of BEST Procedure to Assess Soil Physical Quality in the Baratz Lake Catchment (Sardinia, Italy). *Soil Sci. Soc. Am. J.* 80, 742–755. <https://doi.org/10.2136/sssaj2015.11.0389>
- Chen, L., Sela, S., Svoray, T., Assouline, S., 2013. The role of soil-surface sealing, microtopography, and vegetation patches in rainfall-runoff processes in semiarid areas. *Water Resour. Res.* 49, 5585–5599. <https://doi.org/10.1002/wrcr.20360>

- Di Prima, S., Stewart, R.D., Castellini, M., Bagarello, V., Abou Najm, M.R., Pirastru, M., Giadrossich, F., Iovino, M., Angulo-Jaramillo, R., Lassabatere, L., 2020. Estimating the macroscopic capillary length from Beerkan infiltration experiments and its impact on saturated soil hydraulic conductivity predictions. *J. Hydrol.* 589, 125159.
<https://doi.org/10.1016/j.jhydrol.2020.125159>
- Di Prima, S. 2013. Automatic analysis of multiple Beerkan infiltration experiments for soil hydraulic characterization. In *Proceedings of the 1st CIGR Inter-Regional Conference on Land and Water Challenges*, Bari, Italy (pp. 10-14).
- Federer, W.T., King, F., 2007. *Variations on Split Plot and Split Block Experiment Designs*. John Wiley & Sons, Inc., Hoboken, NJ, USA.
<https://doi.org/10.1002/0470108584>
- Fageria, N., Stone, L., 2006. Physical, chemical, and biological changes in the rhizosphere and nutrient availability. *J. Plant Nutr.* 29, 1327–1356.
<https://doi.org/10.1080/01904160600767682>
- Feng, G., Sharratt, B., Young, F., 2011. Influence of long-term tillage and crop rotations on soil hydraulic properties in the US Pacific Northwest. *J. Soil Water Conserv.* 66, 233–241. <https://doi.org/10.2489/jswc.66.4.233>
- Gabriel, J.L., García-González, I., Quemada, M., Martin-Lammerding, D., Alonso-Ayuso, M., Hontoria, C., 2021. Cover crops reduce soil resistance to penetration by preserving soil surface water content. *Geoderma* 386, 114911.
<https://doi.org/10.1016/j.geoderma.2020.114911>
- Haverkamp, R., Debionne, S., Angulo-Jaramillo, R., de Condappa, D., 2006. Soil properties and moisture movement in the unsaturated zone. In: Delleur, J.W. (Ed.), *The Handbook of Groundwater Engineering*. CRC, pp. 6.1–6.59.
- Haverkamp R. Ross P.J., Smettem K.R.J., Parlange J.Y. 1994. Three-dimensional analysis of

- infiltration from the disc infiltrometer. 2. Physically based infiltration equation. *Water Resources Research*, 30: 2931-2935. <https://doi.org/10.1029/94WR01788>
- Jirků, V., Kodešová, R., Nikodem, A., Mühlhanslová, M., Žigová, A., 2013. Temporal variability of structure and hydraulic properties of topsoil of three soil types. *Geoderma* 204–205, 43–58. <https://doi.org/10.1016/j.geoderma.2013.03.024>
- Lassabatere, L., Di Prima, S., Angulo-Jaramillo, R., Keesstra, S., Salesa, D., 2019. Beerkan multi-runs for characterizing water infiltration and spatial variability of soil hydraulic properties across scales. *Hydrol. Sci. J.* 64, 165–178. <https://doi.org/10.1080/02626667.2018.1560448>
- Lassabatère, L., Angulo-Jaramillo, R., Soria Ugalde, J.M., Cuenca, R., Braud, I., Haverkamp, R., 2006. Beerkan Estimation of Soil Transfer Parameters through Infiltration Experiments-BEST. *Soil Sci. Soc. Am. J.* 70, 521–532. <https://doi.org/10.2136/sssaj2005.0026>
- Minasny, B., McBratney, A.B., 2007. Estimating the Water Retention Shape Parameter from Sand and Clay Content. *Soil Sci. Soc. Am. J.* 71, 1105–1110. <https://doi.org/10.2136/sssaj2006.0298N>
- Moore, D.C., Singer, M.J., 1990. Crust Formation Effects on Soil Erosion Processes. *Soil Sci. Soc. Am. J.* 54, 1117–1123. <https://doi.org/10.2136/sssaj1990.03615995005400040033x>
- Mubarak, I., Mailhol, J.C., Angulo-Jaramillo, R., Ruelle, P., Boivin, P., Khaledian, M., 2009. Temporal variability in soil hydraulic properties under drip irrigation. *Geoderma* 150, 158–165. <https://doi.org/10.1016/j.geoderma.2009.01.022>
- Nciizah, A., Wakindiki, I., 2014. Rainfall intensity effects on crusting and mode of seedling emergence in some quartz-dominated South African soils. *Water SA* 40, 587. <https://doi.org/10.4314/wsa.v40i4.2>
- Neave, M., Rayburg, S., 2007. A field investigation into the effects of progressive rainfall-

- induced soil seal and crust development on runoff and erosion rates: The impact of surface cover. *Geomorphology* 87, 378–390.
<https://doi.org/10.1016/j.geomorph.2006.10.007>
- Palese, A.M., Vignozzi, N., Celano, G., Agnelli, A.E., Pagliai, M., Xiloyannis, C., 2014. Influence of soil management on soil physical characteristics and water storage in a mature rainfed olive orchard. *Soil Tillage Res.* 144, 96–109.
<https://doi.org/10.1016/j.still.2014.07.010>
- Pareja-Sánchez, E., Plaza-Bonilla, D., Ramos, M.C., Lampurlanés, J., Álvaro-Fuentes, J., Cantero-Martínez, C., 2017. Long-term no-till as a means to maintain soil surface structure in an agroecosystem transformed into irrigation. *Soil Tillage Res.* 174, 221–230. <https://doi.org/10.1016/j.still.2017.07.012>
- Philip, J.R., 1987. The quasi-linear analysis, the scattering analog, and other aspects of infiltration and seepage. In: Fok, Y.S. (Ed.), *Infiltration development and application*. Water Resources Research Center, Honolulu, pp. 1–27.
- Ramos, M.C., Pareja-Sánchez, E., Plaza-Bonilla, D., Cantero-Martínez, C., Lampurlanés, J., 2019. Soil sealing and soil water content under no-tillage and conventional tillage in irrigated corn: Effects on grain yield. *Hydrol. Process.* 33, 2095–2109.
<https://doi.org/10.1002/hyp.13457>
- Ries, J.B., Hirt, U., 2008. Permanence of soil surface crusts on abandoned farmland in the Central Ebro Basin/Spain. *CATENA* 72, 282–296.
<https://doi.org/10.1016/j.catena.2007.06.001>
- Šimůnek, J., Angulo-Jaramillo, R., Schaap, M.G., Vandervaere, J.-P., van Genuchten, M.T., 1998. Using an inverse method to estimate the hydraulic properties of crusted soils from tension-disc infiltrometer data. *Geoderma* 86, 61–81. [https://doi.org/10.1016/S0016-7061\(98\)00035-4](https://doi.org/10.1016/S0016-7061(98)00035-4)

- Soil Survey Staff, 2014. *Keys to Soil Taxonomy*, 12th ed. ed. USDA-Natural Resources Conservation Service, Washington, DC.
- Souza, E.S., Antonino, A.C.D., Heck, R.J., Montenegro, S.M.G.L., Lima, J.R.S., Sampaio, E.V.S.B., Angulo-Jaramillo, R., Vauclin, M., 2014. Effect of crusting on the physical and hydraulic properties of a soil cropped with Castor beans (*Ricinus communis* L.) in the northeastern region of Brazil. *Soil Tillage Res.* 141, 55–61.
<https://doi.org/10.1016/j.still.2014.04.004>
- Talukder, R., Plaza-Bonilla, D., Cantero-Martínez, C., Wendroth, O., Castel, J.L., 2022. Soil gas diffusivity and pore continuity dynamics under different tillage and crop sequences in an irrigated Mediterranean area. *Soil Tillage Res.* 221, 105409.
<https://doi.org/10.1016/j.still.2022.105409>
- Usón, A., Poch, R.M., 2000. Effects of tillage and management practices on soil crust morphology under a Mediterranean environment. *Soil Tillage Res.* 54, 191–196.
[https://doi.org/10.1016/S0167-1987\(99\)00099-9](https://doi.org/10.1016/S0167-1987(99)00099-9)
- van Genuchten, 1980. A closed-form equation for predicting the hydraulic conductivity of unsaturated soils. *Soil Sci. Soc. Am. J.* 44, 892–898.
- Vandervaere, J.-P., Peugeot, C., Vauclin, M., Angulo Jaramillo, R., Lebel, T., 1997. Estimating hydraulic conductivity of crusted soils using disc infiltrometers and minitensiometers. *J. Hydrol.* 188–189, 203–223. [https://doi.org/10.1016/S0022-1694\(96\)03160-5](https://doi.org/10.1016/S0022-1694(96)03160-5)
- Watson, K.W., Luxmoore, R.J., 1986. Estimating Macroporosity in a Forest Watershed by use of a Tension Infiltrometer. *Soil Sci. Soc. Am. J.* 50, 578–582.
<https://doi.org/10.2136/sssaj1986.03615995005000030007x>
- Wu, Q., Wang, L., Wu, F., 2016. Effects of structural and depositional crusts on soil erosion on the Loess Plateau of China. *Arid L. Res. Manag.* 30, 432–444.

<https://doi.org/10.1080/15324982.2016.1157837>

Yilmaz, D., Lassabatere, L., Angulo-Jaramillo, R., Deneele, D., Legret, M., 2010.

Hydrodynamic Characterization of Basic Oxygen Furnace Slag through an Adapted

BEST Method. *Vadose Zo. J.* 9, 107. <https://doi.org/10.2136/vzj2009.0039>

Chapter IV

Soil water balance and crop water productivity under different tillage and maize-based crop sequences in a Mediterranean area

Soil water balance and crop water productivity under different tillage and maize-based crop sequences in a Mediterranean area

Rasendra Talukder^{*a}, Jesús Fernández-Ortega^b, Daniel Plaza-Bonilla^b, Carlos Cantero-Martínez^{bc}, Jorge Lampurlanés^{ac}

^aDepartment of Agricultural and Forest Engineering - Agrotecnio-CERCA Center, University of Lleida, Av. Rovira Roure 191, 25198 Lleida, Spain

^bDepartment of Crop and Forest Sciences - Agrotecnio-CERCA Center, University of Lleida, Av. Rovira Roure 191, 25198 Lleida, Spain.

^cAssociate Unit CSIC (Research Spanish Council), Spain

* corresponding author: rasendra.talukder@udl.cat

Abstract

Sustainable agricultural practices aim to maintain year-round ground living cover and improve a variety of agricultural and ecosystem functions and services. In Mediterranean environment with hot, dry summers, irrigation facilities help to keep the ground covered and increases crop yields. The objective of this work was to evaluate the combined impact of tillage systems and crop sequence on soil water balance components, crop biomass and grain yield, crop water use efficiency (WUE_c), and water productivities (WP) under Mediterranean irrigated conditions. The study was carried out on a long-term tillage field experiment (26 years old), in silt loam soils at Agramunt, NE Spain during three consecutive years i.e., 2018-19, 2019-20, and 2020-21. Three different tillage systems (intensive tillage, IT; reduced tillage, RT; and no-tillage, NT) and two crop sequences (short fallow-maize, FM and legume-maize, LM) were compared. Results revealed that water uptake by pea or vetch (LM) during the winter cropping season, decreased the water loss through deep percolation (DP) and depleted soil water content (SWC) greatly than FM, whereas the opposite result was observed in the summer cropping season. Incorporating legume before maize in LM increased significantly maize biomass ((24701 vs.

17773 kg ha⁻¹) and grain yield (11368 vs. 8225 kg ha⁻¹) in 2018-19; and significantly increased maize above ground biomass under RT and NT, and grain yield under IT in 2020-21 compared to FM. Similarly, maize WUE_c for biomass was significantly greater for the LM as compared to FM in 2018-19 and 2020-21. The increase in maize water use efficiency for LM corresponds with greater biomass and grain yield under slightly lower irrigation water application (shorter cycle). Maize water productivities for yield were also significantly greater for the LM as compared to FM because of increased yields and relatively lower supply of irrigation water. Conservation tillage practices i.e., RT and NT tended to increase SWC and reduced runoff and sediment yields compared to IT, and resulted in greater vetch biomass, maize biomass, grain yields and water use efficiency than IT in 2019-20 and 2020-21. Water productivities were also significantly greater for RT and NT compared to IT because of increased yields. In irrigated areas, legume inclusion can be an agricultural strategy ~~that~~ to improves crop yields by increasing water use efficiency. It also contributes to mitigate the negative effects of intense tillage and successfully maintaining yields.

Keywords: Conservation agriculture, Crop diversification, Soil water content dynamics, Soil water budget, water productivity

1. Introduction

In semi-arid Mediterranean areas water is a limiting factor for crop production and changing the land from rainfed to irrigation enhances agricultural production (Ramos et al., 2019). Transpiration and evaporation from the crop and soil, as well as intercepted water, creates significant irrigation demands that increases susceptibility to potential shortages in water resources (Baffaut et al., 2020). Therefore, accurate determination and estimation of soil water balance components i.e., inputs and outputs, under irrigated condition is important for sustainable irrigation water management.

In a water-limited region, ensuring appropriate producer profitability and sustaining the production to meet the growing population's demand, while avoiding non-beneficial water use i.e., deep percolation, leaching and runoff, is a major challenge (Howitt, 2008; Rodrigues and Pereira, 2009; Fernández et al., 2020). In this context, stakeholders are obligated to make accurate decision about irrigation strategy as well as irrigation scheduling methods, among other agricultural management practices. Consequently, to evaluate the impact of different agricultural management practices on soil water balance, crop yield, crop water use, and water productivity under irrigated conditions are required to improve yields, while saving water. However, depending on the agricultural management practices, reliance on irrigation could change the magnitude of some of the soil water balance components at field scale (Graham et al., 2019). Water losses from surface runoff and drainage from root zone increases sediment and nutrient loss, thus impacting both water quantity and quality (Gabriel and Quemada, 2011). Water productivity is the yield produced per unit of water used, i.e., irrigation and/or precipitation. Hence, factors affecting yield or irrigation will likely have an impact on water productivity (Rodrigues and Pereira, 2009; Li et al., 2016). According to Li et al. (2016), agricultural practices had a great impact on irrigation water productivity (WP_I) of cereal crops than climate factors in an arid region of Northwest China with annual mean precipitation of 50-

150 mm. Among agricultural practices, fertilisation and the use of agricultural films contributed 33% and 42%, respectively, to the increase of WP_I .

Intensification of crops in semiarid regions has often been limited because of unsuccessful crop establishment or shortage of water, this is not the case where irrigation is available (Salmerón et al., 2011; Gabriel and Quemada, 2011). Inclusion of legume before cereals as part of crop sequence or rotation, can enhance soil and nutrient conservation and increase crop production and water use efficiency (Salmerón et al., 2011; Huynh et al., 2019).

Changes in agricultural practices viz., traditional single cropping systems (barley or wheat) to legume-maize particularly under irrigated conditions and contrasting soil tillage modifies soil hydro-physical properties and strongly influence its structural stability (Talukder et al., 2022) and thus soil water balance components (Lamm et al., 2009; Huynh et al., 2019; Alfonso et al., 2020), crop yields and water use efficiency (Brunel-Saldias et al., 2018; Gabriel and Quemada, 2011; Huynh et al., 2019).

Tillage is an important soil management practice which alters the most soil processes and functions. There were several studies conducted in Mediterranean areas but non-consistent results have been found under long-term no tillage or reduced tillage in terms of soil physical quality and crops yields (Forte et al., 2017; Lee et al., 2019; Pareja-Sánchez et al., 2019; Franco-Luesma et al., 2020). For instance, NT or RT increases the soil organic carbon content, aggregate stability, enhances crop yields and water use efficiency compared to IT in a silt loam soils under sprinkler irrigation (Pareja-Sánchez et al., 2019). In contrast, Franco-Luesma et al. (2020) reported that IT trended to have greater grain yield and grain N uptake in three consecutive years in a silt loam soils under flood and sprinkler irrigation systems. They pointed out that lower soil bulk density under IT led to optimal conditions for the maize root development and better crop performance than NT. Furthermore, in a study by Forte et al. (2017), both RT and IT had similar maize grain yields and N uptake by crop in a sandy-clay-

loam soil under drip irrigation, although above ground biomass under IT was slightly greater compared to RT due to the breakdown of subsoil compaction under IT.

Maize is an important grain crop which is cultivated under continuous cropping (winter: fallow and summer: maize), and it has increased its surface from 14,000 (MAPAMA, 1945) to 127,000 ha (MAPAMA, 2019). According to Grassini et al. (2011), soil tillage and crop sequence have been identified as the most important factors affecting maize production, apart from sowing and plant population density. However, few studies have been conducted on the effects of crop sequence and soil tillage systems under irrigated conditions on soil water use efficiency and water productivity in maize (Gabriel and Quemada, 2011; Huynh et al., 2019; Baffaut et al., 2020) under the Mediterranean conditions of the Ebro's valley.

The objective of this study was to determine and quantify the soil water balance components, crop biomass and grain yields, crop water use and productivities in a long-term tillage experiment in an irrigated Mediterranean area under various agricultural management practises. We hypothesized that (i) inclusion of legumes in the crop sequence would improve soil hydro-physical properties, and improve crop yield and water productivity, and (ii) reducing the tillage intensity would increase soil water conservation and thus yields.

2. Materials and Methods

2.1 Experimental site and design

The experiment was carried out during the 2018-19, 2019-20 and 2020-21 years in a long-term tillage experiment at Agramunt, NE Spain (41°48' N, 1°07' E, 330 m asl). The climate of the area is semiarid Mediterranean, with a mean annual precipitation of 401 mm and a mean air temperature of 14.1 °C. The soil has a 2% slope and was classified as Typic Xerofluvent according to USDA (Soil Survey Staff, 2014) and the upper (0–28 cm) horizon had a silt loam texture (sand, 30.8%; silt, 57.3%; clay, 11.9%). The experimental field was established in 1996 to compare three tillage systems, intensive tillage (IT), reduced tillage (RT), and no-tillage

(NT), as well as three levels of mineral nitrogen (zero, medium, and high), with a single crop (barley: *Hordeum vulgare* L.) grown under rainfed conditions (Cantero-Martínez et al., 2003). It was transformed to irrigation in 2015 and maize was grown from this year. In 2018, a new factor (crop sequence) was added with two levels, short fallow-maize (FM) and legume-maize (LM), and the experiment transformed to split-plot. More details can be found in Talukder et al. (2022). Only relevant aspects for this study are described below.

Only plots under medium mineral N rate were considered for this study (FM and LM: 200 and 150 kg N ha⁻¹), whereas mineral P and K fertilization were applied at the beginning of each cropping season prior to maize planting based on soil analysis. Tillage applied to the main plots were three levels (i) intensive tillage, IT; (ii) reduced tillage, RT; and (iii) no-tillage, NT. Tillage was done twice on both IT and RT plots in autumn and spring. In IT plots, autumn tillage consisted of a subsoiler pass (depth: 35 cm) followed by a chisel pass (depth: 15 cm) (which helped to incorporate crop residues into the soil nearly 100%) and a roller (to make the surface even), whereas a rototiller (15 cm), followed by a chisel pass and a roller, was used for spring tillage. RT plots, on the other hand, had similar tillage practices in both autumn and spring, consisting of a chisel pass (15 cm) and a roller. NT plots were sprayed with 1.5 L ha⁻¹ of 36 percent glyphosate [N-(phosphonomethyl)-glycine] herbicide without any soil disturbance.

The crop sequences in the subplots had two levels: (i) short fallow-maize (winter: fallow and summer crop: late maturing maize [FAO 700, Pioneer's P1570 hybrid]) and (ii) legume-maize (winter crop: pea for grain [*Pisum sativum* L., var. Furious] in 2018-19, vetch [*Vicia sativa* L., var. Prontivesa] for green manure in 2019-20 and vetch [*Vicia sativa* L., var. Prontivesa] for forage in 2020-21; summer crop: early maturing maize [FAO 400, Pioneer's P0312 hybrid]). According to the farmer's proposal, vetch would have a wider market potential than pea, so in the following years, the crop was changed from pea to vetch. A pneumatic row direct drilling equipment fitted with two-disc furrow openers was used to seeding and planting legume and

maize, respectively. The details of seeding (legume) or planting (maize), tillage operation and harvesting of crops for three consecutive periods are listed in Table S5.

2.2 Components of soil water balance

In the case of winter fallow, evaporation (E) from the soil was used instead of crop evapotranspiration (ET_c), and its durations from autumn tillage to the plating of late maturing maize. On the other hand, the cropping season for legumes and maize was defined as the period from the seeding or plating to the harvest or physiological maturity. The following equation (Eq. 1) was used to calculate soil water balance components: from input and output variables:

$$I + R = ET_c(\text{or } E) + \Delta SWC + R_{off} + DP \quad (1)$$

where I and R are the amount of water received by irrigation and precipitation, respectively. ΔSWC is the change in soil water content. R_{off} and DP are the amount of water losses through surface runoff and deep percolation, respectively.

2.2.1 Precipitation

An automated weather station next to the experimental field was used to record the air temperature ($^{\circ}\text{C}$), relative humidity, precipitation (mm), wind speed (m s^{-1}) and direction, solar radiation (W m^{-2}) every hour.

2.2.2 Irrigation

Irrigation began in March and concluded in October throughout the course of three years. Irrigation was scheduled weekly using the local recommendations of the Department of Agriculture of the Generalitat de Catalunya for the specific crops and growing stage, as farmers do. As every irrigation sector included different crops and growing stages, the irrigation doses were selected according to the most demanding crop. Maximum daily irrigation dose was $90 \text{ m}^3 \text{ ha}^{-1}$, and the precipitation rate of the sprinklers 6 mm h^{-1} (Christiansen Uniformity Coefficient: 78.10). From the second and third year, the irrigation dose was split in two events per day to reduce runoff.

2.2.3 Actual evapotranspiration

Daily weather data were used to estimate reference evapotranspiration (ET_0) by using the FAO CROPWAT 8.0 software (Smith, 1992). To obtain actual evapotranspiration (ET_c), ET_0 was multiplied by the crop coefficients (K_c) (Eq. 2a). In case of maize, the crop coefficients were estimated as a function of thermal time with a model developed in the Ebro's valley field condition (Martínez-Cob, 2008). On the other hand, pea or vetch crop coefficients were taken from FAO crop coefficients list. Additionally, evaporation from the soil surface was computed for the fallow period using $K_c = K_{c \text{ initial}}$ of prior crops (i.e., maize) and assumed that 10 and 30% of the ground surface had residue cover (RT and NT, respectively) (Eq. 2b) (Allen et al., 1998).

$$ET_c = K_c \times ET_0 \quad (2a)$$

$$E = (K_{c \text{ initial}} - \% \text{residue cover}) \times ET_0 \quad (2b)$$

2.2.4 Soil water content

Soil water content was determined monthly (gravimetrically) at 0-30, 30-60 and 60-90 cm soil depth intervals, and a total of 37 times during three consecutive years: 2018-19 (December - November), 2019-20 (January - October) and 2020-21 (December - October).

Soil water content (SWC) in the soil profile was calculated using Eq. 3.

$$SWC = \sum \theta_{vi} Z_i \quad (3)$$

where θ_v is the volumetric water content of the i layer, obtained from gravimetric soil water content and bulk density, Z_i is the layer depth (mm).

Samples from 0-30 cm depth were taken each year to determine the soil bulk density (g cm^{-3}).

Soil bulk density for 30-60 and 60-90 cm depth was 1.31 g cm^{-3} , as determined previously in the same experimental field.

For each crop, the soil water content change (ΔSWC) was computed by subtracting the SWC at the time of sowing from the SWC at the time of harvest.

2.2.5 Surface runoff

In 2018-19, a micro-plot (length: 2 m and width: 1.6 m) together with a collector tank (length: 0.30 m, width: 0.25 m and height: 0.17 m) was installed under IT, RT and NT plots on FM in one replication to collect surface runoff, and a varied volume of runoff was obtained based on tillage systems. As a result, micro-plots were installed to cover the LM plots of the same replication from 2019-20 onwards. The collector tank had no splitters. After heavy precipitation events or every 10-15 days during irrigation application, water from the collector tanks was measured to calculate the total volume of runoff (L) discharge per unit area (m²) (Eq. 4).

$$\text{Runoff (mm)} = \frac{\text{Volume of runoff water (L)}}{\text{Area of the micro-plot (m}^2\text{)}} \quad (4)$$

An aliquot of 150 ml was brought to laboratory to determine the soil losses: sediment yield (t) per unit area (ha) on the runoff water.

$$\text{Sediment yield (t ha}^{-1}\text{)} = \frac{\text{Volume of runoff water (ml)} \times \text{sediment in 150 ml (t)}}{\text{Known volume of water (150 ml)} \times \text{area of the micro-plot (ha)}} \quad (5)$$

2.2.6 Deep percolation

Deep percolation was estimated between every two consecutive soil water content measurements as the residual component of soil water balance equation (Eq. 1).

2.3 Crop variables

Harvesting or chopping took place in May-June for legume crops and in September-October for late maturing and October-November for early maturing maize. For pea, grain was collected using a micro harvester. Pea and vetch biomass was estimated by cutting 0.36 m² of plants at the soil surface level in two areas of each experimental plot. Maize biomass and grain yield were estimated by cutting 2 m long of a central row of plants in three areas of each experimental plot and obtaining its fresh weigh. A sub-sample of two plants of maize was used to assess moisture. The sub-sample was weighed after being dried in the oven for 48 hours at 60 °C. Both

pea and maize biomass and grain yield data are shown at 0% moisture content. The harvest index (HI) was calculated as the ratio between the grain yield and the total biomass.

2.4 Crop water use efficiency and water productivity

Crop water use efficiency (WUE_c) was calculated as the ratio between the total biomass produced by a crop and water used by crop or crop evapotranspiration (ET_c), over the same time period (Viets, 1962; Flexas et al., 2010) (Eq. 6).

$$WUE_c(kg\ ha^{-1}\ mm^{-1}) = \frac{Biomass\ (kg\ ha^{-1})}{ET_c\ (mm)} \quad (6)$$

Crop water productivity (WP_c) was calculated as the ratio between the marketable yield produced by a crop and water consumed by the crop or crop evapotranspiration (ET_c), over the same time period (Howitt, 2008) (Eq. 7).

$$WP_{c1}(kg\ ha^{-1}\ mm^{-1}) = \frac{Grain\ yield\ (kg\ ha^{-1})}{ET_c\ (mm)} \quad (7)$$

According to Rodrigues and Pereira (2009), the use of the total water involved in crop production (TWU) instead of ET_c in the denominator allows to calculate WP_{c2} :

$$WP_{c2}(kg\ ha^{-1}\ mm^{-1}) = \frac{Grain\ yield\ (kg\ ha^{-1})}{TWU\ (mm)} \quad (8)$$

$$TWU = ET_c + N-BWU \quad (9)$$

where, $N-BWU$ is the non-beneficial water use, for instance, the water that is lost through deep percolation and surface runoff, etc.

Furthermore, measuring water productivity in relation to irrigation and total input water (precipitation and irrigation) enables us to understand the important aspects of agricultural management on water productivity, as well as exploring approaches to improve water productivity for efficient water use to maintain crop yield. Irrigation water productivity (WP_I) was calculated as the ratio between the marketable yield produced by a crop and the amount of water that is applied by irrigation or irrigation water use (IWU), over the same time period, with

no distinction on what part was consumed by crop such as ET_c or $N-WBU$ (Rodrigues and Pereira, 2009) (Eq. 10).

$$WP_I(kg\ ha^{-1}mm^{-1}) = \frac{Grain\ yield\ (kg\ ha^{-1})}{IWU\ (mm)} \quad (10)$$

Input water productivity (WP_{I+P}) was calculated as the ratio between the marketable yield produced by a crop and the amount of water received by precipitation and irrigation, over the same time period, with no distinction on what part was consumed by crop such as ET_c or $N-WBU$ (Rodrigues and Pereira, 2009) (Eq. 11).

$$WP_{I+R}(kg\ ha^{-1}mm^{-1}) = \frac{Grain\ yield\ (kg\ ha^{-1})}{Irrigation(mm)+\ Precipitation\ (mm)} \quad (11)$$

2.5 Statistical analysis

Data analysis was performed using the statistical package JMP Pro 16 (SAS Institute Inc, 2022). The least square means and standard errors were calculated for each variable analysed when replications were available. For variables with only one experimental unit (main plot) per management system, the experiment was analysed as an un-replicated factorial (Montgomery, 2012). Analysis of variance (ANOVA) was done for each soil water balance component, yield, water use efficiency and water productivity to assess the significance of the factors and its interactions. Due to the lack of replications, to test the significance of the effects, four-way interactions were considered random and their mean squares used as a conservative estimate of the error means square (Montgomery, 2012). Variables such as biomass and grain yield had subsamples (two or three observations per plot) rather than composite or single samples (one per plot). Thus, for biomass and grain yield, WUE_c and WP , two-way interactions were tested, with subsample error used as an estimate of the experimental error. Student's t-test was used to compare the means of the factors levels when the factors were significant ($p < 0.05$) in the ANOVA.

3. Results

Maize was sown during the second half of April in FM, while in LM, due to the duration of the legume crop, it was sown by the end of June in 2018-19 (pea for grain) and by the end of May in 2010-20 and 2020-21 (vetch for green manure and forage, respectively). Consequently, the duration of the winter cropping season was shorter and the summer cropping season longer in FM than in LM.

The total amount of water received either from precipitation and irrigation (mm) for three consecutive years i.e., 2018-19, 2019-20 and 2020-21 is presented in the Table 11 and Fig. 18. All tillage systems received equal amounts of precipitation and irrigation. However, during the winter cropping season FM and LM received 48.3 vs. 211.1 mm precipitation and 31.8 vs. 126.8 mm irrigation in 2018-19, 169.0 vs. 210.0 mm precipitation and no irrigation in 2019-20, and 84.0 vs. 129.0 mm precipitation and 27.1 vs. 63.0 mm irrigation in 2020-21 (Table 11). During the summer cropping season FM and LM received 223.4 vs. 163.6 mm precipitation, and 730.8 vs. 593.7 mm irrigation in 2018-19, 123.0 vs. 82.0 mm precipitation and 574.8 vs. 581.7 mm irrigation in 2019-20, and 155.3 vs. 110.3 mm precipitation and 719.3 vs. 692.2 mm irrigation in 2020-21 (Table 11).

Table 11: Amount (mm) of precipitation and irrigation for three tillage systems (IT, intensive tillage; RT, reduced tillage; NT, no-tillage) and two crop sequences (FM, short fallow-maize; LM, legume-maize) during the winter and summer cropping seasons of three consecutive years.

Factors	Levels	2018-19		2019-20		2020-21	
		Precipitation	Irrigation	Precipitation	Irrigation	Precipitation	Irrigation
Winter cropping season: Fallow (FM)/ Legume (LM)							
Tillage*		129.7	79.3	189.5	0	106.5	45.0
Crop sequence	FM	48.3	31.8	169.0	0	84.0	27.1
	LM	211.1	126.8	210.0	0	129.0	63.0
Summer cropping season: Maize (on both FM and LM)							
Tillage*		193.5	662.3	102.5	578.3	132.8	705.7
Crop sequence	FM	223.4	730.8	123.0	574.8	155.3	719.3
	LM	163.6	593.7	82.0	581.7	110.3	692.2

*Both winter and summer cropping season, IT, RT and NT received similar amount of water.

3.1 Components of soil water balance

3.1.1 Soil water content dynamics

Soil water content in the soil profile (up to 90 cm depth) was significantly different among sampling dates, crop sequences, and tillage systems throughout the 2018-19, 2019-20, and 2020-21 years (Table S6). Regardless of the year ($p < 0.0001$), *SWC* showed a declining trend over time from the start of the year and reached the lowest *SWC* during May, June in LM, and July in FM. Then, it showed an increasing trend over time, due to frequent irrigation events, up to September or October and after that remained high (Fig. 18). These trends were not so clear in 2019-20. Regardless of the year, FM had greater *SWC* than LM, particularly in 08/5/2019 ($p < 0.03$), 13/3/2020 ($p < 0.04$), 07/10/2020 ($p < 0.001$), 16/4/2021 ($p < 0.009$) and 04/6/2021 ($p < 0.02$) (Fig. 18). Apart from 07/10/2020, all sampling dates were from the early stages of late maturing maize (FM) with low water needs, when relatively less water was applied by irrigation and legumes using water actively. Differences in *SWC* were observed among tillage systems on the following sampling dates viz., 21/12/2018 ($p < 0.05$), 07/10/2020 ($p < 0.02$), 05/3/2021 ($p < 0.002$), 25/8/2021 ($p < 0.05$), and 29/10/2021 ($p < 0.05$). Those sampling dates *SWC* were found in the following order $NT \geq RT \geq IT$ except 21/12/2018 (Fig. 19).

3.1.2 Crop evapotranspiration

Crop evapotranspiration was significantly affected by year ($p = 0.0009$), season (< 0.0001) and crop sequence ($p = 0.001$) but not by tillage system ($p > 0.05$) (Table 12). All tillage systems showed similar values of ET_c (Table 12). A three-way interaction among year, season and crop sequence was found for ET_c ($p = 0.002$). Regardless of the year, LM had significantly greater ET_c compared to FM (E) during the winter cropping season (Fig. 20a). During the summer cropping season, FM had greater ET_c compared to LM in 2018-19 and 2020-21 but not in 2019-20.

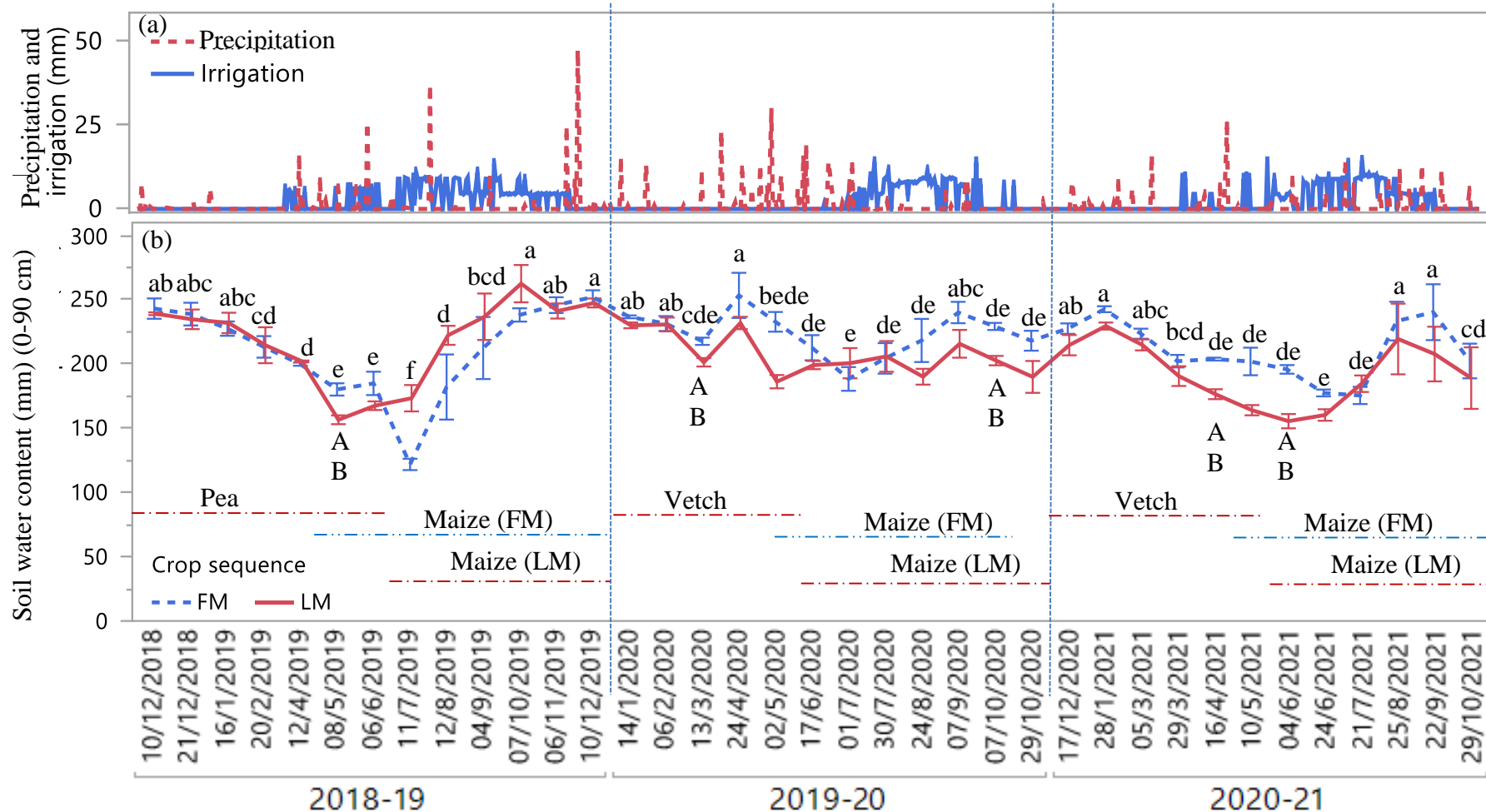


Fig. 18: Amount of precipitation and irrigation (mm) (a) received and total soil water content (mm) (b) dynamics up to 90 cm depth under different crop sequences (FM, short fallow-maize; LM, legume-maize) in three consecutive years (2018-19, 2019-20, 2020-21). Error bars show the standard error. Different lowercase and uppercase letters indicate significant differences among sampling dates and crop sequences respectively ($p < 0.05$). Vertical dashed lines separate the years.

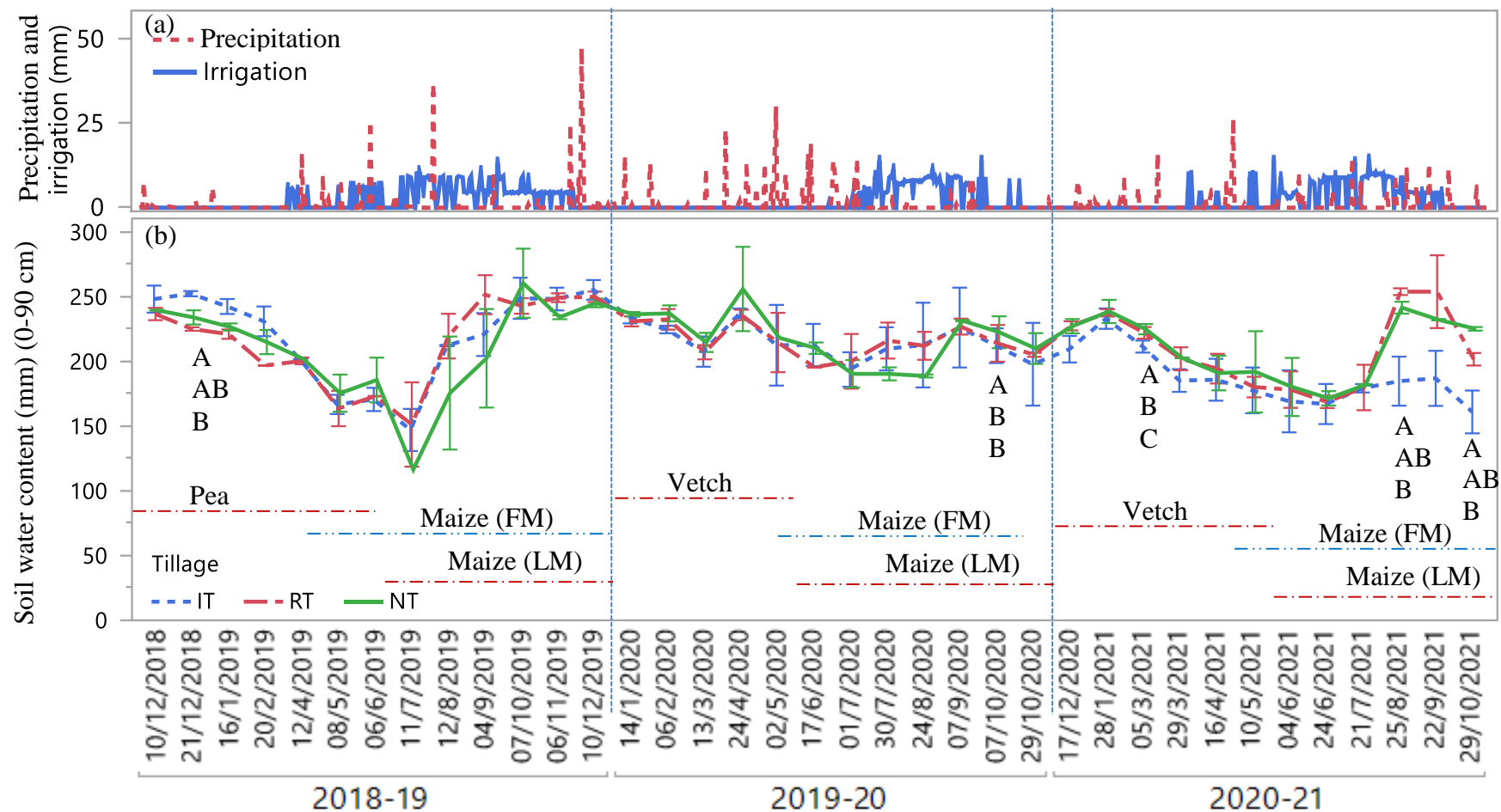


Fig. 19: Amount of precipitation and irrigation (mm) (a) received and total soil water content (mm) (b) dynamics up to 90 cm depth under different tillage systems (IT, intensive tillage; RT, reduced tillage; NT, no-tillage) in three consecutive years (2018-19, 2019-20, 2020-21). Error bars show the standard error. Different uppercase letters indicate significant differences tillage systems for a given date ($p < 0.05$). Vertical dashed lines separate the years.

Table 12: Analysis of variance (p-values) and means comparisons of crop evapotranspiration (ET_c , mm), runoff (R_{off} , mm) and deep percolation (DP , mm) affected by years (2018-19, 2019-20 and 2020-21), seasons (winter and summer cropping season), crop sequences (FM, short fallow-maize; LM, legume-maize) and tillage systems (IT, intensive tillage; RT, reduced tillage; NT, no-tillage) and their interactions. Different uppercase letters within the columns indicate significant differences between treatment means at $p < 0.05$; NS, Non-significant at $p = 0.05$.

Source of variation	ET_c (mm)	R_{off} (mm)	DP (mm)	
Year (CY)	0.0009	0.01	0.0001	
Season (S)	<0.0001	0.006	0.003	
Crop sequence (CS)	0.001	NS	0.007	
Tillage (T)	NS	0.002	NS	
CY \times S	0.0002	0.009	0.001	
CY \times CS	NS	NS	0.03	
CY \times T	NS	0.04	NS	
S \times CS	<0.0001	NS	0.02	
S \times T	NS	0.02	NS	
CS \times T	NS	NS	NS	
CY \times S \times CS	0.002	NS	0.0008	
CY \times S \times T	NS	0.02	NS	
CY \times CS \times T	NS	NS	NS	
S \times CS \times T	NS	NS	NS	
Year				
	2018-19	368.4 A	10.1 A	152.7 A
	2019-20	377.5 B	2.8 B	64.5 B
	2020-21	425.3 B	3.7 B	78.1 B
Season				
	Winter cropping	134.7 B	2.5 B	84.0 B
	Summer cropping	646.1 A	8.6 A	112.8 A
Crop sequence				
	FM	372.3 B	5.1 A	109.5 A
	LM	408.4 A	6.0 A	87.4 B
Tillage				
	IT	394.4 A	13.3 A	95.1 A
	RT	389.1 A	2.8 B	100.9 A
	NT	387.6 A	0.5 B	3.3 A

3.1.3 Surface runoff and deep percolation

Year ($p = 0.01$), season ($p = 0.006$) and tillage ($p = 0.002$) significantly affected runoff but not crop sequence (Table 12). Water losses through R_{off} in FM and LM were similar (Table 12). A significant three-way interaction among year, season and tillage was found for R_{off} ($p = 0.02$). During the winter cropping season, with few irrigation events, water losses through R_{off} were low and not significantly different among tillage systems regardless of year, although tended to

be higher under IT. In contrast, during the summer cropping season of 2018-19 and 2020-21, when most irrigation was applied, IT had significantly higher R_{off} (42.5 and 15.2 mm) than RT (8.7 and 4.6 mm) or NT (1.2 and 1.3 mm) (Fig. 20b). In 2019-20, IT (2.1 mm) and RT (1.0 mm) had low but significantly higher R_{off} than NT (0 mm). Sediment yield was higher under IT than RT and NT with 0.37, 0.02 and 0.0002 t ha⁻¹ year⁻¹ in 2018-19 (Fig. S1). Similarly, in 2019-20 and 2020-21, IT had greater sediment yields than RT and NT but much less than in 2018-19. Both FM and LM yielded comparable amounts of sediment (data not shown).

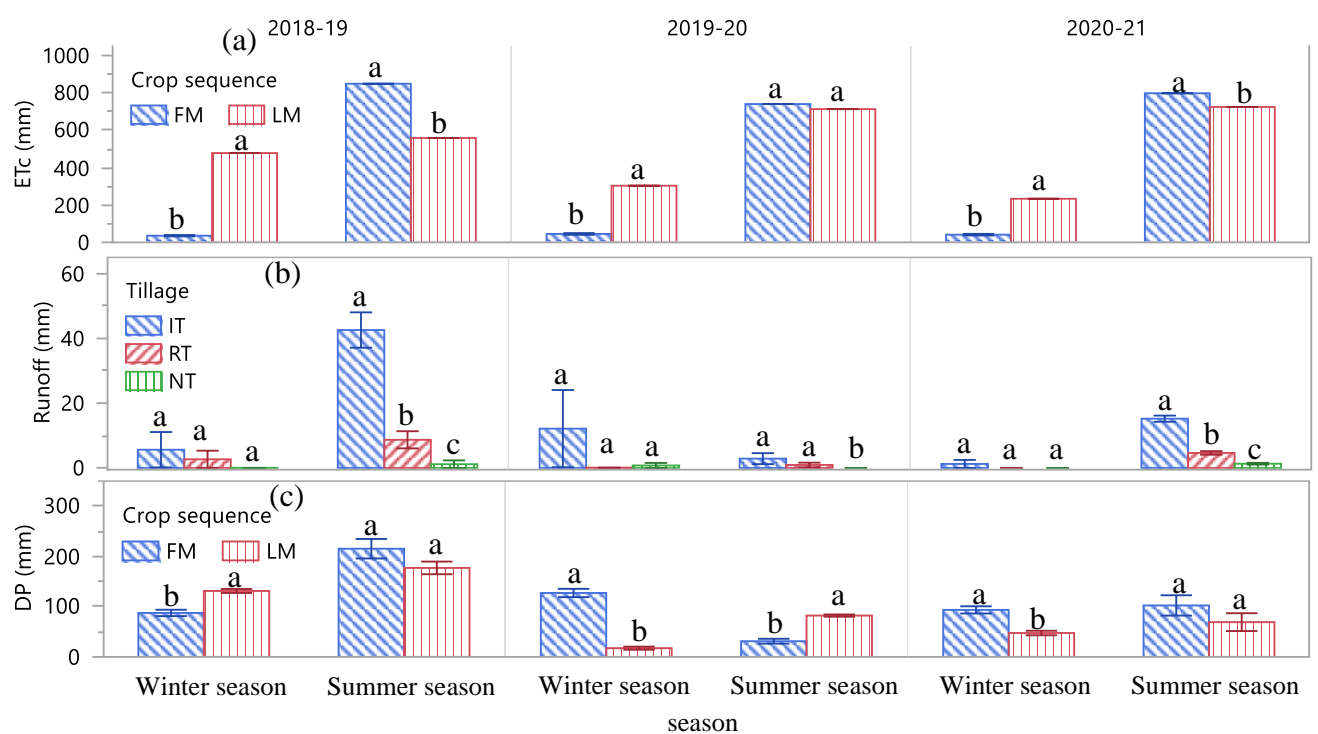


Fig. 20: Crop evapotranspiration (ET_c , mm) (a), runoff (R_{off} , mm) (b), and deep percolation (DP , mm) (c) affected by the interaction among years (2018-19, 2019-20 and 2020-21), seasons (winter and summer cropping season), and crop sequences (FM, short fallow-maize; LM, legume-maize)/tillage systems (IT, intensive tillage; RT, reduced tillage; NT, no-tillage). Error bars show the standard error. Different lowercase letters indicate significant differences between treatments within cropping season ($p < 0.05$).

Deep percolation was significantly affected by year ($p = 0.0001$), season ($p = 0.003$) and crop sequence ($p = 0.007$) but not by tillage system (Table 12). All tillage systems showed similar values of DP (Table 12). During the winter cropping season (Fig. 20c), estimated DP was lower in FM than LM in 2018-19, but higher in FM than LM in 2019-20 and 2020-21 years. During

the summer cropping season, no differences in *DP* were observed between FM and LM except in 2019-20, when LM had significantly greater *DP* than FM.

3.2 Crop variables

Tillage systems did not significantly affect pea above ground biomass, grain yield or harvest index in 2018-19 (Table 13; and Fig. 21 a, d and e), whereas significantly affected vetch above ground biomass in 2019-20 and 2020-21 ($p < 0.001$ and $p < 0.05$ respectively, Table 13).

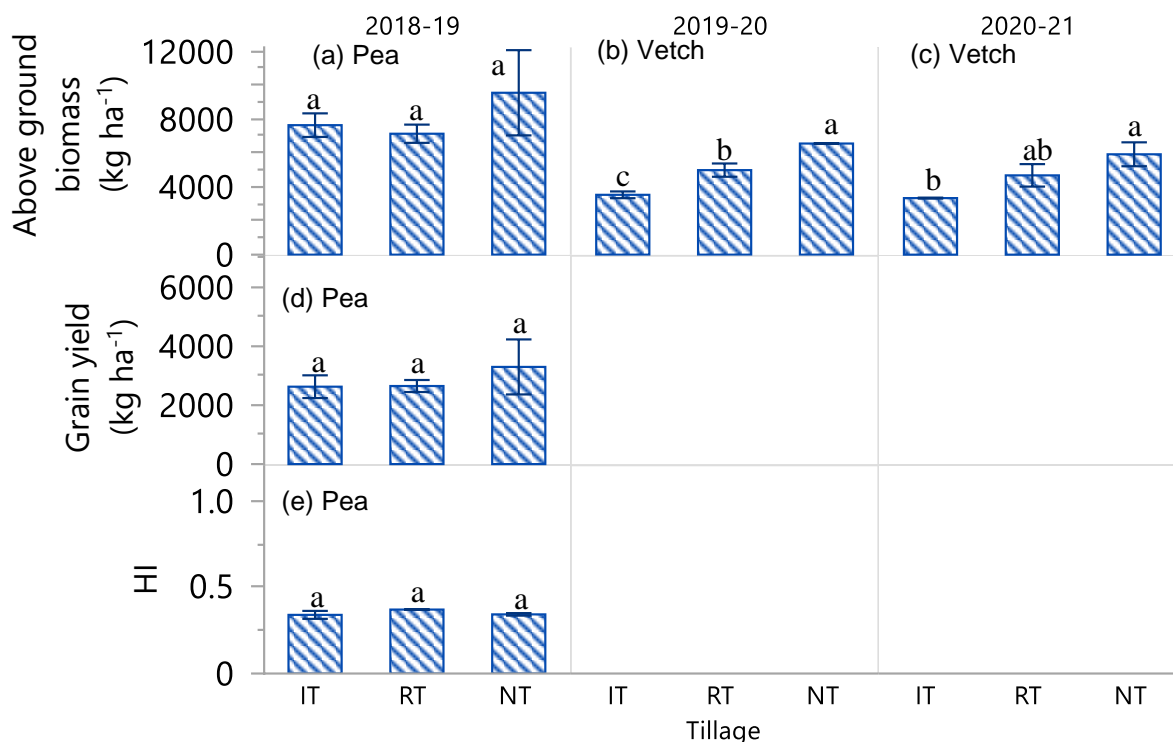


Fig. 21: Above ground biomass (kg ha^{-1}) production in (a) 2018-19, (b) 2019-20 and (c) 2020-21 and pea grain yield (d) (kg ha^{-1}) and harvest index, HI (e) in 2018-19 under different tillage systems (IT, intensive tillage; RT, reduced tillage; NT, no-tillage) during winter cropping season. Error bars show the standard error. Different lowercase letters indicate significant differences between treatments means for a given year and variable ($p < 0.05$). Pea grain data is shown at 0% moisture content.

In 2019-20, the vetch above ground biomass was significantly greater under NT than RT and IT, with 6542, 4977 and 3523 kg ha^{-1} , respectively. In 2020-21, RT (4668 kg ha^{-1}) and NT (5909 kg ha^{-1}) had significantly greater vetch above ground biomass production than IT (3330 kg ha^{-1}) (Fig. 21 b and c). Maize above ground biomass was significantly affected by crop sequence in 2018-19 ($p = 0.008$) and 2020-21 ($p < 0.0001$), whereas grain yield was only

significantly affected in 2018-19 ($p = 0.03$). Above ground biomass was significantly higher in LM compared to FM in 2018-19 and 2020-21 (24701 vs. 17773 and 21706 vs. 12409 kg ha⁻¹, respectively) and grain yield in 2018-19 (11368 vs. 8225 kg ha⁻¹) (Fig. 22).

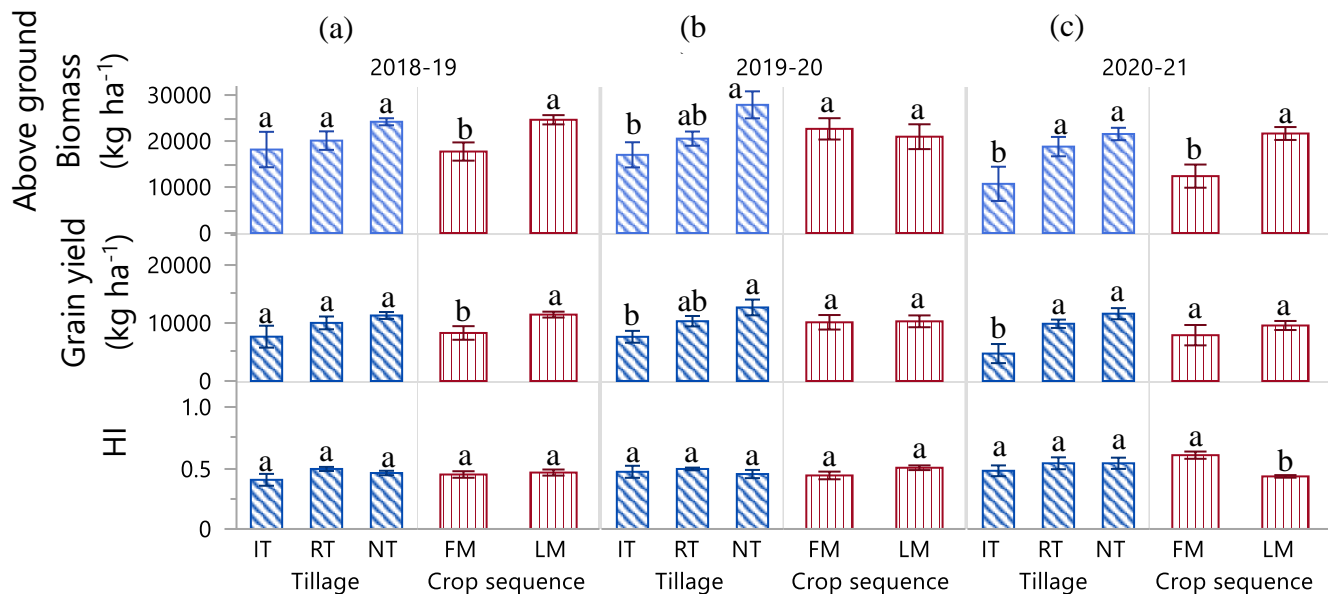


Fig. 22: Maize above ground biomass (kg ha⁻¹), grain yield (kg ha⁻¹), and harvest index (HI) in (a) 2018-19, (b) 2019-20, and (c) 2020-21 under different tillage systems (IT, intensive tillage; RT, reduced tillage; NT, no-tillage) and crop sequences (FM, short fallow-maize; LM, legume-maize) during summer cropping season. Error bars show the standard error. Different lowercase letters indicate significant differences between treatments means ($p < 0.05$). Maize grain data is shown at 0% moisture content.

A significant interaction between tillage systems and crop sequences was observed for above ground biomass ($p = 0.04$) and grain yield ($p = 0.02$) in 2020-21 (Table 13). Regardless of tillage systems, LM tended to have higher above ground biomass than FM, specially under IT (18279 vs. 3172 kg ha⁻¹) and RT (23041 vs. 14651 kg ha⁻¹) (Fig. 23a). Grain yield was significantly lower in FM than LM (1582 vs. 7812 kg ha⁻¹) under IT (Fig. 23b). The maize above ground biomass and grain yield were significantly affected by tillage in 2019-20 ($p = 0.04$) and 2020-21 ($p < 0.0003$) but not in 2018-19 (Table 13). No significant differences were observed for maize above ground biomass and grain yield among tillage systems in 2018-19 (Table 13), whereas NT had significantly higher above ground biomass (27960, 20586 and 17051 kg ha⁻¹ in NT, RT and IT, respectively) and grain yield (12597, 10240 and 7568 kg ha⁻¹ in NT, RT and IT, respectively) than IT in 2019-20, and both NT and RT in 2020-21 (Fig. 22).

The HI was only significantly affected by crop sequence ($p = 0.0003$) in 2020-21, but not by tillage (Fig. 22), and FM showed greater HI compared to LM.

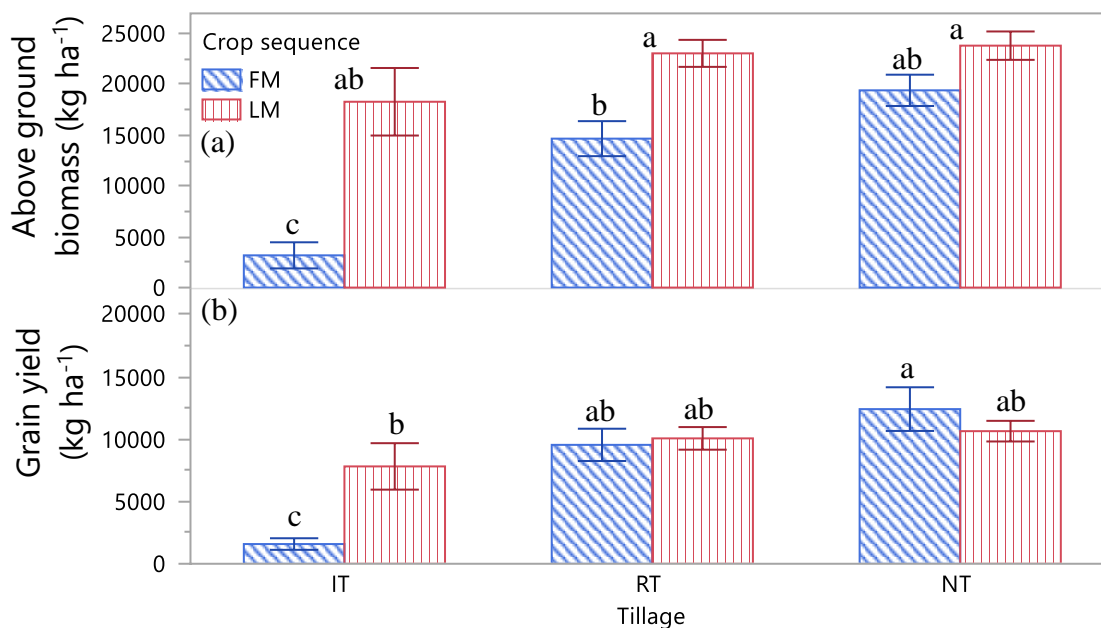


Fig. 23: Maize above ground biomass (kg ha⁻¹) (a) and grain yield (kg ha⁻¹) (b) in 2020-21 as affected by the interaction between tillage systems (IT, intensive tillage; RT, reduced tillage; NT, no-tillage) and crop sequences (FM, short fallow-maize; LM, legume-maize). Error bars show the standard error. Different lowercase letters indicate significant differences within each variable ($p < 0.05$).

3.3 Crop water use efficiency and water productivity

During the winter cropping season in 2019-20 and 2020-21, vetch WUE_c was significantly affected by tillage ($p = 0.0005$ and 0.04 , respectively) but not pea WUE_c in 2018-19 (Table 14). Pea WUE_c were similar under the three tillage systems (Fig. 24), whereas vetch WUE_c were greater under NT than under IT both in 2019-20 and 2020-21, and than under RT in 2019-20. Water productivity was only computed for pea, harvested for grain yield in 2018-19. Although water productivity was always slightly higher for NT (Fig. 24), the difference with RT and IT was only significant for WP_I (25.9, 20.8, 20.6 kg ha⁻¹ mm⁻¹ in NT, RT and IT, respectively) ($p = 0.005$, Table 14).

Table 13: Analysis of variance (p-values) of above ground biomass (kg ha^{-1}), grain yield (kg ha^{-1}) and harvest index (HI) affected by tillage systems (IT, intensive tillage; RT, reduced tillage; NT, no-tillage) and crop sequence (FM, short fallow-maize; LM, legume-maize) and their interactions) during the winter and summer cropping seasons of three consecutive years.

Source of variation	Above ground biomass (kg ha^{-1})			Grain yield (kg ha^{-1})			Harvest index (HI)		
	2018-19	2019-20	2020-21	2018-19	2019-20	2020-21	2018-19	2019-20	2020-21
Winter cropping season: Fallow (FM)-legume (LM)									
Tillage (T)	NS	0.0005	0.04	NS	-	-	NS	-	-
Summer cropping season: Maize (FM and LM)									
Tillage (T)	NS	0.04	0.0003	NS	0.04	0.0005	NS	NS	NS
Crop Sequence (CS)	0.008	NS	<0.0001	0.03	NS	NS	NS	NS	0.0003
T \times CS	NS	NS	0.04	NS	NS	0.02	NS	NS	NS

NS, Non-significant at $p = 0.05$.

Table 14: Analysis of variance (p-values) of crop water use efficiency (WUE_c), crop water productivity (WP_c), irrigation water productivity (WP_I) and input water productivity (WP_{I+P}) affected by tillage systems (IT, intensive tillage; RT, reduced tillage; NT, no-tillage), crop sequences (FM, short fallow-maize; LM, legume-maize), and their interaction) during the winter and summer cropping seasons of three consecutive years.

Source of variation	Crop water use efficiency (WUE_c)			Crop water productivity (WP_c)						Irrigation water productivity (WP_I)			Input water productivity (WP_{I+P})		
	2018-19	2019-20	2020-21	WP_{c1} (Yield/ ET_c)			WP_{c2} (Yield/[$ET_c+N-BWU$])			2018-19	2019-20	2020-21	2018-19	2019-20	2020-21
Winter cropping season: Fallow (FM)-legume (LM)															
Tillage (T)	NS	0.0005	0.04	NS	-	-	NS	-	-	0.005	-	-	NS	-	-
Summer cropping season: Maize (FM and LM)															
Tillage	NS	0.01	<0.0001	NS	0.04	0.0007	NS	0.04	0.0003	NS	0.04	0.0006	NS	0.04	0.0006
CS	<0.0001	NS	0.0002	<0.0001	NS	0.04	0.0001	NS	0.02	0.001	NS	0.008	0.0007	NS	0.04
T \times CS	NS	NS	NS	NS	NS	0.04	NS	NS	NS	NS	NS	0.03	NS	NS	0.04

ET_c , Crop evapotranspiration; $N-BWU$, non-beneficial water use; NS, Non-significant at $p = 0.05$.

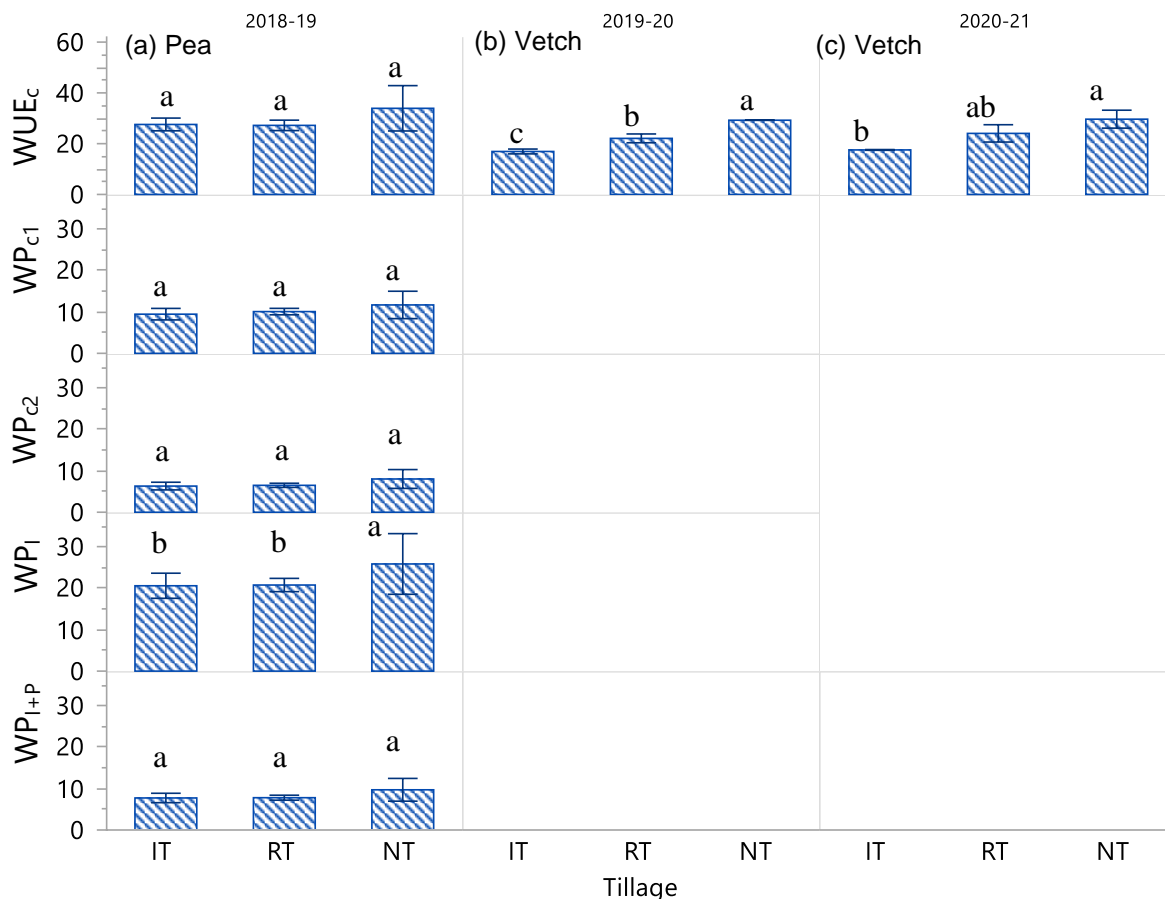


Fig 24: Crop water use efficiency (WUE_c), crop (WP_{c1} : Yield/ ET_c ; and WP_{c2} : Yield/ $[ET_c+N-BWU]$), irrigation (WPI) and input ($WPI+P$) water productivity during the winter cropping season in (a) 2018-19 (Pea), (b) 2019-20 (Vetch) and (c) 2020-21 (Vetch) under different tillage systems (IT, intensive tillage; RT, reduced tillage; NT, no-tillage) and crop sequences (FM, short fallow-maize; LM, legume-maize). Error bars show the standard error. Different lowercase letters indicate significant differences between treatments ($p < 0.05$).

During the summer cropping season, maize WUE_c was significantly affected by tillage in 2019-20 and 2020-21 ($p = 0.01$ and $p < 0.0001$, respectively) and by crop sequence in 2018-19 and 2020-21 ($p < 0.0001$ and $p = 0.0002$, respectively) (Table 14). No significant interaction between tillage and crop sequence was found. In 2018-19, the three tillage systems showed similar maize WUE_c (around $35.6 \text{ kg ha}^{-1} \text{ mm}^{-1}$), while in 2019-20 and 2020-21, NT and also RT in 2020-21, had significantly higher maize WUE_c than IT (Fig. 25). On the other hand, LM had significantly higher maize WUE_c than FM in 2018-19 (50.0 vs. $26.4 \text{ kg ha}^{-1} \text{ mm}^{-1}$) and in 2020-21 (30.9 vs. $16.3 \text{ kg ha}^{-1} \text{ mm}^{-1}$), whereas no differences were found in 2019-20 (Fig. 25). There was no interaction effect between tillage systems and crop sequence on maize WUE_c .

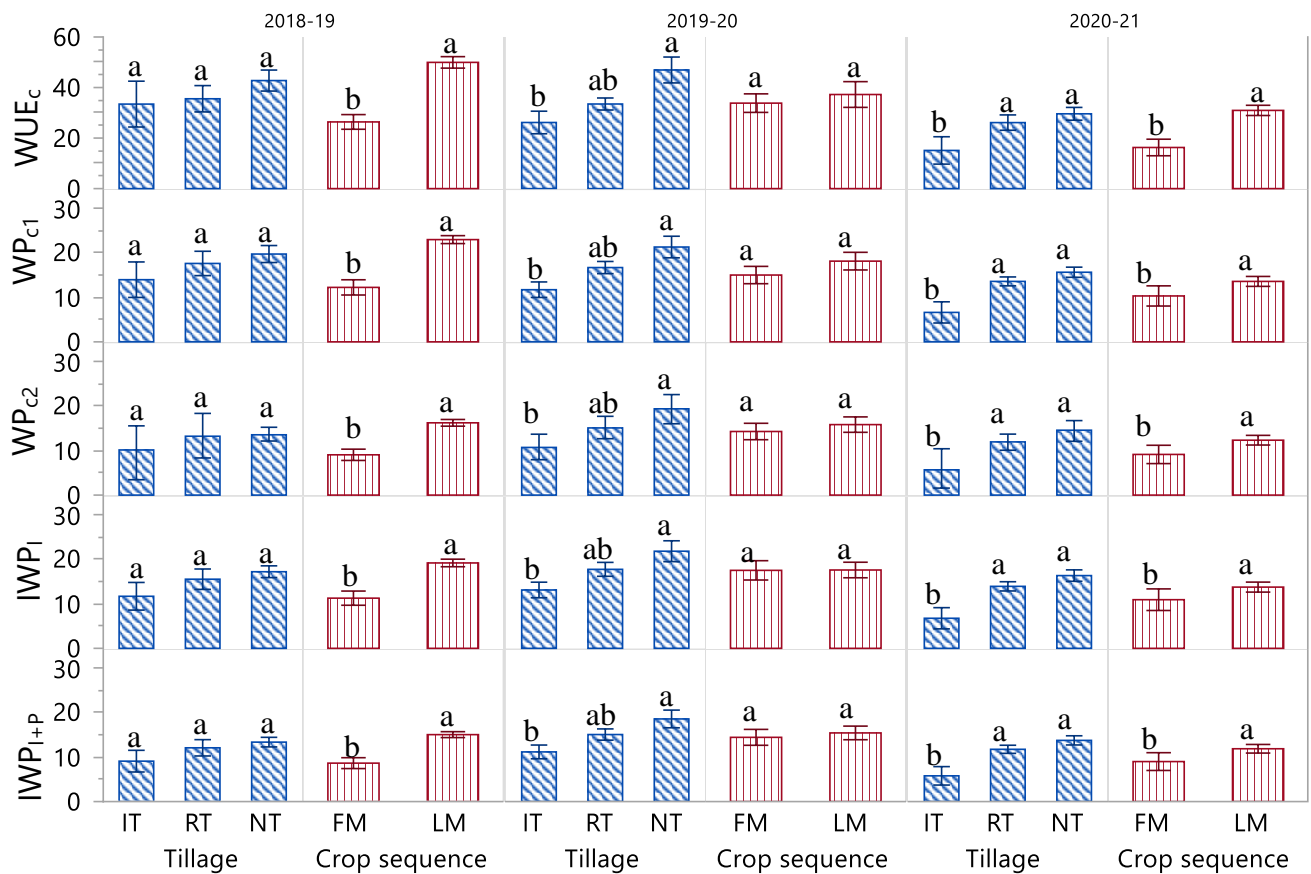


Fig. 25: Crop water use efficiency (WUE_c), crop (WP_{c1} : Yield/ ET_c ; and WP_{c2} : Yield/[$ET_c + N-BWU$]), irrigation (WP_i) and input (WP_{i+p}) water productivity of maize during the summer cropping season in 2018-19, 2019-20 and 2020-21 under different tillage systems (IT, intensive tillage; RT, reduced tillage; NT, no-tillage) and crop sequences (FM, short fallow-maize; LM, legume-maize). Error bars show the standard error. Different lowercase letters indicate significant differences between treatments ($p < 0.05$).

Water productivities during 2019-20 and 2020-21 were significantly affected by tillage but not in 2018-19 (Table 14). Both in 2019-20 and 2020-21, NT and RT had significantly higher WP_{c1} , WP_{c1} , WP_i and WP_{i+p} than IT, whereas no significant differences were observed among tillage systems in 2018-19 (Fig. 25). On the other hand, WP_{c1} , WP_{c1} , WP_i and WP_{i+p} were significantly affected by crop sequence in 2018-19 and 2020-21 but not in 2019-20 (Fig. 25). Both in 2018-19 and 2020-21, LM had significantly higher WP_{c1} , WP_{c2} , WP_i and WP_{i+p} than FM, whereas no significant differences were observed in 2019-20 (Fig. 25). There was a significant interaction effect between tillage and crop sequence on WP_{c1} , WP_i and WP_{i+p} in 2020-21 (Table 14). IT

had significantly greater WP_{c1} , WP_I and WP_{I+P} in LM than FM, whereas no difference was observed between crop sequences for RT and NT (Fig. 26).

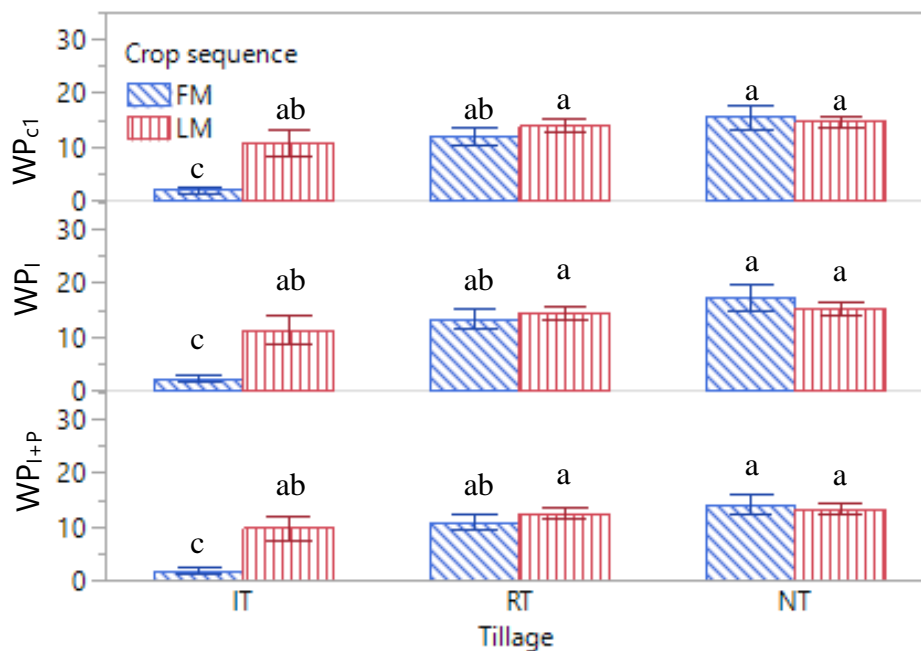


Fig 26: Maize Crop (WP_{c1}), Irrigation (WP_I) and input (WP_{I+P}) water productivity during the summer cropping season in 2020-21 as affected by the interaction between tillage systems (IT, intensive tillage; RT, reduced tillage; NT, no-tillage) and crop sequences (FM, short fallow-maize; LM, legume-maize). Error bars show the standard error. Different lowercase letters indicate significant differences within each variable ($p < 0.05$).

4. Discussion

4.1 Impacts of crop sequence on soil water balance components, yield, crop water use efficiency and productivity

FM showed greater SWC than LM (Fig. 18) particularly, during the winter cropping season. It was expected that fallow period or the initial stages of maize had lower E/ET_c than the vegetative stage of legumes. Due to water uptake by legume, LM had lower SWC than FM, specially at the end of the winter cropping season, as found by Gabriel et al. (2019). Similarly, during the winter cropping season, higher ET_c and less DP in LM compared to FM was the result of legume water uptake (Fig. 20 a and c). Exceptionally, in 2018-19, LM had greater water losses through DP than FM because in this year legume (pea) overlapped in time with late maturing maize for two months and received 126 mm of irrigation water. The consequences

of irrigation were also evident on DP and R_{off} in the summer cropping season. In 2018-19, the required water was applied in one irrigation event per day that generated relatively higher DP and R_{off} . In the subsequent years (2019-20 and 2020-21) irrigation was split in two events per day (early morning and late evening) which reduced DP and, especially R_{off} . In the summer cropping season, lower ET_c in LM is linked to the days need to complete the crop cycle of maize. The late maturing maize (FM) took 40 and 27 more days than early maturing maize in these years. As a result, FM had greater ET_c than LM, whereas no difference on ET_c were found in 2019-20 because both late and early maturing maize were on the field for the similar number of days. During the winter cropping season, water consumption by legume crops reduced the risk of water loss through deep percolation. Beside this, during the winter cropping season in 2018-19 and summer cropping season in 2019-20, significantly greater DP in LM than FM could be related to positive impacts of legume on soil structure stability (Palese et al., 2014; Gabriel et al., 2019). In the same experimental field, it was reported that legume inclusion increased gas diffusivity, macroporosity and pore continuity (Talukder et al., 2022), and improved soil hydraulic properties and pore characteristics (unpublished work). Therefore, better porous systems enhanced infiltration and percolation of rain and irrigation water, consequently led to vertical water movement down to deeper horizons.

The results of this study show that LM had significantly greater maize above ground biomass and grain yield compared to FM in 2018-19 and 2020-21, but did not had an effect in 2019-2020 (Fig. 23). This different result can be due to, firstly, higher disease impact i.e., *Fusarium oxysporum* and weed infestation observed in FM compared to LM in 2018-19 and 2020-21, respectively. Since 2015, maize mono-cropping has been implemented specifically in FM, making this system more vulnerable to disease and weed infestation. Consequently, the biotic stress in FM could decreased the maize above ground biomass and grain yield compared to LM. It is already known that crop diversification with pea or vetch decreases the risk of weeds and

pests infestation in maize grown after them (Ward et al., 2012b). In addition, the early maturing maize could be capable to skip the disease and weed infestation phase due to its late planting. Secondly, pea or vetch enhance the productivity of soils by increasing soil nitrogen and organic carbon content (Gabriel and Quemada, 2011; Huynh et al., 2019). In similar climate and irrigated condition, Gabriel and Quemada (2011) reported that replacing bare fallow with barley or vetch crops in winter did not affect the subsequent maize yield during a 3.5 years study in a silty clay loam soil at Aranjuez, Spain. Similarly, a meta-analysis by Miguez and Bollero, (2005) reported that the introduction of a leguminous crop in winter enhanced maize yield by 37% at 0 kg N ha⁻¹ fertilizer, but this effect reduced when N fertilizer was used.

LM showed greater above ground biomass under IT and RT than FM in 2020-21, and also grain yield was greater under IT (Fig. 23). These greater above ground biomass and grain yield implies that maize performance improved under IT and RT as a consequence of legume inclusion. The benefits of legume inclusion are also linked to the improvement of some soil physical properties that were observed in a parallel study (Talukder et al., 2022), which can counteract the negative effect of intensive tillage in the LM system. Similar pattern of maize yield improvement was reported by Huynh et al. (2019) from a 9-year field study in Germany. They found that crop rotations with legume increased soil nitrogen and carbon content leading to greater maize yield than mono-cropping (maize) both in IT and NT under irrigated condition in a sandy soil.

Water use efficiency and water productivities of maize were significantly higher in LM as compared to FM in 2018-19 and 2020-21 (Fig. 26). The reasons can be: (i) greater biomass and grain yield together with relatively less ET_c (early maturing maize used in LM had lower ET_c compared to long maturing maize used in FM because of less time on field needed to produce the yield) that lead to increased WUE_c and WP_{c1} , (ii) greater grain yield, relatively less ET_c and similar or slightly lower water loss by DP that increased WP_{c2} , and (iii) less irrigation in LM

than FM maize, with proportionally higher yields, that results in higher irrigation and input water productivity. Less water supply in LM resulted in 19 and 6% irrigation water savings in 2018-19 and 2020-21, respectively. Less water application during summer growing season, and greater water depletion during the winter cropping season had no detrimental effects on subsequent maize WUE_c and the different water productivities. Similarly, crop water productivity (grain yield/ ET_c) was compared between soybean (*Glycine max* L. (Merr)) monoculture vs. soybean following a cover crops by oats (*Avena sativa* L.) on a long-term NT clay loam soil in Argentina (Alfonso et al., 2020). They reported that water productivity in soybean improved (4-10%) by the inclusion of a cover crop in the crop sequence. Impacts of tillage systems on soil water balance components, yield, crop water use efficiency and productivity.

4.2 Impacts of tillage systems on soil water balance components, yield, crop water use and productivity

Soil water content changed based on tillage practices at different sampling dates. Conservation tillage practices i.e., RT and NT had significantly higher SWC than IT at the end of the summer cropping season in 2019-20 and 2020-21 (Fig. 19). Other studies have found that NT and RT increased SWC in rain-fed Mediterranean areas due to increased crop surface cover by crop residue and improved soil structure (Ward et al., 2012; Brunel-Saldias et al., 2018). Previous published (and unpublished) work from the same experimental field described the impacts of tillage on soil structure (Pareja-Sánchez et al., 2017; Ramos et al., 2019; Talukder et al., 2022). Long-term NT and RT increased soil structure stability and it was evident in these findings, in brief: (i) increased soil gas diffusivity, macropores and its continuity (Talukder et al., 2022), (ii) reduced the risk of soil crusting and increased infiltration (unpublished results) and (iii) reduced the risk of surface soil sealing and increased crop establishment (19-20%) (Ramos et al., 2019). On the contrary, IT demonstrated lower structural stability due to deterioration of

soil physical properties. These improvements on soil structure under RT and NT greatly affects the results of runoff, crop yield and water productivity in the present study.

Regardless of tillage systems, *DP* was similar, and runoff was very low compared to DP or total input water (Fig. 20 b and c). However, the tendency of increasing surface runoff from NT to IT is due to increased tillage intensity, which makes the soil prone to sealing and crusting. It was widely documented that soil sealing and crusting impeded infiltration and increased runoff (Gabriel et al., 2019; Huynh et al., 2019). Apart from that, RT and especially NT had more crop residue on the surface soil than IT, that acted as a barrier to prevent runoff.

In two of the three years considered, it was observed that both legumes and maize performance varied depending on the tillage practice. In this regard, vetch biomass, and maize biomass and grain yield were significantly greater under NT and RT compared to IT (Fig. 22 and 23). As mentioned previously, IT had lower soil structural stability and showed greater soil degradation in terms of soil hydro-physical properties i.e., lower hydraulic conductivity and infiltration, aggregate stability and soil organic carbon content, pore continuity. As a consequence of soil degradation under IT affected crop establishment, and it was found that maize plant density decreased from 19-20% under IT in the same experimental field (Pareja-Sánchez et al., 2017), resulting in lower maize yields (Pareja-Sánchez et al., 2019). Other investigations of maize productivity under various tillage systems, both under rain-fed and irrigated conditions, showed contradictory or similar results. They stated that soil texture, years of tillage practice, and water input all have an impact on maize yield performance. For instance, Lamm et al. (2009) compared maize yield among IT, RT and NT in a long-term tillage experiment in a silt loam soil under irrigated condition at Colby, Kansas USA. They found that RT and NT significantly increased maize yield compared to IT due to residue retention that reduced evaporation loss and enhanced water use under those tillage systems. Contrarily, in a 9-year field study, in northeast Germany, Huynh et al. (2019) working on a sandy soil, reported that a negative impact of NT

started from the fourth year, and reduced the maize yield significantly as compared to IT to the rest of the year, both under irrigated and non-irrigated condition. They pointed out that high compaction and low water availability of NT negatively affect seedling emergence and crop establishment. In a case study of many experimental sites particularly from southern Africa where average precipitation was 631 mm year⁻¹, Erenstein et al. (2012) found that conservation tillage practices (RT and NT) greatly increased maize yield. Exceptionally, under extreme water limited condition due to low precipitation maize yield was lower under RT and NT compared to IT. They noted that higher bulk density in NT caused poor root penetration, which hindered the establishment of seedling roots.

Crop water use efficiency (WUE_c) of vetch and maize, and crop water productivities (WP) of maize were significantly higher under RT and NT as compared to IT in 2019-20 and 2020-21 (Fig. 25). All tillage systems received the same amount of water either by rain and/or irrigation and water losses by ET_c were also relatively equal (Table 12). Therefore, greater biomass of vetch, and greater biomass and grain of maize under RT and NT significantly increased water use efficiency and water productivity of these crops compared to IT. Our results are in agreement with the results of Lamm et al. (2009) who found that slightly increased water use efficiency by maize under RT and NT correspond with greater grain yields for these tillage systems. Further, water productivity (grain yield/ ET_c) also tended to be greater for these tillage systems compared to IT because of increased yields under RT and NT.

5. Conclusions

Inclusion of legume in the crop sequence increases the water consumption and depletion from soil during the winter cropping period. However, under irrigated conditions, water depletion is unlikely to have a negative impact on following maize cropping season. The maize grown after the legume produces more biomass and grain yield, and as a consequence, crop water use efficiency and water productivities of maize increases. Under intensive tillage legume inclusion

could mitigate the negative effects of tillage and get similar biomass and grain yield production than conservation tillage systems.

Conservation tillage practices such as reduced tillage and no tillage, reduces surface runoff without increasing deep percolation. These in turns significantly increases crop biomass, and grain yields and hence water use efficiency and water productivity. In some studies of soil water balance to determine the water used by the crop, the surface runoff and deep percolation are often assumed to be zero or negligible, which is an error that overestimate the crop evapotranspiration. Under field conditions, these two variables can become quite important, and they should be taken into account specially under irrigated conditions and in fields which are not completely flat. To split the daily irrigation dose in two events as proven to be useful to reduce runoff and deep percolation losses in low infiltration soils.

Acknowledgments

The authors thank the advice given by Professor Maria Concepción Ramos, and the support of the field and laboratory technicians Carlos Cortés and Silvia Martí, and the farmer Xavier Penella. The authors gratefully acknowledge support for this research from the Research Spanish Agency (DISOSMED Project – AGL2017-84529-C3-R). Rasendra Talukder also sincerely acknowledges the fund provided by University of Lleida to support PhD fellowship. Daniel Plaza-Bonilla is Ramón y Cajal fellow (RYC-2018-024536-I) co-funded by MICIN/AEI/10.13039/501100011033 and European Social Fund.

References

Alfonso, C., Barbieri, P.A., Hernández, M.D., Lewczuk, N.A., Martínez, J.P., Echarte, M.M.,

Echarte, L., 2020. Water productivity in soybean following a cover crop in a humid environment. *Agric. Water Manag.* 232, 106045.

<https://doi.org/10.1016/j.agwat.2020.106045>

Allen, R.G., Pereira, L.S., Raes, D., Smith, M., 1998. Crop evapotranspiration-Guidelines for

computing crop water requirements-FAO Irrigation and drainage paper 56. Fao, Rome 300, D05109.

- Baffaut, C., Baker, J.M., Biederman, J.A., Bosch, D.D., Brooks, E.S., Buda, A.R., Demaria, E.M., Elias, E.H., Flerchinger, G.N., Goodrich, D.C., Hamilton, S.K., Hardegree, S.P., Harmel, R.D., Hoover, D.L., King, K.W., Kleinman, P.J., Liebig, M.A., McCarty, G.W., Moglen, G.E., Moorman, T.B., Moriasi, D.N., Okalebo, J., Pierson, F.B., Russell, E.S., Saliendra, N.Z., Saha, A.K., Smith, D.R., Yasarer, L.M.W., 2020. Comparative analysis of water budgets across the U.S. long-term agroecosystem research network. *J. Hydrol.* 588, 125021. <https://doi.org/10.1016/j.jhydrol.2020.125021>
- Brunel-Saldias, N., Seguel, O., Ovalle, C., Acevedo, E., Martínez, I., 2018. Tillage effects on the soil water balance and the use of water by oats and wheat in a Mediterranean climate. *Soil Tillage Res.* 184, 68–77. <https://doi.org/10.1016/j.still.2018.07.005>
- Cantero-Martínez, C., Angas, P., Lampurlanés, J., 2003. Growth, yield and water productivity of barley (*Hordeum vulgare* L.) affected by tillage and N fertilization in Mediterranean semiarid, rainfed conditions of Spain. *F. Crop. Res.* 84, 341–357. [https://doi.org/10.1016/S0378-4290\(03\)00101-1](https://doi.org/10.1016/S0378-4290(03)00101-1)
- Lamm, F. R., Aiken, R. M., Abou Kheira, A. A., 2009. Corn Yield and Water Use Characteristics as Affected by Tillage, Plant Density, and Irrigation. *Trans. ASABE* 52, 133–143. <https://doi.org/10.13031/2013.25954>
- Fernández, J.E., Alcon, F., Diaz-Espejo, A., Hernandez-Santana, V., Cuevas, M. V., 2020. Water use indicators and economic analysis for on-farm irrigation decision: A case study of a super high density olive tree orchard. *Agric. Water Manag.* 237, 106074. <https://doi.org/10.1016/j.agwat.2020.106074>
- Flexas, J., Galmes, J., Galle, A., Gulias, J., Pou, A., Ribas-carbo, M., Tomàs, M., Medrano,

- H., 2010. Improving water use efficiency in grapevines: potential physiological targets for biotechnological improvement. *Aust. J. Grape Wine Res.* 16, 106–121.
<https://doi.org/10.1111/j.1755-0238.2009.00057.x>
- Forte, A., Fiorentino, N., Fagnano, M., Fierro, A., 2017. Mitigation impact of minimum tillage on CO₂ and N₂O emissions from a Mediterranean maize cropped soil under low-water input management. *Soil Tillage Res.* 166, 167–178.
<https://doi.org/10.1016/j.still.2016.09.014>
- Franco-Luesma, S., Cavero, J., Plaza-Bonilla, D., Cantero-Martínez, C., Tortosa, G., Bedmar, E.J., Álvaro-Fuentes, J., 2020. Irrigation and tillage effects on soil nitrous oxide emissions in maize monoculture. *Agron. J.* 112, 56–71.
<https://doi.org/10.1002/agj2.20057>
- Gabriel, J.L., Quemada, M., 2011. Replacing bare fallow with cover crops in a maize cropping system: Yield, N uptake and fertiliser fate. *Eur. J. Agron.* 34, 133–143.
<https://doi.org/10.1016/j.eja.2010.11.006>
- Gabriel, J.L., Quemada, M., Martín-Lammerding, D., Vanclooster, M., 2019. Assessing the cover crop effect on soil hydraulic properties by inverse modelling in a 10-year field trial. *Agric. Water Manag.* 222, 62–71. <https://doi.org/10.1016/j.agwat.2019.05.034>
- Graham, S.L., Laubach, J., Hunt, J.E., Eger, A., Carrick, S., Whitehead, D., 2019. Predicting soil water balance for irrigated and non-irrigated lucerne on stony, alluvial soils. *Agric. Water Manag.* 226, 105790. <https://doi.org/10.1016/j.agwat.2019.105790>
- Grassini, P., Thorburn, J., Burr, C., Cassman, K.G., 2011. High-yield irrigated maize in the Western U.S. Corn Belt: I. On-farm yield, yield potential, and impact of agronomic practices. *F. Crop. Res.* 120, 142–150. <https://doi.org/10.1016/j.fcr.2010.09.012>
- Howitt, R., 2008. *Water Productivity in Agriculture: Limits and Opportunities for*

- Improvement. *Vadose Zo. J.* 7, 390–391. <https://doi.org/10.2136/vzj2007.0085br>
- Huynh, H.T., Hufnagel, J., Wurbs, A., Bellingrath-Kimura, S.D., 2019. Influences of soil tillage, irrigation and crop rotation on maize biomass yield in a 9-year field study in Müncheberg, Germany. *F. Crop. Res.* 241, 107565. <https://doi.org/10.1016/j.fcr.2019.107565>
- Lee, H., Lautenbach, S., Nieto, A.P.G., Bondeau, A., Cramer, W., Geijzendorffer, I.R., 2019. The impact of conservation farming practices on Mediterranean agro-ecosystem services provisioning—a meta-analysis. *Reg. Environ. Chang.* <https://doi.org/10.1007/s10113-018-1447-y>
- Li, X., Zhang, X., Niu, J., Tong, L., Kang, S., Du, T., Li, S., Ding, R., 2016. Irrigation water productivity is more influenced by agronomic practice factors than by climatic factors in Hexi Corridor, Northwest China. *Sci. Rep.* 6, 37971. <https://doi.org/10.1038/srep37971>
- MAPAMA, 1945. Anuario de Estadística del MAPA.
- MAPAMA, 2019. Anuario de Estadística del MAPA.
- Martínez-Cob, A., 2008. Use of thermal units to estimate corn crop coefficients under semiarid climatic conditions. *Irrig. Sci.* 26, 335–345. <https://doi.org/10.1007/s00271-007-0097-5>
- Miguez, F.E., Bollero, G.A., 2005. Review of corn yield response under winter cover cropping systems using meta-analytic methods. *Crop Sci.* <https://doi.org/10.2135/cropsci2005.0014>
- Montgomery, D.C., 2012. *Design and Analysis of Experiments Ninth Edition*, Eighth ed. ed. John Wiley & Sons, Cary, North Carolina, USA.
- Palese, A.M., Vignozzi, N., Celano, G., Agnelli, A.E., Pagliai, M., Xiloyannis, C., 2014. Influence of soil management on soil physical characteristics and water storage in a

- mature rainfed olive orchard. *Soil Tillage Res.* 144, 96–109.
<https://doi.org/10.1016/j.still.2014.07.010>
- Pareja-Sánchez, E., Plaza-Bonilla, D., Álvaro-Fuentes, J., Cantero-Martínez, C., 2019. Is it feasible to reduce tillage and N use while improving maize yield in irrigated Mediterranean agroecosystems? *Eur. J. Agron.* 109, 125919.
<https://doi.org/10.1016/j.eja.2019.125919>
- Pareja-Sánchez, E., Plaza-Bonilla, D., Ramos, M.C., Lampurlanés, J., Álvaro-Fuentes, J., Cantero-Martínez, C., 2017. Long-term no-till as a means to maintain soil surface structure in an agroecosystem transformed into irrigation. *Soil Tillage Res.* 174, 221–230. <https://doi.org/10.1016/j.still.2017.07.012>
- Ramos, M.C., Pareja-Sánchez, E., Plaza-Bonilla, D., Cantero-Martínez, C., Lampurlanés, J., 2019. Soil sealing and soil water content under no-tillage and conventional tillage in irrigated corn: Effects on grain yield. *Hydrol. Process.* 33, 2095–2109.
<https://doi.org/10.1002/hyp.13457>
- Rodrigues, G.C., Pereira, L.S., 2009. Assessing economic impacts of deficit irrigation as related to water productivity and water costs. *Biosyst. Eng.* 103, 536–551.
<https://doi.org/10.1016/j.biosystemseng.2009.05.002>
- Salmerón, M., Isla, R., Cavero, J., 2011. Effect of winter cover crop species and planting methods on maize yield and N availability under irrigated Mediterranean conditions. *F. Crop. Res.* 123, 89–99. <https://doi.org/10.1016/j.fcr.2011.05.006>
- Smith, M. (Martin), 1992. CROPWAT : a computer program for irrigation planning and management.
- Soil Survey Staff, 2014. *Keys to Soil Taxonomy*, 12th ed. ed. USDA-Natural Resources Conservation Service, Washington, DC.

Talukder, R., Plaza-Bonilla, D., Cantero-Martínez, C., Wendroth, O., Castel, J.L., 2022. Soil gas diffusivity and pore continuity dynamics under different tillage and crop sequences in an irrigated Mediterranean area. *Soil Tillage Res.* 221, 105409.

<https://doi.org/10.1016/j.still.2022.105409>

Viets, F.G., 1962. Fertilizers And The Efficient Use Of Water, in: *Advances in Agronomy*. Academic Press, pp. 223–264. [https://doi.org/10.1016/S0065-2113\(08\)60439-3](https://doi.org/10.1016/S0065-2113(08)60439-3)

Ward, P.R., Flower, K.C., Cordingley, N., Weeks, C., Micin, S.F., 2012. Soil water balance with cover crops and conservation agriculture in a Mediterranean climate. *F. Crop. Res.* 132, 33–39. <https://doi.org/10.1016/j.fcr.2011.10.017>

Supplementary Tables

Table S5: Date of tillage operation, sowing or planting, chopping or harvesting from 2018-19 to 2020-21.

Date	Tillage operation	Sowing (pea/ vetch) or planting (maize)	Chopping or harvesting
Period: 2018-19			
26 Oct. 2018	IT and RT plots (FM and LM)	Pea, LM	-
12 Apr. 2019	-	late maturing maize, FM	-
18 June 2019	IT and RT plots, LM	-	Pea (Harvesting)
27 June 2019	-	Early maturing maize, LM	-
14 Oct. 2019	-	-	Late maturing maize, FM
19 Nov. 2019	-	-	Early maturing maize, LM
Period: 2019-20			
18 Dec. 2019	IT and RT plots (FM and LM)	-	-
10 Jan. 2020	-	Vetch, LM	-
01 May 2020	IT and RT plots, FM	-	-
02 May 2020	-	Late maturing maize, FM	-
21 May 2020	IT and RT plots, LM	-	Vetch (Chopping)
28 May 2020	-	Early maturing maize, LM	-
23 Sep. 2020	-	-	Late maturing maize, FM
21 Oct. 2020	-	-	Early maturing maize, LM
Period: 2020-21			
30 Nov. 2020	IT and RT plots (FM and LM)	-	-
03 Dec. 2020	-	Vetch, LM	-
21 Apr. 2021	IT and RT plots, FM	-	-
22 Apr. 2021	-	Late maturing maize	-
19 May 2021	IT & RT plots (LM)	Early maturing maize	Vetch (Harvesting)
4 Nov. 2021	-	-	Maize (FM and LM)

Table S6: Analysis of variance (p-values) of soil water content (SWC) up to 90 cm soil depth, affected by sampling dates, tillage systems (IT, intensive tillage; RT, reduced tillage; NT, no-tillage), crop sequences ((FM, short fallow-maize; LM, legume-maize) and their interactions in three consecutive years (2018-19, 2019-20 and 2020-21).

Source of variation	Soil water content in profile		
	2018-19	2019-20	2020-21
Sampling date (SD)	<0.0001	<0.0001	<0.0001
Crop sequence (CS)	0.03	<0.0001	<0.0001
Tillage (T)	0.004	0.03	0.002
SD × CS	NS	NS	NS
T × CS	NS	NS	NS
SD × T × CS	NS	NS	NS

NS, non-significant (p > 0.05).

Supplementary Figure

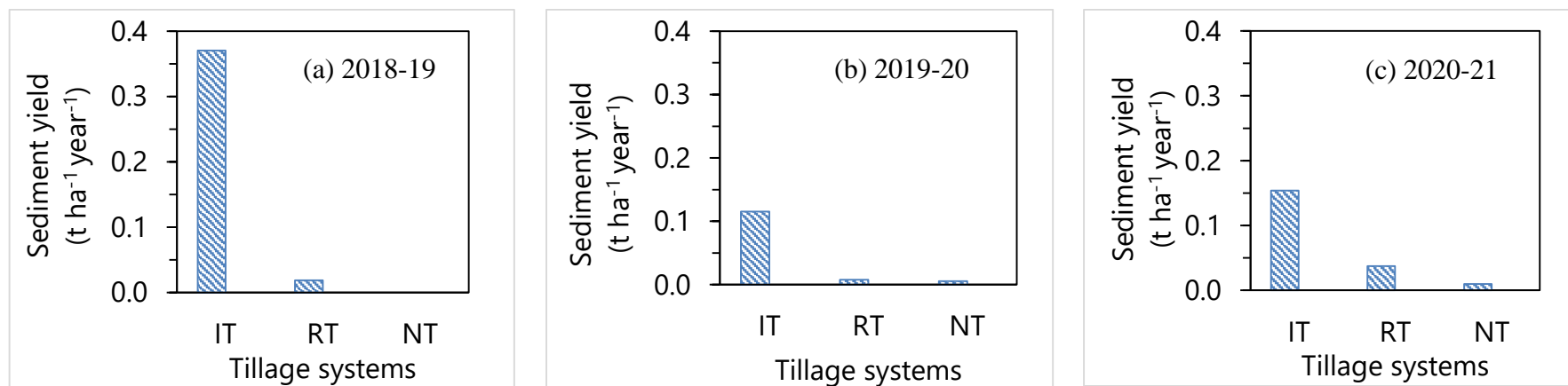


Fig S1: Sediment yield ($t\ ha^{-1}\ year^{-1}$) under different tillage systems (IT, intensive tillage; RT, reduced tillage; NT, no-tillage) in 2018-19 (a), 2019-20 (b) and 2020-21(c).

General discussion

General discussion

1. Crop sequence and tillage effects on spatio-temporal variations of soil hydro-physical properties

In the irrigated Mediterranean area, inclusion of legumes before maize as part of crop sequence or rotation, intensified soil and crop management activities such as tillage, planting, and harvesting, can potentially triggering temporal variations on soil properties. However, the effect of those intensification activities was not clearly seen on the temporal dynamics of gas diffusivity, air-filled porosity, soil water content and pore continuity comparing fallow-maize and legume-maize systems. But an increasing trend on these properties were observed in legume-maize system compared to fallow-maize. For instance, crop diversification: replacing fallows by legumes, increased soil aeration (gas diffusivity), and tended to increase saturated and near saturated (0 to -3 cm H₂O Ψ) soil hydraulic conductivity after sowing of legume under NT in 2018-19. The growth of legume roots enhanced pore continuity and increased the number of functional pores per unit area, which was the most likely responsible process for this improvement. However, such differences between IT and NT did not remain over time, thanks to legumes that mitigated the deleterious effect of tillage in IT. This indicates importance of leguminous crops on soil hydro-dynamic properties on the short term.

In addition, it was found that LM had greater air-filled porosity (0.113 vs. 0.105 cm³ cm⁻³), macroporosity (0.120 vs. 0.099 cm³ cm⁻³) and specific hydraulic conductivity of that pore size class, and pore continuity (0.30 vs. 0.29) than FM. The soil pore system configuration is responsible for air and water exchange through soil, which is dominated by pore size (macropores vs. micropores), hydraulically active pores and their continuity. For example, air and water movement in soil primarily control by macropores and its continuity compared to micropores. In this work, presence of crops potential improved soil pore system characteristics and consequently, enhanced soil aeration and hydraulic behavior. We hypothesized that, the

improvement of pore characteristics under legume-maize system may result from development of root channels, and the absence of soil disturbance in NT probably helps maintain these channels as relatively continuous macropores.

In summary, replacing fallow by legumes in a maize-based crop sequence improved air and water fluxes in soil particularly through macropores by generating preferential paths and improved soil pore system characteristics i.e., pore continuity, greater effective porosity, and number of pores per unit area. Apart from this, improvement of soil pore characteristics are also indicators of better soil structural development under legume-maize system (Abdollahi et al., 2014; Villarreal et al., 2020).

Likewise crop sequence, based on tillage systems temporal dynamics of soil hydro-physical properties were found in the three consecutive cropping years from 2018-19 to 2020-21. The difference on soil hydro-physical properties among tillage systems could be associated with soil structure components e.g., form, stability and resilience. The long-term contrasting tillage maintained for more than 26 years had a great impact on soil structuring. Regarding this, previous soil management led to different state of initial soil structure: increase tillage intensity (NT < RT < IT) is proportional to greater soil structure degradation. Continuous tillage (26 years) both in IT and RT created surface crust due to lower structural stability and it was more evident after spring tillage compared to autumn tillage, which resulted in reduced infiltration, and decreased surface soil hydraulic conductivity, K_s and sorptivity, S . The negative effects of soil crust on S and K_s were greater under IT than RT, and little under long-term NT. On the other hand, long-term NT showed similar or significantly higher values of soil hydro-physical properties over time which implies that soil under NT has a more stable structure and improved soil hydraulic conductivity due to a more effective porous system i.e., higher number of effective pores and pore continuity. In this regard, in the same experimental area Plaza-Bonilla et al. (2013) reported that long-term NT promotes soil aggregates stability by increasing the

percentage of stable macro-aggregates and the proportion of carbon in micro-aggregates compared to IT. Similarly, Pareja-Sánchez et al. (2017) found that lower soil organic carbon concentration and lower structural stability of IT increased the risk of surface crusting and lowered infiltration. Those findings imply that long-term NT had stable structure and more resilience to soil hydro-physical properties degradation and crusting, enhancing soil infiltration, gas and water fluxes compared to IT.

Apart from that, soil inversion by tillage loosens the soils and increases air-filled porosity and coarse mesoporosity under IT; and in the same time the breakdown of soil aggregates creates discontinuity among pores. As a consequence, although IT had greater air-filled porosity and coarse mesoporosity, it did not increase the air and water movement in the soil because of lower pore continuity. But this is not the case for NT that, due to less disturbance, showed a higher pore continuity. In addition, residue retention under NT stimulated the soil fauna activity and as a consequence, bio-pores and channels created by fauna increased pore continuity as well as soil aeration and water flux.

Overall, to understand the different hydro-physical process responsible for plant growth and development during crop succession, measurements or sampling considering intervention made by agricultural management need to be done to get the completed scenario because these differences are linked to the seasonal/yearly effects.

Spatial variations of soil hydro-physical properties (within vs. between crop rows) were observed in three consecutive cropping years (2018-19 to 2020-21). In row crops, measurement and determination of different soil variables varied depending on the position i.e., W-row vs. B-row. This implies that position itself has an impact on soil hydro-physical properties. The result of this study indicates that W-row shows better soil hydro-physical properties in terms of soil gas and water transport because of lower bulk density, greater air-filled porosity, macroporosity, coarse mesoporosity, effective porosity and number of effective pores per unit

area. The lower bulk density and greater porosity W-row could be related to local disturbance (very shallow depth) that happened at the time of seeding or planting by the seeding machine which opens the slot and loosens the soils. The little alternation of pore continuity occurred by local disturbance recovered or restored during the crop root development over time. In addition, the presence of plant roots and its growth and development especially W-row creates preferential flow channels. As a results, W-row had greater aeration and easier water movement than B-row. Similarly, the surface soil hydraulic conductivity (K_s) was around three times higher W-row than B-row (Table 10). The difference on K_s was due to crust formation, more prominent B-row. Row crops are unable to cover the whole soil surface, especially during the vegetative stages, which exposes more soil surface to water drop impact. The presence of the crops W-row, led to the weakening or lowering of crust development by intercepting raindrops and irrigation water, and reducing the falling energy when reaching the surface (Neave and Rayburg, 2007). Furthermore, plant roots strengthened the stability of surrounding aggregates by decaying roots biomass W-row, leading to a reduction in aggregate physical dispersion caused by water action (Fageria and Stone, 2006). The results of this work are consistent with the previous study performed by Pareja-Sánchez et al. (2017) in the same experimental area. They reported that, penetration resistance was greater B-row compared to W-row, particularly under IT because of less crop residues water runoff occurred mainly through the surface between rows. Under irrigated conditions, aggregates that break apart (splash effect) and are transported to soil depressions, are likely to clog the pores and reduced the continuity of pores and restrict the infiltration and percolation processes.

Generally, measurements of soil attributes are performed B-row. This particular choice is due to easier to perform the field activities i.e., accessible to install or set up the instrument, collection of samples etc. On the other hand, ignorance of W-row is due to difficulties that

arises from standing plants. Using B-row values only for modelling purposes may lead to inaccurate results.

2. Crop sequence and tillage effects on soil and water conservation, yields, water use efficiency and water productivity

In comparison to fallow, cultivation of legume reduced the risk of water loss through deep percolation. However, during winter (2018-19) and summer cropping season (2018-19) under irrigated condition LM showed greater *DP* than FM. In 2018-19, greater *DP* under LM can be due to the fact that the sprinkler installation did not allow to apply irrigation water as per crop requirement. The overlapping of late maturing maize (early planted) with early maturing maize (late planted) had different water requirement, but water was applied considering early planted maize (higher water than necessary applied for late planted maize). Further, this particular year irrigation dose was applied as a single irrigation event. As a result, water losses through *DP* were greater under LM than FM.

This study showed that maize performance was better under LM compared to FM. These differences could be due to positive impacts of legume on soil pore system characteristics (Palese et al., 2014; Gabriel et al., 2019). As previously mentioned, legume-maize systems enhanced air and water movements in soil because of greater amount of macropores and its continuity. Greater water flux makes it easier to utilise the water that is available for growing crops and may increase crop yields, especially for maize. Beside this, incorporation of legume before maize helped to reduce the risk of biotic stress. In this line, continuous maize cultivation since 2015 has retained the disease inoculums associated with maize residue and weed seedbank prevalent in the experimental plot have a detrimental impact on maize yield. As a result, it was observed that continuous mono-cropping in FM had faced a severe disease i.e., *Fusarium oxysporum* and weed infestations in 2018-19 and 2020-21, respectively. However, this is not the case for LM due to a delay in planting date for early maturing maize, which helped it to

escape disease and weed infestation. Therefore, the early maturing maize in LM had significantly greater above ground biomass and grain yield compared to FM in 2018-19 and 2020-21, but did not have an effect in 2019-2020 (Fig. 23). In addition, we hypothesised that legume (pea or vetch) increases the productivity of soils by incorporating soil nitrogen and organic carbon content from the residue retention (Gabriel and Quemada, 2011; Huynh et al., 2019). Further, LM showed greater above ground biomass under IT and RT than FM in 2020-21, and also grain yield was greater under IT (Fig. 23). These results highlighted that under intensive tillage legume inclusion counteract the detrimental effect of tillage operation and maintain similar crop production compared to conservation tillage i.e., RT and NT.

In 2018-19 and 2020-21, the early maturing maize grown after the legume had greater above ground biomass and grain yield. As a consequence, maize water use efficiency and water productivities increased significantly. Apart from that, greater water depletion during the winter cropping season, and less water application during summer cropping season had no adverse effects on subsequent maize WUE_c and the different water productivities. Nevertheless, the lack of yield reduction under legume-maize system was an important finding because soil water depletion by additional crops in Mediterranean area is a concern for subsequent main crops. These results illustrate that introduction of legumes in a crop sequence could maintain yield of main crops and also is benefited by environmental aspects e.g., improving soil structure.

Conservation tillage i.e., RT and NT improved soil and water conservation by reducing the surface runoff. It was evident that both sediment and water losses were greater under IT compared to RT and NT (during summer cropping season regardless of cropping year mean runoff ranges from: 42.5-2.9, 8.7-0.9, 1.3-0 mm in IT, RT and NT, respectively). The tendency of increasing surface runoff from NT to IT is due to increased tillage intensity, which makes the soil prone to sealing and crusting that strongly reduced infiltration (Gabriel et al., 2019; Huynh et al., 2019).

Similarly, both tillage systems (RT and NT) showed greater vetch biomass, and maize biomass and grain yield compared to IT (Fig. 22 and 23). The above ground biomass and grain yield reduction under IT could be linked to several causes related to soil structural stability and hydro-physical properties. As mentioned previously, IT had lower soil structural stability and showed greater soil degradation in terms of soil hydro-physical properties i.e., lower hydraulic conductivity and infiltration, pore continuity. As a consequence of soil degradation under IT, crop establishment was affected by IT in the same experimental field (Pareja-Sánchez et al., 2017), resulting in lower maize yields (Pareja-Sánchez et al., 2019).

Moreover, all tillage systems had received the same amount of water but greater biomass of vetch, and greater biomass and grain yield of maize under RT and NT significantly increased water use efficiency and water productivity of these crops compared to IT.

Therefore, the legume-maize sequence can be a management strategy where condition allows, not only because of the impact on crop yields but also because of improvements on soil hydro-physical properties. Under intensive tillage, legume inclusion would counteract the negative effect of tillage and sustain crop yields.

General conclusions

General conclusions

1. Introducing a legume before the maize increases soil macroporosity and produces a more continuous porous system, which increases soil gas diffusivity (better soil aeration) and hydraulic conductivity. This can alleviate the negative effect of intensive tillage by maintaining pore continuity, and reduce tillage requirements by providing increase aeration and water movements under no-tillage systems.
2. Long-term no-tillage, although increases soil bulk density and reduces porosity, increases pore continuity among macropores as well as reduces blocked pores avoiding deleterious effects on soil gas and water transport. No-tillage creates a continuous and stable pore organization system, which is one of the driving factors in gas and water transport through soils.
3. Within the row of crops, effective porosity, number of effective pores and pore continuity are greater compared to between crop rows, leading to higher soil gas diffusivity, saturated and unsaturated hydraulic conductivity. Spatial variations of soil hydro-physical properties and pore characteristics should be taken into consideration when measuring soil gas emissions and water flux as those variables may vary depending on the position of measurements.
4. The initial enhancements of porosity by intensive tillage, are lost very easily in the short term because of settlement that occurs due to rain and irrigation. In addition, the weak structural stability of surface soil under intensive tillage makes it prone to crust formation, leading to decreased sorptivity, hydraulic conductivity and number of actively conducting pores.
5. No-tillage and reduced tillage can be a management choice in Mediterranean areas, also under irrigated conditions, due to better structural stability, resilience to surface crust

formation, and enhanced soil hydraulic properties, that can improve the efficiency of using rain and irrigation water by reducing runoff.

6. Within the row of crops, the protective effect of the crop canopy on the soil reduces the risk of crust development, and preferential water flow increases surface soil hydraulic conductivity and sorptivity.
7. The inclusion of legumes in crop sequence increases the water consumption and depletion from the soil during the winter cropping season and reduces the risk of water losses by deep percolation.
8. Legume-maize system leads to greater biomass and grain yield, crop water use efficiency and water productivities due to reduce impact of biotic stresses.
9. Greater grain yield, water use efficiency and water productivities of maize after legumes under intensive tillage indicates that legume inclusion mitigates the negative effects of tillage and sustains the system production compared to fallow-maize system.
10. Conservation tillage practices such as reduced tillage and no-tillage, enhance soil water infiltration and percolation and reduces surface runoff and sediment yield in crust prone soils. These in turns significantly increases vetch biomass, maize biomass, and grain yields and water use efficiency and water productivities.
11. The effective use of water generates greater maize yields and consequently increases water productivity. These findings highlighted the importance of conservation tillage practices that enhances yields, water use efficiency and productivity, and envisages their potentialities to save water in irrigated systems which can be important where irrigation water is expensive, and crucial to overcome climate change effects.

References

- Abdollahi, L., Munkholm, L.J., Garbout, A., 2014. Tillage System and Cover Crop Effects on Soil Quality: II. Pore Characteristics. *Soil Sci. Soc. Am. J.* 78, 271–279.
<https://doi.org/10.2136/sssaj2013.07.0302>
- Fageria, N., Stone, L., 2006. Physical, chemical, and biological changes in the rhizosphere and nutrient availability. *J. Plant Nutr.* 29, 1327–1356.
<https://doi.org/10.1080/01904160600767682>
- Gabriel, J.L., Quemada, M., 2011. Replacing bare fallow with cover crops in a maize cropping system: Yield, N uptake and fertiliser fate. *Eur. J. Agron.* 34, 133–143.
<https://doi.org/10.1016/j.eja.2010.11.006>
- Gabriel, J.L., Quemada, M., Martín-Lammerding, D., Vanclooster, M., 2019. Assessing the cover crop effect on soil hydraulic properties by inverse modelling in a 10-year field trial. *Agric. Water Manag.* 222, 62–71. <https://doi.org/10.1016/j.agwat.2019.05.034>
- Huynh, H.T., Hufnagel, J., Wurbs, A., Bellingrath-Kimura, S.D., 2019. Influences of soil tillage, irrigation and crop rotation on maize biomass yield in a 9-year field study in Müncheberg, Germany. *F. Crop. Res.* 241, 107565.
<https://doi.org/10.1016/j.fcr.2019.107565>
- Neave, M., Rayburg, S., 2007. A field investigation into the effects of progressive rainfall-induced soil seal and crust development on runoff and erosion rates: The impact of surface cover. *Geomorphology* 87, 378–390.
<https://doi.org/10.1016/j.geomorph.2006.10.007>
- Palese, A.M., Vignozzi, N., Celano, G., Agnelli, A.E., Pagliai, M., Xiloyannis, C., 2014. Influence of soil management on soil physical characteristics and water storage in a mature rainfed olive orchard. *Soil Tillage Res.* 144, 96–109.
<https://doi.org/10.1016/j.still.2014.07.010>

-
- Pareja-Sánchez, E., Plaza-Bonilla, D., Álvaro-Fuentes, J., Cantero-Martínez, C., 2019. Is it feasible to reduce tillage and N use while improving maize yield in irrigated Mediterranean agroecosystems? *Eur. J. Agron.* 109, 125919.
<https://doi.org/10.1016/j.eja.2019.125919>
- Pareja-Sánchez, E., Plaza-Bonilla, D., Ramos, M.C., Lampurlanés, J., Álvaro-Fuentes, J., Cantero-Martínez, C., 2017. Long-term no-till as a means to maintain soil surface structure in an agroecosystem transformed into irrigation. *Soil Tillage Res.* 174, 221–230. <https://doi.org/10.1016/j.still.2017.07.012>
- Plaza-Bonilla, D., Cantero-Martínez, C., Viñas, P., Álvaro-Fuentes, J., 2013. Soil aggregation and organic carbon protection in a no-tillage chronosequence under Mediterranean conditions. *Geoderma* 193–194, 76–82.
<https://doi.org/10.1016/J.GEODERMA.2012.10.022>
- Villarreal, R., Lozano, L.A., Salazar, M.P., Bellora, G.L., Melani, E.M., Polich, N., Soracco, C.G., 2020. Pore system configuration and hydraulic properties. Temporal variation during the crop cycle in different soil types of Argentinean Pampas Region. *Soil Tillage Res.* 198, 104528. <https://doi.org/10.1016/j.still.2019.104528>